Southeastern Geology: Volume 25, No. 3
February 1985

Edited by: S. Duncan Heron, Jr.

Abstract

Academic journal published quarterly by the Department of Geology, Duke University.

SOUTHEASTERN GEOLOGY

PUBLISHED AT DUKE UNIVERSITY DURHAM, NORTH CAROLINA

VOL. 25, NO. 3 FEBRUARY, 1985

SOUTHEASTERN GEOLOGY

PUBLISHED QUARTERLY

AT

DUKE UNIVERSITY

Editor in Chief:
S. Duncan Heron, Jr.

Managing Editor:
James W. Clarke

This journal welcomes original papers on all phases of geology, geophysics, and geochemistry as related to the Southeast. Transmit manuscripts to S. DUNCAN HERON, JR., BOX 6729, COLLEGE STATION, DURHAM, NORTH CAROLINA 27708. Observe the following:

1) Type the manuscript with double space lines and submit in duplicate.
2) Cite references and prepare bibliographic lists in accordance with the method found within the pages of this journal.
3) Submit line drawings and complex tables as finished copy.
4) Make certain that all photographs are sharp, clear, and of good contrast.
5) Stratigraphic terminology should abide by the North American Stratigraphic Code (Am. Assoc. Petroleum Geologists Bulletin, v. 67, p. 841-875).

Proofs will be sent authors.

Reprints must be ordered prior to publication; prices available upon request. Subscriptions to Southeastern Geology are $9.00 per volume (US and Canada), $11.00 per volume (foreign). Inquiries should be sent to: SOUTHEASTERN GEOLOGY, BOX 6729, COLLEGE STATION, DURHAM, NORTH CAROLINA 27708. Make checks payable to: Southeastern Geology.

SOUTHEASTERN GEOLOGY

Table of Contents

Vol. 25, No. 3

February, 1985

STRATIGRAPHIC SECTION THROUGH THE ST. MARYS FORMATION, MIOCENE, AT LITTLE COVE POINT, MARYLAND

LUCY MCCARTAN U.S. Geological Survey, Reston, Virginia 22092

B. W. BLACKWELDER Tenneco Oil Exploration and Production, Box 2511, Houston, Texas 77001

E. M. LEMON, JR. U.S. Geological Survey, Reston, Virginia 22092

ABSTRACT

The cliff at Little Cove Point, Maryland, exposes a Miocene regressive marginal marine sequence. Only the top meter, which is Holocene wind-blown sand, does not belong to the Miocene sequence. The Little Cove Point section is the most complete record of the St. Marys Formation available in a single exposure.

Previous workers considered only the shelly beds at the base and the interbedded sand and mud above to be Miocene; overlying beds, predominantly sand and gravel, were assigned to the Pleistocene. Our study has revealed a relatively simple succession of sedimentary facies: fossiliferous silty clay grading upward to silty fine sand (shallow shelf, subtidal environment; 0-12 m altitude in cliff face), overlain by 3 m of interbedded sand and silt (open bay, intertidal to shallow subtidal environment), overlain by 12 m of beach sand.

Although weathering processes have leached the deposit and produced diagenetic minerals throughout the section, there is no apparent change in source material nor is there a zone of reworked weathering products. We conclude, therefore, that the entire 27 m sequence was deposited during a single sedimentary cycle. The only two notable changes in environment of deposition are found at the base and top of the interbedded sand and silt, where the shelf facies grades abruptly upward into bay sediment, which is in turn succeeded by beach deposits. The few hiatuses in the section are apparently of minor magnitude.

INTRODUCTION

Depositional cycles have been recognized in sequences of all ages in the Atlantic Coastal Plain (Owens and Sohl, 1969; Colquhoun, 1974; McCartan and others, 1982; Riggs and others, 1982). Newell and Rader (1982) described major cycles in the Chesapeake Group of Virginia and Maryland, and Kidwell (1982) found smaller-scale cyclicity within the Calvert and Choptank Formations. The 27 m cliff at Little Cove Point, Md., provides an excellent vertical record of the regressive phase of a middle Miocene cycle of the Chesapeake Group. The section will serve as a lithostratigraphic standard for comparison of small, isolated exposures and drill-hole samples of deposits belonging to the same sedimentary cycle. Fossiliferous strata of this cycle extend inland only a few kilometers, but unfossiliferous sandy beds, presumably of the same age, extend for tens of kilometers. By Walther's Law (translated in Reineck and Singh, 1975, p. 160), the upper part of the Little Cove Point section is the seaward extension of the lithologically similar updip strata, and the section will be a key element in further study of the updip deposits.

Location, Name and Age of Deposit, and Stratigraphic Position

Little Cove Point is on the western shore of Chesapeake Bay in Calvert County, Maryland, and is owned by the Chesapeake Ranch Club residential community (fig. 1). It is a headland dominated by a wave-cut cliff about 27 m high that is being actively eroded (figs. 2 and 3). On the basis of mollusks (table 1), ostracodes, and foraminifera, all the fossiliferous strata (lowest 12 m) are middle Miocene (Gernant and others, 1971; Blackwelder and Ward, 1976; Forester, 1980).

Both the lower, fossiliferous strata, and the overlying unfossiliferous strata are here referred to the St. Marys Formation. The St. Marys Formation, which is the middle of the Chesapeake Group (Darton, 1891; Dall, 1892), overlies the Choptank Formation. Following the revisions of Blackwelder and Ward (1976) and Ward (in press), the St. Marys Formation includes Shattuck's (1904) Zones 20 and 21 (beds at Camp Conoy, and near and below sea level at Little Cove Point), Zones 22 and 23 (at Little Cove Point), and Zone 24 (in St. Marys County). We consider Zone 24 the downdip equivalent of the unfossiliferous sand above Zone 23 at Little Cove Point.

The log and samples from an auger hole about a half kilometer west of the measured section (figs. 1 and 2) have been correlated with the measured section. The auger samples are generally less weathered than those from the cliff and so are helpful in determining the original mineralogy.

PREVIOUS WORK

The richly fossiliferous Miocene strata along the western shore of Chesapeake Bay have been studied for more than 100 years. The first stratigraphic reports were by Darton (1891), Harris (1893), and Shattuck (1904). Shattuck recognized three lithologic and fossil "zones" at Little Cove Point. He assigned the fossiliferous beds in the lower half of the section to the Miocene St. Marys Formation and the overlying unfossiliferous sand to the Pleistocene (fig. 2). Gernant (1971) discussed Miocene paleoecology based on Shattuck's stratigraphy. Blackwelder and Ward (1976) briefly discussed paleoecology and assigned the fossiliferous beds to the informal "Little Cove Point unit", now considered a member of the St. Marys Formation (Ward, in press). Ward (personal commun., 1984), believes the fossiliferous beds of the St. Marys Formation in the type area (St. Marys County) to be slightly younger than those at Little Cove Point, and probably a subtidal facies equivalent of the open bay and beach facies at Little Cove Point. Blackwelder and Ward (1976) found distinct biostratigraphic breaks between the St. Marys Formation and the overlying Eastover Formation (Pliocene) and the underlying Choptank Formation (their definition), and minor breaks within the St. Marys Formation. Kelley (1983) studied eight mollusk lineages from Little Cove Point and the remainder of the Calvert County cliffs, and used the stratigraphy of Blackwelder and Ward (1976).

Gibson (1971) and Newell and Rader (1982) considered the regional implications of the Maryland and Virginia Miocene, including the Little Cove Point sequence. Gibson (1971) estimated the extent and thickness of the St. Marys Formation, and found that the axis of the basin trends east-west and lies just south of Little Cove Point (fig. 2). Newell and Rader (1982) found evidence for interfingering of the St. Marys and Choptank Formations in Virginia, and argued that the St. Marys Formation contains deposits of the shallowest-water facies of a long-term depositional cycle containing the Calvert and Choptank Formations as well. Owens and Denny (1979) found a coarse-grained deltaic marine sequence on the Delmarva Peninsula that contained shallow-water fossils in the lower part ("Manokin" beds) characteristic of the St. Marys Formation at Little Cove Point, and deeper water fossils in the upper part ("Pokomoke" beds) characteristic of the Eastover Formation. Hornblende is abundant in the coarse deltaic deposits (Owens and Denny, 1979) as well as in the St. Marys Formation at Little Cove Point, but is rare in the Choptank Formation and absent from the Calvert Formation (Glaser, 1971; Anderson, 1948). Thus, Newell and Rader's (1982) evidence suggests that the St. Marys Formation is depositionally allied with the Calvert and Choptank Formations, but Owens and Denny's data suggest that it is genetically closer to the Eastover Formation.

THE LITTLE COVE POINT SECTION

The Little Cove Point sequence can be described in three parts (figs. 2 and 3): the lowest 12 m is upward coarsening, fossiliferous silty clay to muddy fine sand (subtidal, shallow shelf facies); the middle 3 m is interbedded silt and sand (intertidal to shallow subtidal, open bay facies); and the uppermost 12 m is burrowed, fine-to-coarse pebbly sand (beach facies). Evidence presented in this part of the paper for the three depositional lithofacies and for the continuity of the sequence will be discussed in a subsequent part of the paper.

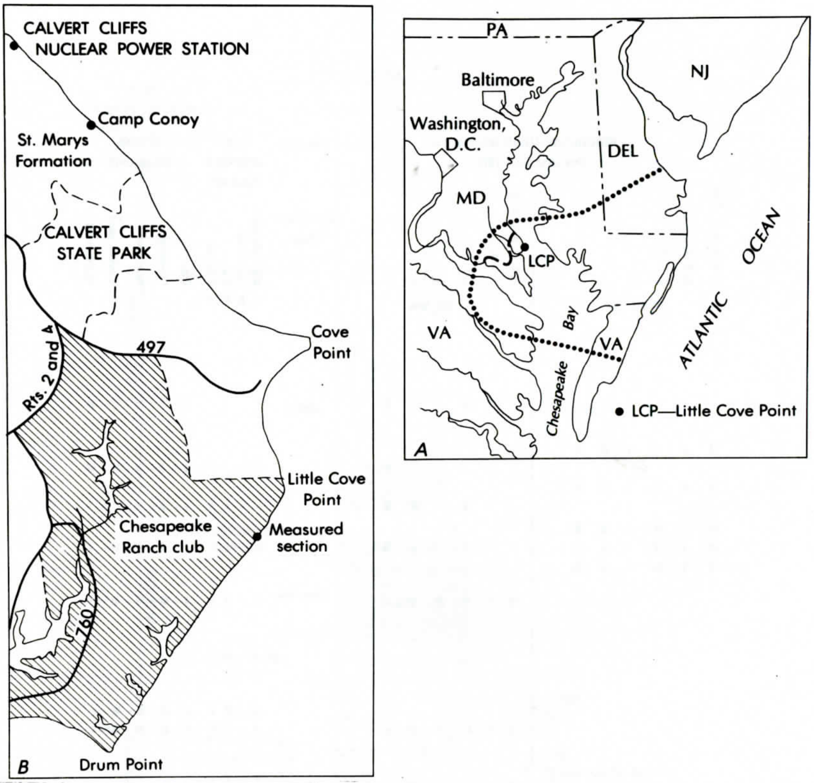

Figure 1. Maps showing location of Little Cove Point, Maryland, on the western shore of Chesapeake Bay. A. Dashed line crossing the two southern Maryland peninsulas just west of Little Cove Point marks the approximate inland edge of intertidal and subtidal deposits in the St. Marys Formation (modified from Blackwelder and Ward, 1976). Dotted line is approximate lnland edge of St. Marys Formation beach deposits (modified from Gibson, 1971). B. Measure section and auger hole south of Litle Cove Point. Lined pattern shows Chesapeake Ranch Club property.

Organic activity is evident throughout the Little Cove Point section (table 1, fig. 2). Mollusk-shell ghosts, occasional calcitic shell remnants, and pyritized forams, diatoms, and plant fragments are found near beach level; shell beds are preserved up to about 10 m; and burrows are found in beds from the base to within about 5 m of the top of the section.

The base of the St. Marys Formation is exposed at Camp Conoy (fig. 1B), and was penetrated in the auger hole west of Little Cove Point. The uppermost beds of the underlying Boston Cliffs Member of the Choptank Formation are "greenish-brown, clayey fine sand" with an irregular, eroded surface (Blackwelder and Ward, 1976). The mature heavy mineral suite characterizing the top of the Choptank Formation is superseded by a distinctly immature suite in the St. Marys Formation (fig. 2). The basal greenish-gray silty clay of the St. Marys can be traced southward past Little Cove Point. At Camp Conoy the clay at the base of the St. Marys Formation is 3 m thick; at the Little Cove Point section, less than one meter of the clay is exposed. Phosphate pebbles present at the upper surface of the clay at Camp Conoy are missing in the measured section, where the contact is marked by a concentration of burrows in the top of the clay and an abrupt increase in silt and fine sand above the clay. The clay was called the Conoy Member of the Choptank Formation by Gernant (1971), was then relegated to the base of the informal "Little Cove Point unit" between the Choptank and St. Marys Formations by Blackwelder and Ward (1976), and is now considered the base of the expanded St. Marys Formation (Ward, in press).

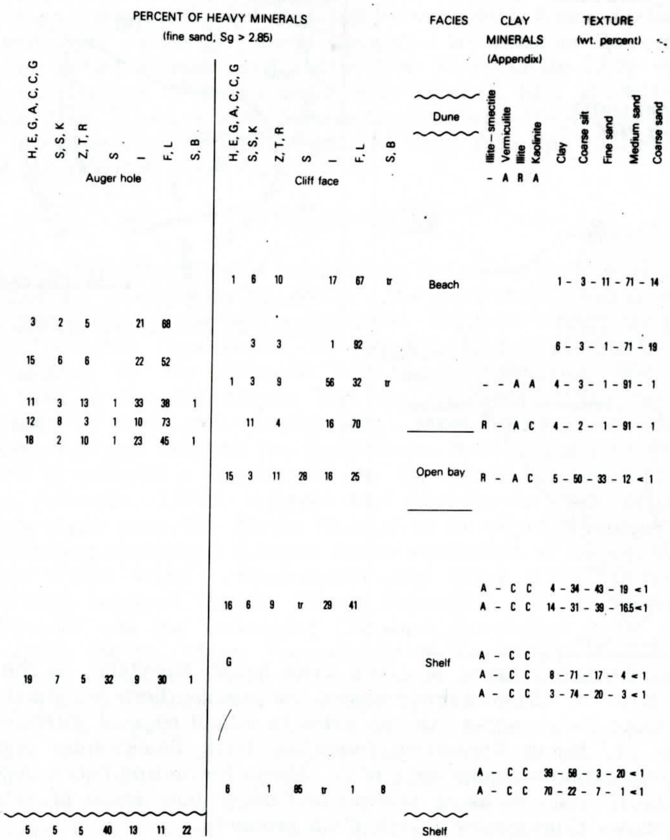

Figure 2. Stratigraphic section through the Miocene St. Marys Formation at Little Cove Point, Maryland. The two primary lithologic trends evident in this section--upward coarsening and upward increase in shallow-water sedimentary structures--are characteristic of a regressive (progradational) shoreline sequence (Reineck and Singh, 1975). Clay minerals were identified by x-ray diffractometry (A, abundant; C, common; P, rare; -, negligible; see also the Appendix); the heavy minerals were identified in oils with a petrographic microscope. The left columns give heavy mineral percentages from the auger hole and the measured section. The wavy line represents

The top of the St. Marys Formation has been eroded in Calvert County and replaced in some areas by a thin (up to 2 m thick) cover of well-sorted fine sand to poorly-sorted silty fine sand. In the Little Cove Point section, the lower half of this sand is hard due to soil processes. Youth of the sand is indicated by the presence of illite (Appendix), feldspar, and epidote. These minerals are rare to absent in samples from the underlying Miocene beach facies (fig. 2). The mineralogy and the fact that the sand is presently accumulating point to a Holocene age. This unit is excluded from further discussion.

Minor biostratigraphic breaks within the St. Marys Formation noted by Blackwelder and Ward (1976) reflect changing environmental conditions through time. The most significant break is between the faunas at Little Cove Point, Calvert County, and Windmill Point, St. Marys County (Blackwelder and Ward, 1976, Appendix 2).

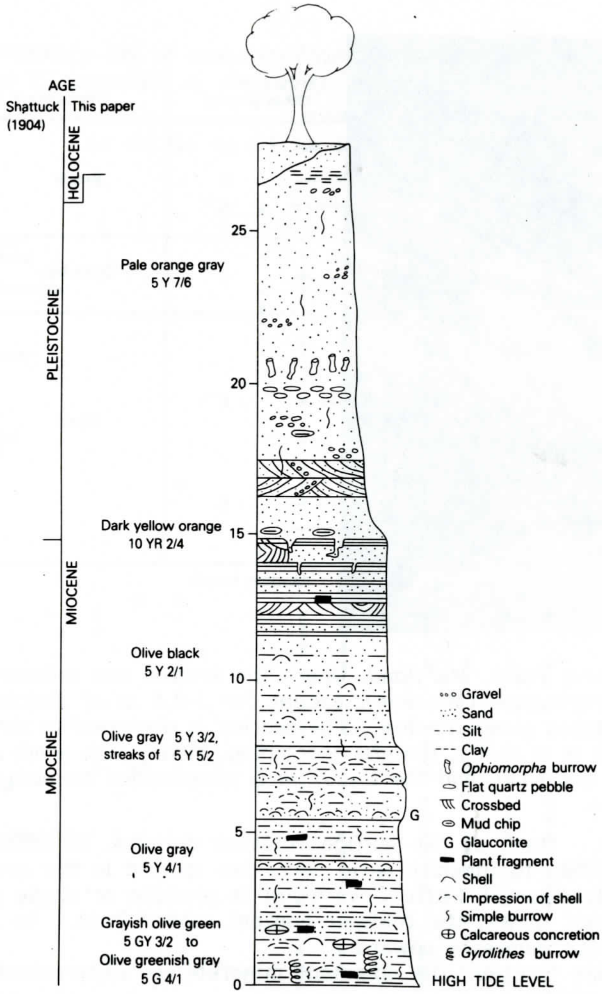

the unconformity between the St. Marys and Choptank Formations. Differences in maturity of the mineral suites in the auger hole and the cliff are discussed in the text. The symbols, starting at the left, represent hornblende, epidote, garnet, andalusite, chlorite, chloritoid, and glauconite (easily weathered non-opaque heavy minerals); staurolite, kyanite, and sillimanite (moderately resistant); zircon, tourmaline, and rutile (very resistant to weathering); sulfide (includes many replaced plant fragments and microfossils); ilmenite; iron oxide and leucoxene (ilmenite weathering product); bone and shell fragments.

Shelf Facies

The shelf facies consists of shelly, bioturbated, olive-black to grayish green silty clay to silty fine sand, which coarsens upward. Plant fragments are disseminated throughout the facies; shells are both disseminated and in discrete beds, and are found both in life position and in post-death accumulations. Shelf-facies beds are generally massive due to intense bioturbation, but shell accumulations impart the bedding at some levels.

The mineralogy of the lowest 12 m of the Little Cove Point section is the most variable and least mature of the three units. In the non-opaque fraction of the heavy minerals, moderately fresh glauconite, hornblende, epidote, and garnet are abundant. At the base, the opaque fraction of heavy minerals consists mainly of sulfides with a

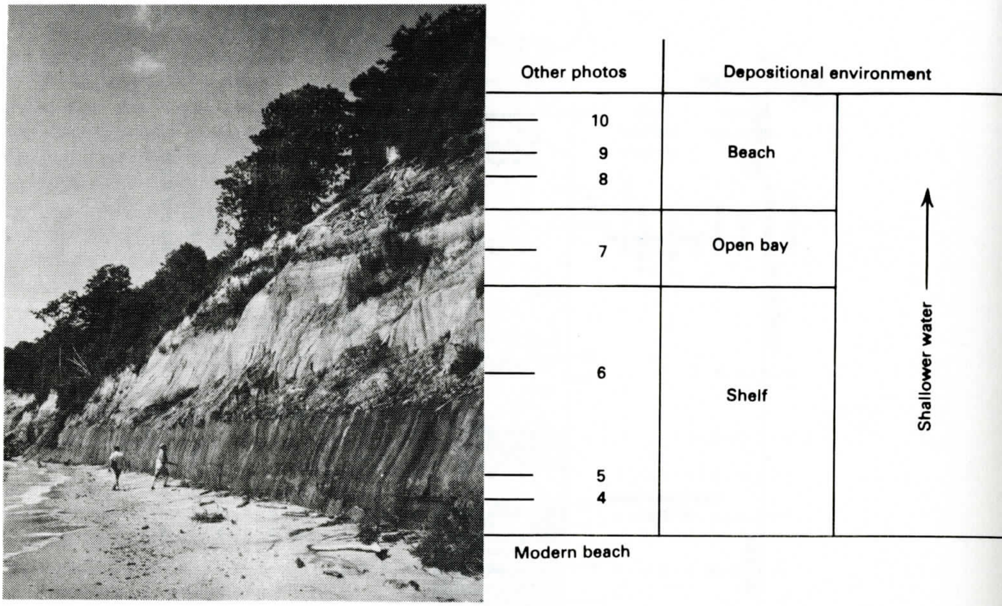

Figure 3. Little Cove Point, Maryland, where the section was measured. The entire cliff is St. Marys Formation (Miocene), except for 1-1.5 m of Holocene wind-blown material at some places along the top. The section is discussed in three parts in the text: the lowest 12 m is shelly, upward coarsening, muddy fine sand; the middle 3 m is interbedded mud and sand; and the top 12 m is crossbedded medium sand containing pebbles and burrows.

trace of leucoxene. Much of the sulfide replaces diatoms, foraminifers, and plant fragments. The sulfide to ilmenite ratio decreases upward in the section.

Most of the feldspar at Little Cove Point is perthite or single phase potassium feldspar. In the shelf facies, the feldspar content ranges from 5 to 15 percent, and alteration to kaolinite increases upward.

In the clay size fraction, the dominant minerals are illite-smectite mixed layer clay, illite, and kaolinite.

Of the 46 species and 52 genera of mollusks in table 1, 5 species and 41 genera are extant (Abbott and Dance, 1982). *Nucula proxima* prefers subtidal, sandy mud substrates, and is found from Nova Scotia to Texas. *Hiatella arctica* lives only in very cold waters. *Thracia conradi* has been found in depths between subtidal and 300 m from eastern Canada to New York. *Crepidula fornicata* attaches to rocks and shells in the subtidal zone in the eastern United States. *Lunatia heros* lives in intertidal to offshore sandy areas from the Gulf of St. Lawrence to North Carolina. The modern habitats of these species suggests that the shelf facies of the St. Marys Formation was deposited in a shallow subtidal environment and was slightly cooler than at present.

Only 8 of the 41 genera (other than the 5 noted above) have narrow depth and substrate tolerances. All 8 genera (*Anadara, Modiolus, Lucina, Cardium, Mercenaria, Periploma, Urosalpinx,* and *Busycon*) occupy habitats less than 30 m deep, and several prefer intertidal conditions. *Urosalpinx*, in addition, is usually found attached to oyster banks.

The most striking fossil in the lowest 2-3 m of this section is *Gyrolithes* a sand-filled, vertical corkscrew burrow (fig. 4). *Gyrolithes* is the previously named genus to which Hantzschel (1975) assigned Mansfield's (1927) *Xenohelix marylandica.*

The infaunal gastropod *Turritella* occurs in lenses 1-2 m above the base. In some fine sandy mud layers, the *Turritella* shells are current oriented parallel to the bedding planes (fig. 5) rather than in life position with the long axes crossing the bedding planes.

The most prominent shell bed, 1 m thick (fig. 6), is near the top of the steepest

Table 1. Preliminary list of mollusks from the shelf facies at Little Cove Point (R, rare; C, common; A, abundant)

	Altitude, in meters above sea level																	
	0.3	0.6	0.9	1.4	2.4	4.0	5.5	6.1	6.4	6.5	6.7	7.0	7.6	8.2	8.8	9.1	10.3	10.7
Pelecypoda																		
Nucula proxima				R	R		R											
Yoldia laevis	R	R		C	R	R	R	R	R	R	R	R	C					
Anadara sp. (elongate)							R											
Anadara covepointensis					R	R	R		R			R						
Modiolus ducateli						R		R	R	R	R	R						
Chesapecten covepointensis					R	R		C	R	C	A	R				R		
Astarte sp.					R													
Margaretaria sp.					R													
Lucina anodonta					R	R	R		R									
Parvilucina crenulatus					R	R	C	R	R	R								
Cardium sp.					R	C	C	C	R	C	A			R	R	R	R	R
Chione sp.						R												
Dosinia acetabulum						C	C	A	R	C		C						
Clementia							R	R	R	R	R							
Mercenaria (elongate)					R	R	C											
(arched)								C	C	R?	R	R				?		
Callocardia					R	R												
Spisula delumbis			R			R		R	R	R		R						R
Mactra subcuneata						R	A	C	C	C	A	C	C	R			R	
Ensis sp.					C		R	R	C	C	C	C	C					
Tellina "agilis"													R					
Aligena sp.					R						R							
Mesodesma mariana							C	R	R	R								
Hiatella arctica									R									
Periploma sp.		R	R															
Corbula inaequalis	R				C	C		R		R	R	R		R				
Pandora lata	R					R	R		R									
Thracia conradi						R	R											
Panopea sp.							R		R	R	R	R						
Gastropoda																		
Teinostoma nanum					R	R	R	R	R	R		R						
Teinostoma liparum					R				R									
Turritella plebeia	R	R		C	C	A	A	C	C	C	C	C	C			R		
Turritella variabilis					R	R	R								R			
Epitonium sayana								R	R	R	R	R						
Crucibulum costatum						R	R	R	R		R	R						
Crepidula fornicata (small)						R	R	R	R	R	R	R						
Crepidula plana							R		R	R								
Polinices duplicatus						R	R	R	C	R	C	C						
Lunatia heros					R	C	C	C	A	C	C	R						
Sinum sp.						R		R			R	R						
Urosalpinx rusticus										R	R							
Trophon tetricus										R								
Typhis acuticosta						R	R		R		R	R						
Ecphora sp.						R	R	R	R	R		R						
Nassarius peralta						C	C	C	A	C	C							
Bulliopsis marylandica						R	R	R	C	R	R							
Mitrella communis						C	A	C	A	C	C							
Busycon rugosum							R	R	R	R	C							
Busycon fusiforme								R			R						R	
Scalispira?							R											
Cancellaria lunata								R			R	R						
Cancellaria sp.												R						
Drillia limatula						R	R	R	R	R								
Drillia incilifera								R	R	R	R	R						
Mangelia parva						C	A	C	C	A	C	C						
Pleurotoma communis					R	C	C	C	C	C	R	C						
Terebra inornata						C	C	C	C	C	C	C						
Terebra simplex							R	R	R	R								
Turbonilla sp.					R	R	R	R	R	R	R							
Acteon ovoides						R		R			R	R						
Acteon shiloensis							R		R			R	R					
Volvula iota							R	R	R		R		R					
Scaphopoda																		
Dentalium caduloide							R	R	R	R	R		R					
Discinisca						R			R									
Balanus (large)						C	R		R	R	A	A						
Echinoderm? spines (reg.)							R			R								
Hydrozoans								R				C						
Reptile bones												R						
Wood fragments												R						

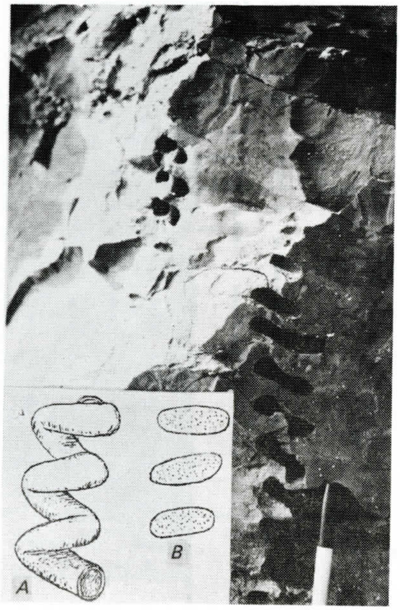

Figure 4. Gyrolithes, *corkscrew-shaped burrows, filled with black sand, are present in fractured, dewatered mud near the base of the section (see fig. 3 for location). Jarosite, a yellow sulfate mineral, coats the fractures; shell casts and molds are present. A. Three dimensional view. B. Vertical section through sand-filled* Gyrolithes. *C. Photograph of base of Little Cove Point section.*

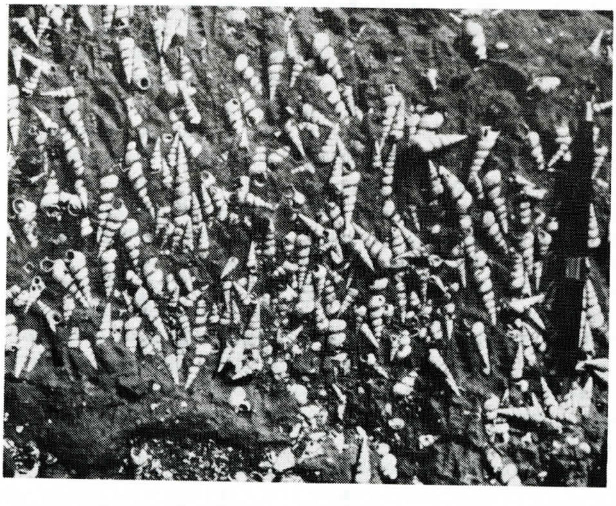

Figure 5. Current-oriented Turritella *shells on a bedding plane surface from a layer of fine sandy mud near the base of the section. Shells were aligned bimodally by tidal traction. Photograph of fallen block.*

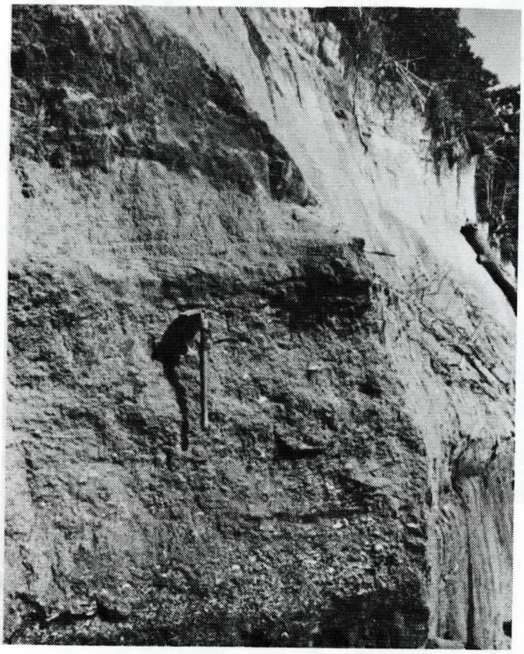

Figure 6. Shell bed, about 1 m thick, in the shelf facies; contains a diverse molluscan fauna, abundant glauconite, and wood and bone fragments at the top. See fig. 3 for location.

part of the cliff (figs. 2 and 3) and contains a diverse fauna (table 1, 6.1 to 7.0 m) as well as abundant glauconite. Wood and bone fragments are present near the top of this layer.

Open-bay Facies

The middle part of the section (12-15 m altitude) consists of alternating sand and clayey silt beds (fig. 7) without shells but containing abundant small sand-filled burrows near the top and crossbeds in some sandier parts. Clayey silt beds are up to 2 cm thick and sand beds are as much as 3 cm thick. Many "beds" are laminae only a few millimeters thick.

In the auger hole (fig. 1), this facies is represented by 4 m of dark gray olive shelly fine sand that is silty in the lower 2 1/2 m. The interbedded and non-interbedded lithologies of the open-bay facies can also be found grading laterally into each other north of Little Cove Point. The mineralogy of the interbedded sand and clay unit is essentially similar to that of the unit below.

Beach Facies

The uppermost 12 m is medium-to-coarse sand and fine gravel containing burrows and cross beds (figs. 2, 8, 9, 10), similar in scale and character to upper shoreface features in the Gulf of Gaeta, Italy (Reineck and Singh, 1975). Mud clasts typically as much as 3 cm long are found near the base of this unit and discoidal quartz pebbles as long as 2 cm are present in scattered lenses. The upper 5 m of the section is essentially massive.

Beach facies sand in the auger hole is siltier and more poorly sorted than at the cliff. This variability of sorting is characteristic of the facies northward along the cliff.

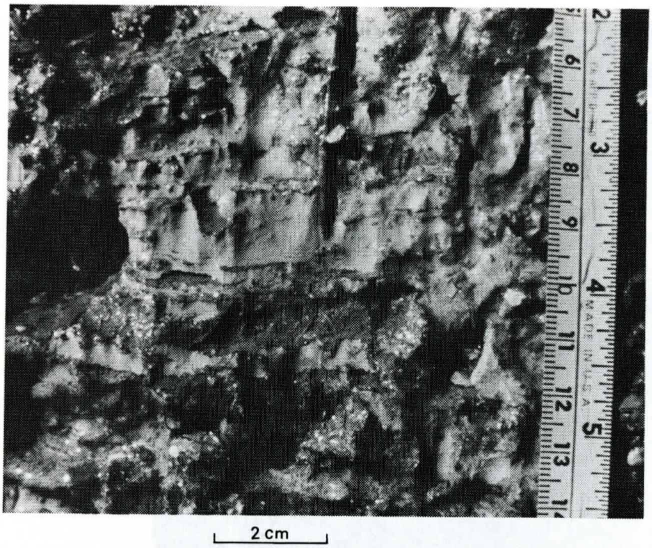

Figure 7. Small ripple crossbeds occur in the sand beds, and thin, vertical burrows cross the bedding of the interbedded sand and mud constituting the middle 3 m of the section. See fig. 3 for loction.

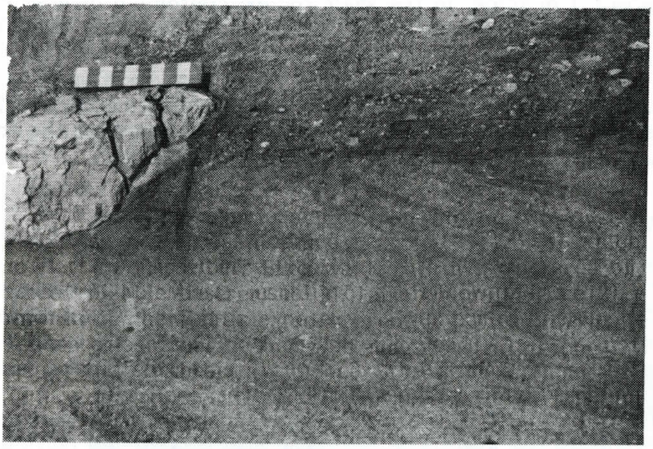

Figure 8. Megaripple crossbeds outlined with intraformational mud clasts derived from the immediately underlying interbedded mud and sand interval. This is an abrupt facies change rather than an unconformity. See fig. 3 for loction.

A mature heavy-mineral suite consisting mainly of iron oxide, leucoxene (weathering product of ilmenite), ilmenite, and zircon, characterizes the beach facies at the cliff and in the upper, most weathered part of the auger hole. Iron oxide cement forms crusts up to 10 cm thick in several layers.

A mud clast at the base of the sand beds is almost entirely illite and kaolinite; mixed layer clay, dominant in underlying facies, is essentially absent in the clast. Lepidocrocite, an ephemeral diagenetic iron hydroxide, is also present in the clast. Interstitial clay 2 m from the top of the cliff contains abundant vermiculite and kaolinite, weathering products of illite, illite-smectite, and feldspar. Feldspar ranges from 0 to 5 percent in the beach facies and is typically absent.

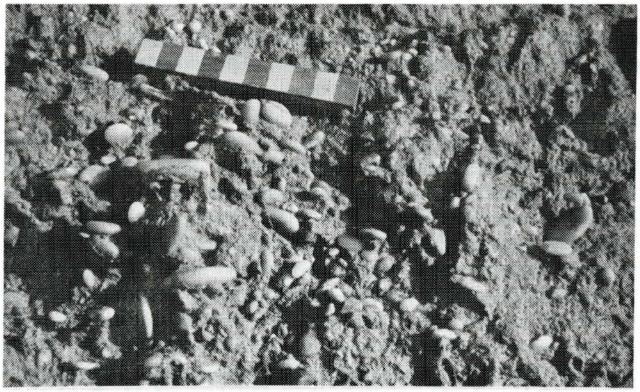

Figure 9. Flat quartz pebbles in the upper half of the section indicate a beach environment. See fig. 3 for location.

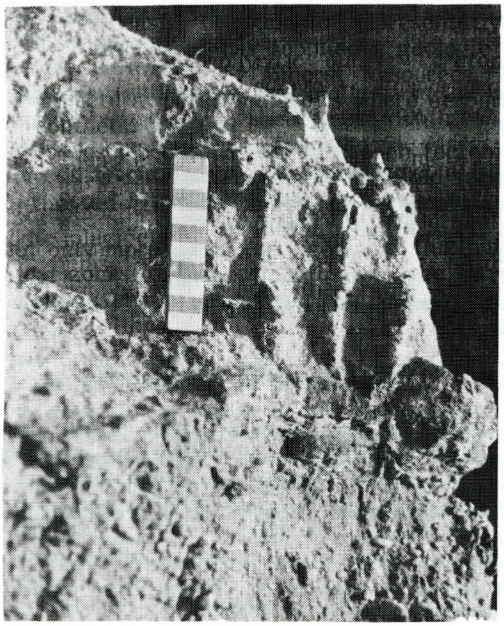

Figure 10. Ophiomorpha burrows in the upper half of the section suggest lower beachface environment. See fig. 3 for location.

DISCUSSION

Sedimentology

Upward coarsening in the Little Cove Point section in addition to the massive appearance at the base, laminated bedding in the middle, and crossbedding in the upper half, suggests gradual shoaling and progradation with time (Allen, 1970; Reineck and Singh, 1975). The orderly succession of progressively higher energy lithofacies records a single depositional regression unbroken by major hiatuses.

The alternation of grain sizes in the middle 3 m probably reflects two processes: a change in sediment supply due to migration of distal and proximal facies in a small-scale wave-dominated delta (Miall, 1976), and a change in energy conditions due to the waxing and waning of tides in an open bay such as the North Sea (Dörjes and others, 1970). The abundance of plant fragments, plant fragments and microfossils replaced by pyrite, and secondary sulfate near the base of the section, reflect deltaic sedimentation (Rainwater, 1966; see also Altschuler and others, 1983), and the abundance of normal salinity organisms (table 1) requires circulation at least as unrestricted as an open bay (Abbott and Dance, 1982).

Shoreface conditions are suggested by the overlying medium-to-coarse sand, abundant megaripple crossbedding (Clifton and others, 1971; Reineck and Singh, 1975), discoidal quartz pebbles (Kuenen, 1964), and lenses containing many *Ophiomorpha* burrows. Mud clasts, just above the contact between the sand and the underlying alternating mud and sand beds, indicate penecontemporaneous deposition and erosion of mud within a relatively small area, and juxtaposition of quiet and vigorous energy conditions. Similar variability of hydraulic conditions is suggested by poorer sorting in the beach facies of the auger hole as well as northward along the cliff, and is characteristic of many modern depositional areas (Gulf of Mexico, Bernard and others, 1970; Atlantic coast, Howard and Reineck, 1972; North Sea, Dörjes and others, 1970).

The abrupt change from muddy sediment in the lowest 15 m of the section to sand without mud above the 15 m level records a change from lower water energy to greater energy but does not necessarily reflect a significant time gap. A long pause in sedimentation such as inferred by Shattuck (1904) would be marked by reworked weathering products (for example, gibbsite or iron oxide clasts, or abundant worn shells or phosphate clasts), a new heavy-mineral suite suggesting a different source area, or an abrupt and unexpected change in depositional sequence. Such indicators of regional unconformities are common in other Atlantic Coastal Plain stratigraphic successions (Glaser, 1971; Owens and Sohl, 1969; Owens and others, 1983).

At Little Cove Point, the lithologic trends support the conclusion that the sands constituting the beach facies rest upon open bay and shallow shelf facies in a single regressive depositional cycle (see also Bernard and others, 1970, Howard and Reineck, 1972, and Reineck and Singh, 1975, for Holocene examples, and discussion in Newell and Rader, 1982). The single bed containing sparse but notable wood and bone fragments is a few centimeters thick and occurs in the middle of the bay facies; sand content increases above the "bone bed". This suggests a minor hiatus after which the water depth decreased slightly.

Mineralogy and Weathering

The original mineralogy and abundance of shells in the Little Cove Point section can be inferred by removing the overprint of weathering processes. Certain minerals such as hornblende, epidote, garnet, feldspar, and illite-smectite mixed layer clay are more easily altered during weathering than are others, such as tourmaline, zircon, and kaolinite (see Appendix and Owens and others, 1983). Calcium carbonate shells tend to dissolve most readily in permeable, sparsely shelly sands with mobile, acidic groundwater. Conversely, shells tend to be preserved in populous shell beds by the buffering action of abundant calcium carbonate, in mud by the impeding of ground water flow, and with basic ground water conditions. Combinations of these conditions produce a variety of results, including the massive appearance of much of the upper third of the section.

The weathering profile in the auger hole west of the measured section is thinner than at the cliff because the ground water moves more rapidly at the cliff, which intersects the water table almost vertically. This difference in weathering profile is reflected in the mineralogy (fig. 2) and abundance of shells at the two sites. Easily weathered non-opaque minerals are 15 percent of the heavy mineral suite as high as 3 m above the base of the beach facies in the auger hole; at the cliff, 15 percent weatherable non-opaques are present only up to 2 m below the base of the beach facies--a 5 m difference in comparable weathering between the two locations.

Shells are present in the auger hole to the top of the bay facies (15 m altitude); at the cliff, shells are found only between about 4 m and 8 m elevation, 4 m below the lowest bed of the bay facies. Shell "ghosts" are present between 8 m and 10 m altitude. Casts and molds are present in the lowest 4 m of the section but shell material is rare and in an advanced stage of dissolution. No aragonite remains. Dissolution is apparently due to the action of sulfuric acid, produced by oxidation of abundant authigenic sulfide in the lower part of the shelf facies. A by product of this process is the presence of jarosite, an iron sulfate, which coats all fractures and exposed surfaces at the base of the cliff face.

Judging from the mineralogy of the less weathered parts of the two sections (data from text, fig. 2, and Appendix), we can estimate the average mineralogy and shell abundance for the three facies at the time of deposition. Shells were most abundant in the several beds near the middle of the shelf facies, present in the bay facies, and rare in the beach facies. Sand mineralogy was about 90 percent quartz, 7 percent feldspar, and 3 percent heavy minerals. The detrital heavy mineral suite was about half ilmenite and half non-opaque minerals, of which most were easily weathered. Syndepositional or reworked glauconite was locally abundant. The three dominant clays were illite-smectite mixed layer material, illite, and kaolinite.

Soon after deposition, iron sulfide minerals formed in the shelf and bay facies under locally reducing conditions enhanced in both facies by relatively impermeable muddy sediment and rich organic material in the form of plant fragments, and in the shelf facies by abundant diatoms and forams as well.

During subsequent uplift and weathering, the present distribution of primary and secondary minerals evolved. Now the dominant components of the most thoroughly weathered beds are quartz, iron and aluminum oxides, vermiculite (from illite and illite-smectite) and kaolinite (detrital and as a feldspar weathering product).

Paleoecology

Environments associated with the extant mollusks in the Little Cove Point section strongly suggest an intertidal to shallow shelf water depths and a warm temperate to cool temperate climate for the shelf facies of the St. Marys Formation.

The succession of dominant species in the lower half of the Little Cove Point section (table 1) is a response to slight differences in substrate, water depth, degree of transportation of the assemblage, and preservation (Gernant, 1971; Blackwelder and Ward, 1976; Abbott and Dance, 1982).

Ostracodes (Forester, 1980) and benthic foraminifera (R. Z. Poore, 1981, written commun.) from the shelly part of the sequence also reflect a subtidal, shallow shelf environment of deposition.

Diatoms are present only in the basal 3 to 4 m of the St. Marys Formation (1 m at Little Cove Point) but are abundant in both the Calvert and Choptank Formations (Andrews, 1978). Conditions are amenable to the preservation of diatoms in many beds in the lower half of the section (oxidation of sulfide minerals produces acidic ground water, which inhibits the dissolution of the silica tests of diatoms), yet diatoms are essentially absent throughout most of the section. Perhaps the nutrients necessary for diatom blooms were not present in the required abundance during deposition of the St. Marys Formation, or the accumulation of clastic sediment greatly diluted the diatoms. In either case, the St. Marys Formation records a set of conditions different from those present during deposition of the older Calvert and Choptank Formations.

SUMMARY AND CONCLUSIONS

Interpretation of trends in texture, sedimentary structures and bed forms, sand and clay mineralogy, and fossils, has led to the following conclusions:

1. The St. Marys Formation at Little Cove Point, Maryland, is the regressive part of a single cycle of marine deposition without significant breaks in sedimentation, in which supratidal and intertidal deposits overlie shallow subtidal (shelf) deposits. Previous workers interpreted the 12 m of unfossiliferous St. Marys Formation beach sediment at Little Cove Point as fluvial Pleistocene deposits, assuming incorrectly that the abrupt change in lithology from mud and sand below to sand above was evidence for an unconformity.

2. The section is deeply weathered, and the leaching and diagenesis are more complete at the top than at the base of the section. The weathering profile is several meters thicker at the cliff than in the auger hole a half kilometer to the west. The most significant post-depositional trends are an upward decrease in shells and easily weatherable minerals such as hornblende, epidote, feldspar, illite-smectite mixed layer clay, illite, and sulfides, and an increase in the relative abundance of resistant detrital

minerals such as quartz, zircon, tourmaline, and detrital kaolinite, and authigenic components such as iron oxides, vermiculite, and secondary kaolinite.

3. Recognition of the lateral variability of the St. Marys Formation due to the distribution of primary depositional facies and subsequent differential weathering is essential to regional mapping of the unit.

ACKNOWLEDGMENTS

We wish to thank many workers for their contributions to this study. J. P. Owens first noted that the section is a single regressive sequence. N. L. Sohl, L. W. Ward, T. M. Cronin, and J. E. Hazel discussed the paleoecology of mollusks and ostracodes. S. M. Kidwell and S. D. Heron reviewed the manuscript and made several valuable suggestions for its improvement.

Appendix Clay mineralogy

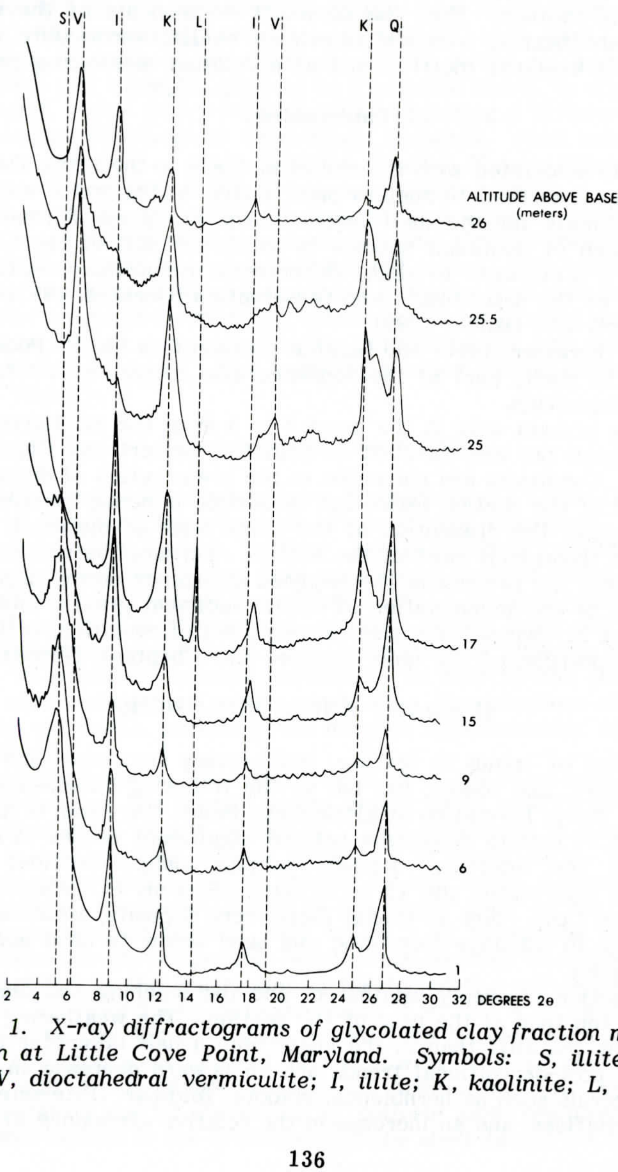

Appendix Figure 1. X-ray diffractograms of glycolated clay fraction minerals from the measured section at Little Cove Point, Maryland. Symbols: S, illite-smectite mixed layer material; V, dioctahedral vermiculite; I, illite; K, kaolinite; L, lepidocrocite; Q, quartz.

The less than two micrometer size fraction was obtained by centrifugation for clay-mineral analysis. This size fraction was suspended in water, pipetted on glass slides and allowed to dry. Four slides were made for each sample: untreated (Appendix fig. 1), glycolated, baked at 350°C, and baked at 550°C. X-ray diffraction patterns were obtained from a "Diano" diffractometer using CuKa radiation, and graphite monocrometer. The four x-ray patterns produced were compared, noting the degree 2Θ and dx spacings of each peak. Kaolinite and chlorite were differentiated by observing the 7.2 and 14 angstrom peak intensities before and after baking at 550°C. Chlorite was, for the most part, negligible. Glycolated samples with non-expanding peaks at 14 angstroms retained their 14 angstrom peaks after potassium-saturation indicating dioctahedral vermiculite.*

Changes in clay mineral proportions in a vertical sequence of samples--rather than the absolute quantity of each mineral in every sample--was the goal of the analysis. The most important trends are: 1) the decrease of illite-smectite upward from 1 m to 17 m; 2) the appearance of dioctahedral vermiculite and the lack of illite at the top of the St. Marys Formation weathering profile (25 m and 25.5 m); 3) the presence of lepidocrocite at 17 m; and 4) the reappearance of illite in the uppermost sample. Vermiculite forms during weathering at the expense of illite-smectite and illite. Lepidocrocite is an ephemeral iron hydroxide found only in a very active part of a weathering profile (the "weathering front"). Illite in the uppermost sample is windblown, probably reworked from the sediment sloughing from the upper part of the cliff face. Stephansson and Owens (1970) and Knechtel and others (1966) presented other studies of St. Marys Formation and clays.

**Any use of trade names in this report is for descriptive purposes only and does not constitute endorsement by the U.S. Geological Survey.*

REFERENCES CITED

Abbott, R. T., and Dance, S. R., 1982, Compendium of seashells: New York, E. P. Dutton, 411 p.

Allen, J. R. L., 1970, Physical processes of sedimentation: New York, American Elsevier, 248 p.

Altschuler, Z. S., Schnepfe, M. M., Silber, C. C., and Simon, F. O., 1983, Sulfur diagenesis in Everglades peat and origin of pyrite in coal: Science, v. 221, p. 221-227.

Anderson, J. L., 1948, Cretaceous and Tertiary subsurface geology: The stratigraphy, paleontology, and sedimentology of three deep test wells on the Eastern Shore of Maryland: Maryland Geol. Survey Bull. 2, p. 1-113.

Andrews, G. W., 1978, Marine diatom sequence in Miocene strata of the Chesapeake Bay region, Maryland: Micropaleontology, v. 24, p. 371-406.

Bernard, H. A., Major, C. F., Jr., Parrott, B. S., LeBlanc, R. J., Sr., 1970, Recent sediments of southeast Texas, a field guide to the Brazos alluvial and deltaic plains and the Galveston barrier island complex: Guidebook 11, Bureau of Econ. Geol., Univ. of Texas at Austin, 16 p.

Blackwelder, B. W. and Ward, L. W., 1976, Stratigraphy of the Chesapeake Group of Maryland and Virginia: Geol. Soc. America Guidebook for Field Trip 7b, 55 p.

Clifton, H. E., Hunter, R. E., and Phillips, R. L., 1971, Depositional structures and processes in the non-barred high-energy nearshore: Jour. of Sed. Petrology, v. 41, p. 651-670.

Colquhoun, D. J., 1974, Cyclic surficial stratigraphic units of the middle and lower Coastal Plains, central South Carolina, *in* Oaks, R. Q., Jr., and DuBar, J., eds., Post-Miocene Stratigraphy Central and Southern Atlantic Coastal Plain: Logan, Utah, Utah State Univ. Press, p. 179-190.

Dall, W. H., 1892, Correlation papers; Neocene: U.S. Geol. Survey Bull. 84, 349 p.

Darton, N. H., 1891, Mesozoic and Cenozoic formations of eastern Virginia and Maryland: Geol. Soc. America Bull., v. 2, p. 431-450.

Dörjes, J., Gadow, S., Reineck, H.-E., and Singh, I. B., 1970, Sedimentologie und Makro-benthos der Nordergrunde und der Aussenjade (Nordsee): Senckenbergiana Mari-tima, v. 2, p. 31-59.

Forester, R. M., 1980, A systematic revision of the ostracode species described by Ulrich and Bassler and by Malkin from the Chesapeake Group in Maryland and Virginia: U.S. Geol. Survey Professional Paper 1128, 25 p.

Gernant, R. E., 1971, Invertebrate biofacies and paleoenvironments, *in* Gernant, R. E., Gibson, T. G., and Whitmore, F. C., Jr., Environmental history of Maryland Miocene: Maryland Geol. Survey, Guidebook 3, p. 19-30.

Gernant, R. E., Gibson, T. G., and Whitmore, F. C., Jr., 1971, Environmental history of Maryland Miocene: Maryland Geol. Survey, Guidebook 3, 58 p.

Gibson, T. G., 1971, Miocene of the middle Atlantic Coastal Plain, *in* Gernant, R. E., Gibson, T. G., and Whitmore, F. C., Jr., Environmental history of Maryland Miocene: Maryland Geol. Survey, Guidebook 3, p. 1-15.

Glaser, J. D., 1971, Geology and mineral resources of southern Maryland: Maryland Geol. Survey Rept. of Investigations 15, 85 p.

Hantzschel, W., 1975, Trace fossils and problematica, Part W, Miscellanea, Treatise on Invertebrate Paleontology: Geol. Soc. America and Univ. of Kansas, p. W65.

Harris, G. D., 1893, The Tertiary geology of Calvert Cliffs, Maryland: Am. Jour. Science, 3rd. ser., v. 45, p. 21-31.

Howard, J. D., and Reineck, H.-E., 1972, Georgia coastal region, Sapelo Island, U.S.A.: Sedimentology and biology. IV. Physical and biogenic sedimentary structures of the nearshore shelf: Senckenbergiana Maritima, v. 4, p. 47-79.

Kelley, P. H., 1983, Evolutionary patterns of eight Chesapeake Group molluscs: evidence for the model of punctuated equilibria: Jour. Paleontology, v. 57, p. 581-598.

Kidwell, S. M., 1982, Stratigraphy, invertebrate taphonomy, and depositional history of the Miocene Calvert and Choptank Formations, Atlantic Coastal Plain: unpublished Ph.D. dissertation, Yale University, New Haven, Connecticut, 514 p.

Knechtel, M. M., Hamlin, H. P., and Hosterman, J. W., 1966, Expandable clay in St. Marys Formation of southern Maryland: Maryland Geol. Survey Rept. of Investigations 4, 17 p.

Kuenen, P. H., 1964, Experimental abrasion: 6. Surf action: Sedimentology, v. 3, p. 29-43.

Mansfield, W. C., 1927, Some peculiar fossil forms from Maryland: Proceedings of the U.S. National Museum, v. 71, p. 1-9.

McCartan, L., Owens, J. P., Blackwelder, B. W., Szabo, B. J., Belknap, D. F., Kriausakul, N., Mitterer, R. M., and Wehmiller, J. F., 1982, Comparison of amino acid racemization geochronometry with lithostratigraphy, biostratigraphy, uranium-series coral dating, and magnetostratigraphy in the Atlantic Coastal Plain of the southeastern United States: Quaternary Research, v. 18, p. 337-359.

Miall, A. D., 1976, Facies models 4. Deltas: Geoscience Canada, v. 3, p. 215-227.

Newell, W. L., and Rader, E. K., 1982, Tectonic control of cyclic sedimentation in the Chesapeake Group of Virginia and Maryland, *in* Lyttle, P. T., ed., Central Appalachian Geology: NE-SE Geol. Soc. America Field Trip Guidebook, p. 1-27.

Owens, J. P., and Denny, C. S., 1979, Upper Cenozoic deposits of the central Delmarva Peninsula, Maryland and Delaware: U.S. Geol. Survey Professional Paper 1067-A, 28 p.

Owens, J. P., Hess, M. M., Denny, C. S., and Dwornik, E. J., 1983, Post-depositional alteration of surface and near-surface minerals in selected Coastal Plain formations of the Middle Atlantic States: U.S. Geol. Survey Professional Paper 1067-F, 45 p.

Owens, J. P., and Sohl, N. F., 1969, Shelf and deltaic paleo-environments in the Cretaceous-Tertiary formations of the New Jersey Coastal Plain, *in* Subitsky, S., ed., Geology of Selected Areas in New Jersey and Eastern Pennsylvania and Guidebook to Excursions: New Brunswick, N. J., Rutgers University Press, p. 235-278.

Rainwater, E. H., 1966, The geological importance of deltas, *in* Shirley, M. L., and Ragsdale, J. A., eds., Deltas in their Geologic Framework: Houston Geological Society, p. 1-15.

Reineck, H.-E., and Singh, I. B., 1975, Depositional Sedimentary Environments: (corrected reprint of the first edition) New York, Springer Verlag, 439 p.

Riggs, S. R., Lewis, D. W., Scarborough, A. K., and Snyder, S. W., 1982, Cyclic deposition of Neogene phophorites in the Aurora area, North Carolina, and their possible relationship to global sea-level fluctuations: Southeastern Geol., v. 23, p. 189-204.

Shattuck, G. B., 1904, Geologic and paleontologic relations with a review of earlier investigations, *in* Clark, W. B., Shattuck, G. B., and Dall, W. H., eds., The Miocene Deposits of Maryland: Maryland Geol. Survey, Miocene Volume, p. 33-94.

Stefansson, Karl, and Owens, J. P., 1970, Clay mineralogy of selected samples from the middle Miocene Formations of southern Maryland: U.S. Geol. Survey Professional Paper 700-B, p. B150-B156.

Ward, L. W., Stratigraphy of outcropping Tertiary beds along the Pamunkey River—central Virginia Coastal Plain: Guidebook for the 21st Annual Field Conference of the Atlantic Coastal Plain Geol. Association, in press.

Woodring, W. P., 1957, Marine Pleistocene of California: Geol. Soc. America Memoir 67, p. 589-598.

A COMPARATIVE WEATHERING STUDY OF THE EAST FARRINGTON ADAMELLITE AND THE CONCORD SYENITE

STEVEN J. FRITZ — Department of Geology, Texas A&M University, College Station, Texas 77843

ABSTRACT

Two mineralogically similar rocks in the North Carolina Piedmont not only have different weathering rind morphologies but also different sequences of elemental mobilization. The East Farrington adamellite develops a few, thick rindlets that are clay-rich. Here, kaolinization is concomitant with physical disaggregation, resulting in severe depletions of Ca, Na and Sr. Weathering of the Concord syenite produces many thin rindlets that are limonitic rather than argillaceous and little elemental depletion occurs in this rind system. The factor controlling this dissimilarity appears to be texture of the parent rock. The perthite matrix of syenite is not easily penetrated by solution channels; hence, channel propagation is not retarded. This results in a proliferation of rindlets having limonitic products. In the adamellite, kaolinization of plagioclase blunts rindlet production, resulting in a few, clay-rich rindlets with significant elemental depletions.

INTRODUCTION

Weathering rinds generally represent the first stages of chemical weathering. Preserved in a weathering rind system is the early history of alteration of the fresh rock core. Interpreting this history is made easier by recognizing that all rinds once had chemical and mineralogical compositions similar to those in the fresh rock core. If care is taken to sample only those rocks least affected by physical weathering, then weathering rinds become ideal for studying the changes occurring in early stages of chemical weathering. A weathering rind system can be characterized by its morphology, mineralogical stabilities and elemental distribution. Factors that control these characteristics are: mineralogy and texture of the parent rock, fabric of the rock, chemical nature of the pore water, physiography, local topographic relief, climate and time.

Igneous rocks in the North Carolina Piedmont develop two distinct weathering rind morphologies: 1) a weathering rind system consisting of a few, thick, clay-rich rindlets categorized into inner and outer rindlets (Types I and II of Fritz and Ragland, 1980); and 2) a weathering rind system composed of many thin, clay-poor rindlets of a single morphology (Type III of Fritz and Ragland, 1980). The degree of chemical weathering is strikingly different in these two weathering rind systems. In the former system, residual weathering results in removal of Na and Ca concomitant with kaolinization of plagioclase. This is typical of the weathering of the East Farrington adamellite, Lilesville granite and Mount Airy granite. The rindlets in the Type III weathering rind system are remarkably fresh and alteration tends to produce weathering products that are limonitic rather than argillaceous. This is typical of weathering rinds produced on the Pee Dee gabbro and Concord syenite (Fritz, 1976). Figure 1 is a drawing of the weathering rind morphologies typically found in outcrops of the East Farrington adamellite and the Concord syenite.

In this study the weathering rind characteristics of the mineralogically similar East Farrington adamellite and Concord syenite are compared to determine what factors control their dissimilar types of alteration. Because both lithologies are unmetamorphosed plutons in the North Carolina Piedmont, the fabric, physiographic and climatic variables are minimized.

PROCEDURES

A weathering rind outcrop was sampled when the following criteria were met: 1) there were no detectable faults or dikes in the local outcrop areas; 2) the fresh parent

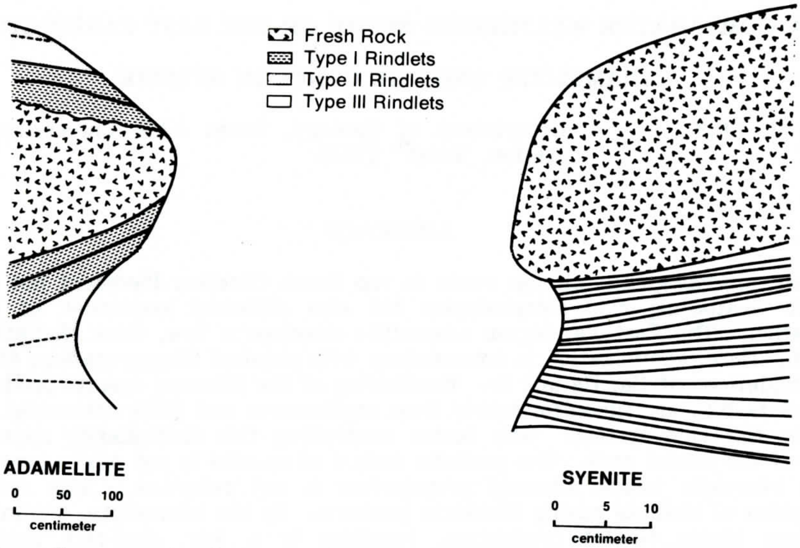

Figure 1. Cross-sectional views of the two typical weathering rind morphologies developed on plutonic igneous rocks in the North Carolina Piedmont. Adamellite and granite rind systems have profiles similar to that portrayed by the left sketch. Syenite and gabbro rind systems are represented on the right.

rock was devoid of metamorphic foliation; 3) the outcrop was preferably a nearly vertical exposure in order to expose as many rindlets as possible; and 4) an uninterrupted fresh-to-weathered sequence was visible. Weathering rind sequences were collected outward from the fresh rock core. As any individual outcrop commonly had more than one weathering rind profile, a problem arose as to which fresh rock core an outer rindlet belonged. In such cases, the curvature of outer rindlet contacts was compared to the curvature of the contact between the fresh rock and innermost rindlets. If the contacts were parallel, then the parent rock of the outer weathering rindlet was identified.

Powders of bulk samples were split into two parts, with one fraction to be used for X-ray fluorescence analysis according to the preparation scheme outlined by Baird (1961). The other split was dissolved using the HF-H_3BO_3 decomposition technique developed by Bernas (1968). Each sample was analyzed in duplicate for 17 elements. Sodium, K, Mg, Al and total Fe were performed on a Perkin-Elmer Model 303 atomic absorption unit. FeO analyses were performed by titrimetry (Schafer, 1966). Silica was determined colorimetrically by a method described by Shapiro (1974). Weight percent water was determined by loss on ignition, corrected for fixed humidity prior to heating as well as for oxidation of the sample's FeO. Analyses for Ca, Ti and Mn were performed by X-ray fluorescence using a standard vacuum path Norelco spectograph equipped with a W-tube and a LiF (220) diffracting crystal. All trace element analyses were also performed by X-ray fluorescence. Rubidium, Sr and Zr analyses were performed with a W-tube and flow proportional counter. Barium was analyzed using a flow proportional counter and Cr-tube. Zinc, Ni and Cu were analyzed using a scintillation counter as the detector and a Mo-tube as the primary X-ray source.

FAST FARRINGTON ADAMELLITE WEATHERING RINDS

The East and West Farrington igneous complex covers an area of about 140 square km and is located in Orange and Chatham Counties, North Carolina. Fullagar (1971) determined the age of the complex as 519 $\pm$48m.y. Wagener (1964) found the rocks of the East Farrington complex to be gradationally zoned with the center portion of the stock primarily consisting of medium-grained leucogranodiorite and the border rocks being finer grained and having more K-feldspar than the center. Two weathering rind profiles were sampled on a low relief road cut on Manns Chapel Road, Chatham County.

Weathering Rind Morphology

There are two morphologically distinct sequences in weathering rind systems of the East Farrington adamellite. Adjacent to the fresh rock core are the innermost rindlets of the Type I morphology (Figure 1). These rindlets are indurated and retain the textural relationships of the fresh rock. Hand specimens show plagioclase altered to whitish clay minerals and local limonite stains confined to rims of mafic minerals. These innermost rindlets are least altered and these youngest rindlets grade into Type II rindlets at distances of 0.3 to 0.7 m from the fresh rock contact.

The outermost rindlets are non-indurated sandy rubble and are categorized as Type II rindlets. Embedded in a matrix of silty sand are pebbles of rock fragments. Borders between individual rindlets are diffuse and are commonly lost between 1 and 1.5 m from the fresh rock contact. Thicknesses of individual rindlets are variable, ranging from 0.2 to 0.7 m. Weight percent of the clay fraction of these rindlets ranges from 10 to 14 percent (Table 1).

Mineralogical Stabilities

Quartz, perthitic K-feldspar and plagioclase volumetrically account for about 20, 30 and 45 percent of the rock, respectively. Magnetite, ilmenite, pyrite, chloritized biotite, zircon, apatite and epidote are minor accessories. Maximum grain sizes of the major phases range from 0.8 to 1.2 mm, and they are set in a fine groundmass consisting of small intergrowths of quartz and K-feldspar. Plagioclase is subhedral and locally covered with small amounts of clay minerals. Biotites are partially altered to chlorite. The alterations of biotite and plagioclase plus the presence of epidote suggest deuteric alteration of the East Farrington complex (Wagener, 1964).

A well-developed weathering rind profile commonly contains two or more rindlets of Types I and II. Thin sections were made of two adjacent Type I rindlets in the East Farrington profile. Sample D2 was taken from the freshest Type I rindlet which is 0.3 m thick and is in direct contact with the parent rock. Sample D4 is texturally similar to D2, yet visibly more altered. The inner contact of D4 is with D2, and beyond its outer contact is a clay-silt rind of Type II morphology.

In D2, both plagioclase and perthitic K-feldspar are partially altered to clay minerals. Twinning planes of plagioclase are partially obscured by clay minerals. The iron-bearing epidotes and chloritized biotites are the most extensively altered minerals. Emanating from these minerals are channels that are partially filled with limonitic material (Figure 2). Initially, the channel thicknesses are about 0.06 mm, but commonly pinch out at distances 1 to 2 mm away from the altered minerals. The channels serve as conduits for incoming pore water and as outlets for dissolved alteration products. These channels connect centers of maximum chemical alteration, the chloritized biotite and epidote. A few channels are filled with material that gives no hint of crystallinity upon petrographic examination. This material is optically

Table 1. Weight percent of clay-sized fraction in selected weathering rind samples of the East Farrington adamellite (Efa) and the Concord syenite (Cs).

Sample	Rind Type	Weight percent of clay fraction *
EFa D2	I	3.7
EFa D4	I	4.8
EFa D6	II	11
EFa D7	II	14
Cs A2	inner rindlet	0.6
Cs A4	outer rindlet	1.4
Cs A6	talus	4.7

*procedures for determining weight percent of the < 2 μ fraction were patterned after Folk (1968).

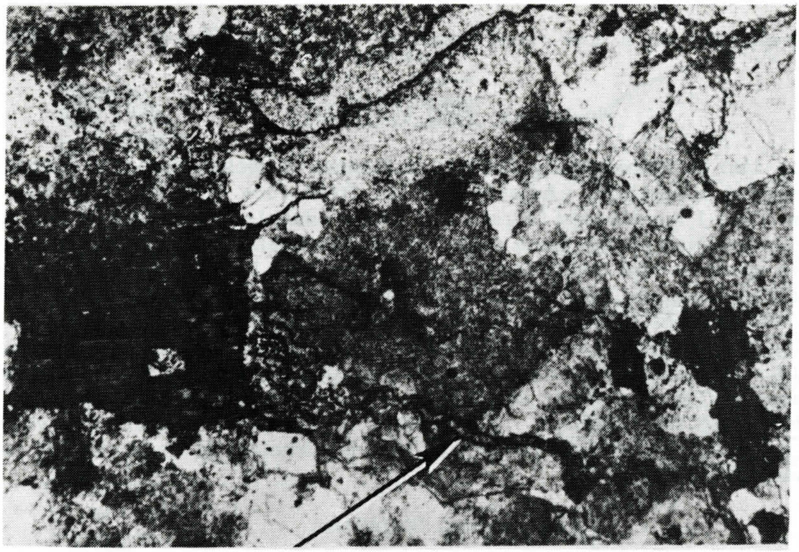

Figure 2. Photomicrograph (in plane light) showing a limonite-filled channel (pointed to by arrow) emanating from altered biotite to the left. The channel cuts through plagioclase, K-feldspar and quartz. Long axis of the photo is 2.7 mm.

isotropic and is thus believed to be amorphous. As these channels are in the vicinity of quartz grains, the channel fill is thought to be amorphous silica.

Surfaces of plagioclase and K-feldspar in sample D4 have a higher proportion of clay minerals than feldspars from the fresher, inner rindlet. The channel system previously described is more extensive in this sample and greater lengths of the channels are filled with limonite. In sample D2, quartz grains are broken by small channels (0.05 mm wide), and channels are filled with amorphous silica or limonite stain. Further physico-chemical attack of quartz is evidenced in outer rindlets. Hand picked quartz from sandy rubble typical of Type II rindlets can be broken with one's fingers. Weight percent of clay-sized material of both these Type I rindlets lies between 3 and 5 percent (Table 1). Oriented and non-oriented mounts of the $< 2\mu$ fraction in Type I rindlets gave only broad X-ray diffraction patterns, indicative of the non-crystalline nature of the clay minerals. In contrast, the $< 2\mu$ fraction of the outermost clay silt rindlets of Type II morphology showed a moderately crystalline dehydrated halloysite.

Elemental Distributions

Chemical Trends

Figures 3, 4 and 7 show elemental percentages of a representative weathering rind profile from the East Farrington adamellite and the Concord syenite. Analyses for all profiles are listed in Table 2. Weathering profiles B and D are separated by only 5 meters such that the elemental distributions discussed below for profile B in Figures 3 through 7 also hold for profile D. Their similar behavior is reflected in their compositions listed in Table 2.

Plagioclase from the adamellite profile constitutes between 40 and 50 modal percent of the rock and is the major Na- and Ca-bearing phase. The release of Ca and Na is thus attributed to the breakdown of plagioclase. Plagioclase in outer Type I rindlets is barely recognizable in thin section, but it does retain its grain boundaries. Leaching of alkalis from plagioclase in this stage of alteration is detectable, though not pronounced. Advanced stages of chemical attack occurs only after a rindlet loses its physical coherence. This is evidenced in the Type II rindlet samples showing severe depletions of Ca and Na in these samples (Figure 3).

Table 2. *Chemical analyses of samples from weathering rind profiles representing the East Farrington adamellite (profiles B and D) and the Concord syenite (profiles A and B). Major elements are expressed in weight percent and trace elements as ppm. In those cases where FeO was not analyzed (N/A), the total iron is expressed as Fe_2O_3.*

Sample	cm from fresh rock Contact	SiO_2	Al_2O_3	TiO_2	FeO	ΣFe_2O_3	MnO	CaO	MgO	K_2O	Na_2O	H_2O	Cu	Zn	Ni	Ba	Rb	Sr	Zr
B1	0	71.18	14.03	0.40	0.52	2.14	0.07	0.93	0.52	3.92	4.99	0.89	<1	86	4	762	81	197	275
B2	21	72.68	14.26	0.58	0.50	2.36	0.10	0.72	0.44	4.00	4.46	1.24	3	77	5	771	70	227	336
B3	44	71.30	14.92	0.50	0.44	2.07	0.08	0.61	0.41	3.82	4.51	1.57	3	77	7	750	75	217	277
B4	59	73.84	13.65	0.59	0.47	2.54	0.07	0.47	0.47	4.34	4.15	1.05	5	76	5	805	76	168	362
B5	88	71.71	15.24	0.52	0.23	2.32	0.08	0.55	0.42	3.94	4.15	2.07	2	81	6	758	74	188	319
B6	103	49.31	29.74	0.66	0.19	5.56	0.02	0.11	0.34	1.12	0.47	12.05	7	75	11	241	76	54	130
B7	141	48.12	31.04	0.79	0.05	5.67	0.03	0.05	0.38	1.05	0.19	12.19	6	90	17	244	90	48	127
D1	0	70.66	14.68	0.47	N/A	2.14	0.08	0.94	0.53	3.81	5.24	0.84	2	71	2	709	68	261	295
D2	21	72.29	14.99	0.43	N/A	2.07	0.08	0.79	0.46	3.90	5.00	0.86	1	69	6	851	65	295	280
D3	35	72.68	14.78	0.51	N/A	2.25	0.08	0.88	0.47	3.88	4.86	1.23	<1	65	6	748	69	256	321
D4	62	71.36	15.54	0.44	N/A	1.93	0.08	0.72	0.37	3.78	4.70	1.63	2	44	3	773	68	214	254
D5	88	70.13	16.85	0.36	N/A	2.89	0.06	0.32	0.37	3.95	3.05	3.35	4	49	7	832	80	139	254
D6	115	46.21	32.37	0.76	N/A	5.72	0.02	0.18	0.39	0.94	0.24	13.72	7	78	16	240	81	57	101
A1	0	59.23	17.34	1.25	2.68	6.16	0.16	3.30	1.65	3.84	6.35	0.18	12	118	10	1380	16	418	603
A2	9	55.99	15.65	2.00	3.58	8.24	0.27	4.50	2.44	3.46	5.73	0.39	8	159	8	1270	13	369	679
A3	29	57.68	16.38	1.70	2.91	8.09	0.22	4.13	2.15	3.41	5.98	0.37	11	107	3	1360	10	399	987
A4	44	60.10	17.77	1.25	2.45	6.36	0.17	3.65	1.53	3.44	6.40	0.35	10	79	7	1370	8	424	694
A5	71	61.73	17.35	0.98	1.49	4.66	0.13	2.86	1.21	3.91	6.71	0.46	13	73	8	1470	10	461	578
A6	85	59.32	17.67	1.43	2.00	6.85	0.18	3.11	1.45	3.60	6.01	0.50	13	96	11	1290	8	411	826
A-talus		62.04	18.58	0.90	N/A	4.58	0.13	2.80	0.94	3.98	6.65	0.35	5	46	4	1410	12	397	344
B1	0	59.96	16.98	1.49	N/A	7.01	0.19	3.78	1.93	3.61	6.09	0.24	5	123	7	1350	14	417	875
B2	21	55.97	15.73	2.16	N/A	8.93	0.28	4.38	2.59	3.62	5.54	0.12	9	144	7	1230	15	350	1150
B3	30	60.34	17.97	1.29	N/A	5.96	0.17	3.42	1.46	3.67	6.43	0.54	8	86	7	1400	12	361	527
B4	67	58.14	16.83	1.62	N/A	7.68	0.20	3.96	2.04	3.53	5.96	0.22	10	103	7	1300	14	402	852

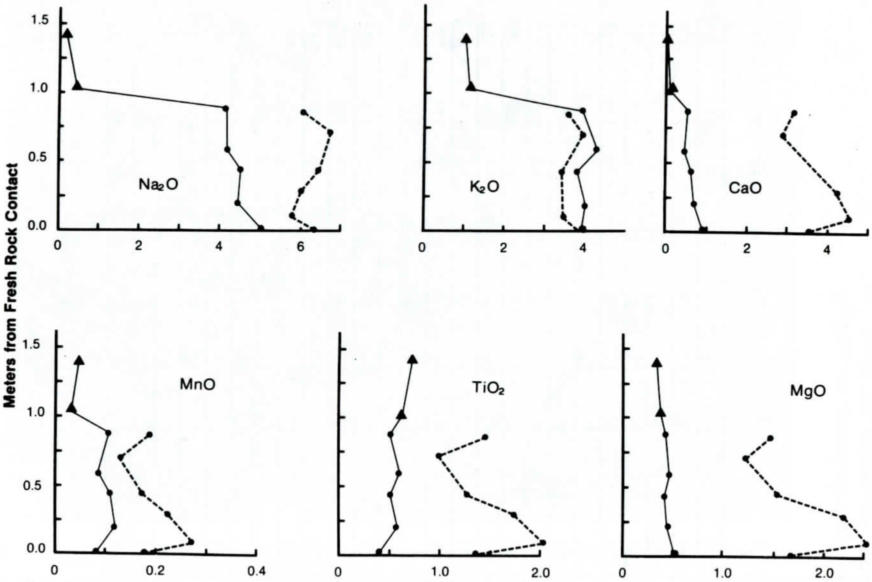

Figure 3. Distribution of weight percents of six major elements versus distance from fresh rock contact. The fresh rock is represented at the bottom of each profile. Samples of profile A (excluding A-talus) of the Concord syenite are connected with dashed lines and solid lines connect samples of profile B of the East Farrington adamellite. In this and subsequent figures, samples depicted by triangles in the adamellite profile are Type II rindlets.

The uniform concentration of K in Type I rindlets testifies to the stability of K-feldspar in the inner system. X-ray diffraction of clay-rich, outer, Type II rindlets indicates small amounts of K-feldspar, which probably accounts for the 1 percent K_2O in these extremely altered samples.

Magnesium shows little depletion. Harriss and Adams (1966) studied the chemistry of soil profiles over two selected granites in Georgia and Oklahoma and found Mg depleted over soils of those rocks. Johnson and others (1968), and Dennen and Anderson (1962) also found Mg depleted in soil profiles developed over granitic rocks. Chloritized biotite is the only major Mg-bearing mineral in the profile and thin sections show this mineral altering as early as the innermost weathering rindlets. Evidently, the degradation of this mica does not result in significant release of magnesium. This element is probably incorporated into clay structures.

Concentration of iron remains fairly constant in Type I rindlets (Figure 4). Thin sections of samples from inner rindlets show marked alteration of Fe-bearing minerals and the subsequent precipitation of the Fe as amorphous limonite stains (Figure 2). Thus, iron is liberated from lattice sites of Fe-bearing minerals but immediate oxidation in the vicinity of the alteration decreases the solubility of the Fe and causes precipitation. Supporting chemical evidence for this assertion is presented in Figure 5 which shows that, with increasing alteration, the FeO/Fe_2O_3 ratio decreases. Secondary ferric oxides are thus produced at the expense of ferrous oxides during alteration. The residual 0.35 percent FeO in clay-silt rindlets of profile B is probably due to the stability of magnetite. Silt-sized magnetite was identified in the outermost clay-silt rindlets. The three-fold increase of total Fe in the outermost rindlets in an artifact caused by removal of the more mobile elements.

Titanium does not show much variation in concentration within profile B. The increase in Ti in the outermost rindlets is likely attributed to the stability of ilmenite in the silt fraction of these samples.

Most of the Mn in the parent rocks is probably concentrated in biotites. Manganese released from a mineral in an oxidizing environment with a basic pH should precipitate in the form of hydrous Mn (IV) oxides (Krauskopf, 1957). Krauskopf (1967)

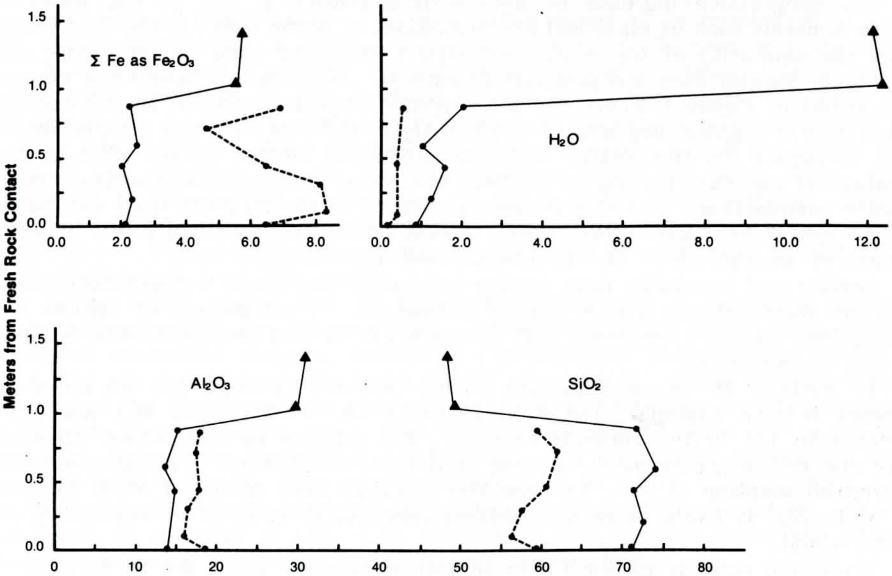

Figure 4. Distribution of weight percents of water, silica, alumina and total iron expressed as Fe_2O_3 versus distance from fresh rock contact for profile B of the adamellite and profile A of the syenite.

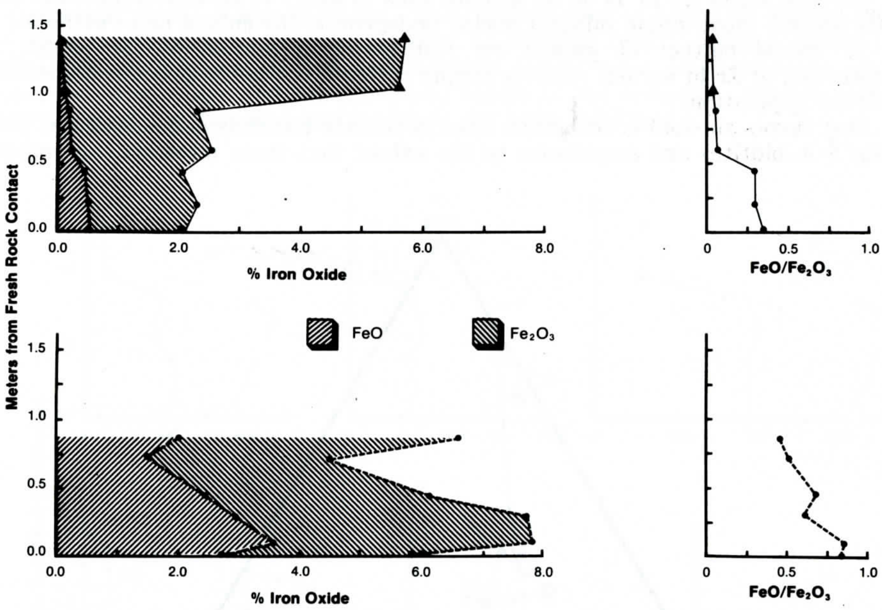

Figure 5. A plot of the distribution of FeO and Fe_2O_3 in profile B of the adamellite (top) and profile A of the syenite (bottom). Note that with increased weathering the FeO/Fe_2O_3 ratio decreases. This is a surer indication of weathering severity than total iron distribution within the profile.

states that Fe commonly precipitates before Mn in weathering solutions filtering through igneous rocks. He attributed this to a gradual rise in pH of the weathering solution which allows Fe compounds to reach their solubility limit before Mn compounds. The small depletion of Mn in comparison to the apparent enrichment of Fe in outer rindlets could be explained by this mechanism.

The progressive increase in H_2O with alteration is due to the formation of hydrous minerals such as clays and hydrous oxides of ferric iron. In the East Farrington profile the similarity of the Al_2O_3 and H_2O curves, and their mirror image with the SiO_2 curve, suggest clay and products (Figure 4). Variation of these three components is presented in Figure 6 where the three components are summed to 100 percent and plotted on a triangular diagram. The SiO_2-Al_2O_3-H_2O diagram was utilized by Goldich (1938) to depict the progressive kaolinization of the Morton gneiss. The progressive alteration of the East Farrington rindlets also shows end products trending toward the kaolinite composition. The clay mineral identified in the clay-silt rinds was halloysite, a polymorph of kaolinite (Grim, 1968). Grant (1975) found kaolinite and halloysite as products of weathering of the Panola adamellite in Georgia.

Barium and potassium have similar ionic radii and hence the weathering behavior of barium should closely follow that of potassium. A comparison of Figures 3 and 7 indicate that barium's depletion with alteration of K-feldspar and biotite is similar to the fate of potassium.

In contrast to the K depletion in the clay-silt rindlets, the Rb concentration increases in these rindlets. The K/Rb ratio for the fresh rock is 400, and this ratio decreases to 125 in the clay-silt rindlets. The relative enrichment of Rb over K is either due to the preferential leaching of K from biotites and feldspars and/or to the preferential sorption of Rb. Because the hydrated ionic radius of Rb is smaller than that of K, Rb^+ is likely to be more effectively sorbed by clays in weathering profiles (Mason, 1966).

Strontium substitutes for Ca in silicate minerals. Thus, the Sr curve in Figure 7 should parallel the Ca curve in Figure 3. Comparison of the two elements indicates similar behavior, even though acid-soluble apatite contains Sr and Ca in different stoichiometric proportions than plagioclase.

The vast majority of Zr in an igneous rock is likely to be concentrated in zircons. Zircons are the most stable mineral during pedogenesis (Krumbein and Pettijohn, 1938). Thus Zr should neither be gained nor lost during formation of the profile. The concentration of Zr in various rindlets simply reflects the heterogeneous distribution of the zircon population.

Zinc favors six-fold coordination sites in silicate minerals and substitutes for Fe^{+2} and Mg^{+2} in biotites and amphiboles to the extent that these minerals can contain 500

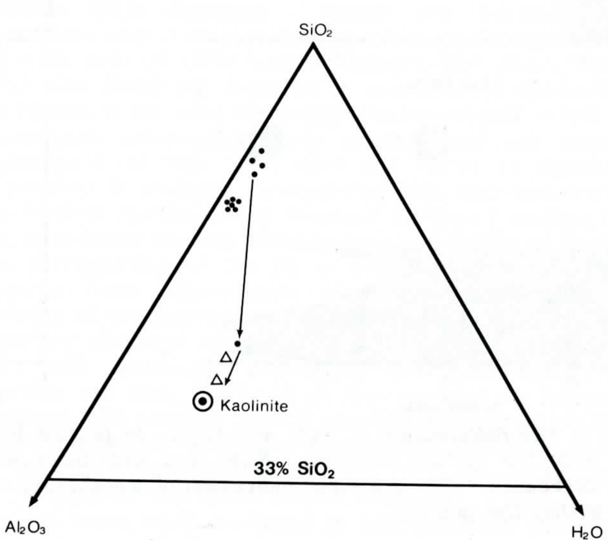

Figure 6. Weight percents of silica, alumina and water for each sample are normalized to 100% and plotted on this ternary diagram. Fresh and weathered samples of syenite profile A plot as a tight group, indicating little clay formation during weathering. Relative position of the adamellite samples in profile B are indicated by arrows. The kaolinization trend is clearly evident. Triangular points indicate Type II samples.

to 1000 ppm Zn (Wedepohl, 1972). Zinc also favors four-fold sites in spinels such that zinc's substitution for Fe^{+2} in magnetites commonly results in Zn concentrations of over 2000 ppm in this mineral. The relative constancy of Zn concentration in the two East Farrington profiles is attributed to the stability of Zn-bearing magnetite.

In igneous rocks Cu tends to concentrate in sulfide phases. Trace amounts of pyrite were identified in thin sections of the fresh adamellite. Copper must be released to the weathering rind profile because no pyrite was observed in thin sections of outer rind material. Once released, Cu tends to remain within the profile as Figure 7 shows this element retains its concentration levels in outer rinds. Copper's enrichment in the clay-silt rindlets may be due to preferential sorption. Short (1958) found Cu enrichment in the clay fraction of soil profiles overlying granites in Colorado and Missouri. Copper's relative enrichment could also be an artifact caused by removal of other elements from the profile.

Butler (1953) stated that Ni frequently follows Mg in magmatic cycles where sulfide concentrations are low or absent. He found that the Mg/Ni ratio decreased in weathered adamellite samples, indicating a preferential concentration of Ni. Butler found that silt from this profile had a Mg/Ni ratio of 440. Butler's observation on the behavior of the Mg/Ni ratio is also seen in the East Farrington weathering rinds. The Mg/Ni ratio decreases from about 1200 in the fresh rock to about 150 in the clay-rich Type II rindlets of the East Farrington profiles. The only major Mg-bearing mineral in the fresh rock is biotite. The relative increase of Ni in the outer rindlets cannot be due to biotite stability as biotite is completely absent in Type II rindlets. Short (1958) also found Ni enriched in the $< 2\mu$ fraction of soil samples overlying granites and invoked a sorption mechanism to explain this enrichment.

CONCORD SYENITE WEATHERING RINDS

The Concord gabbro-syenite complex is intruded into granite-gneiss country rock in Cabarrus County, North Carolina. The Concord syenite forms an arcuate pattern on the gabbro periphery. Previous studies by Morgan (1963), Cabaup (1969), Fullagar (1971), Bell (1960) and Butler and Ragland (1969) have concerned the geophysical properties, origin, age and petrochemical nature of the complex. Studies pertaining to weathering of the Concord syenite have not been published.

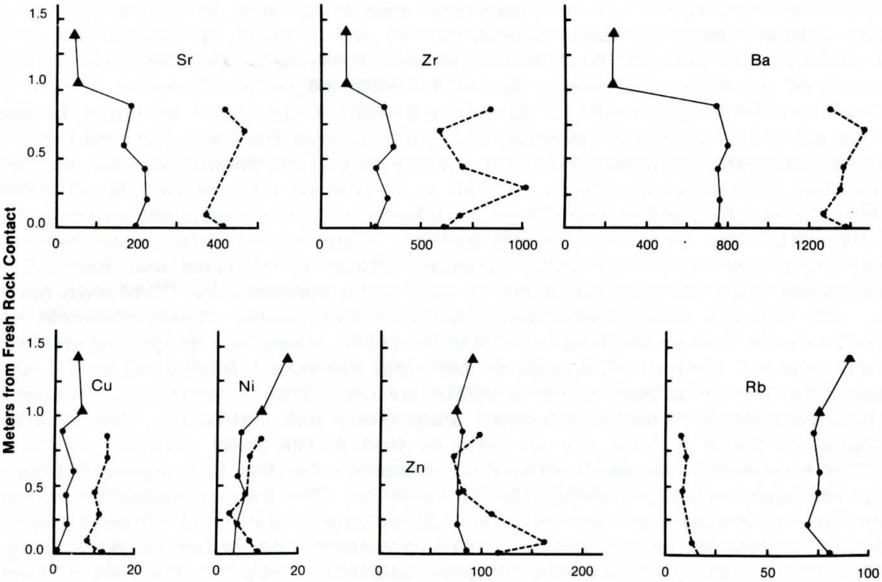

Figure 7. Distribution of trace elements (expressed as ppm) for profile B of the adamellite and profile A of the syenite.

In hand specimen, the Concord syenite is a pink colored, coarse-grained rock in which phenocrysts of K-feldspar can exceed 3 cm in maximum dimension. Thin sections show the large, pink phenocrysts to be perthitic intergrowths. In fact, the bulk of the entire rock is a maze of perthites, antiperthites and myrmekitic intergrowths with subordinate amounts of ferromagnesian minerals.

Weathering Rind Morphology

Within a gravel pit in the Concord syenite were found large > 10 meters in diameter) boulders having as many as 30 weathering rindlets. Although the term 'boulder' implies transport, this term can be employed to denote large in-place rock masses rounded by weathering (Stokes and Varnes, 1955). Weathering rinds were best developed on the flanks of these in-place boulders, and few to no rindlets were found on top of the boulders. In-place boulders at the quarry edge had extensive rinds that were peripheral about the core of fresh syenite.

Weathering rinds of the Concord syenite represent a radical departure from rind morphologies of the East Farrington adamellite. The syenite was found to have only one rind morphology, but this rind morphology persisted to produce a proliferation of rindlets of the same type (Figure 1). The rindlets are clay deficient. Outer, more altered rindlets contain less than 2 percent clay-sized material (Table 1). All rindlets are indurated and are 0.5 to 2 cm thick. The width of the curviplanar spallation cracks between the rindlets is less than 0.5 mm in the outer zones. These outer rindlets break off from the boulder as the spallation crack widens. Talus at the foot of the boulders consists of rock fragments contained within a silty-sand matrix, which contains less than 5 percent clay-sized material (Table 1).

Mineralogical Stabilities

Perthitic intergrowths volumetrically constitute between 80 and 90 percent of the fresh Concord syenite. Both perthites and antiperthites are present, the former being the dominant type. Maximum dimension of the perthite grains is 2 to 3 cm. Quartz is present in amounts less than 10 percent and occurs either as grains surrounded by perthite, individual anhedra between intergrowths or intergrowths with both feldspars. Magnetite is the dominant opaque mineral, and along with ilmenite accounts for 1 to 2 percent of the rock. A clinopyroxene exhibiting blue to green pleochroism is aegirine-augite. Many of these clinopyroxenes are mantled by hornblendes, and both these minerals are present in amounts less than 5 percent. Biotites, constituting 1 to 3 percent of the rock, are usually in contact with magnetite; however, a few biotites are found enclosed by perthites. Zircon and apatite are found as minor accessories.

Sample A3 is a rindlet collected about 0.3 m from the fresh rock contact. A thin section of this sample shows that most pyroxenes and amphiboles are so intensely Fe-stained that their cleavage planes, as well as their grain boundaries, are often obscured by these stains. Emanating from these weathered mafic minerals are solution channels (less than 0.05 mm wide) filled with limonite stain. These stains are restricted to borders peripheral to the perthitic matrices (Plate 3b of Fritz and Ragland, 1980). Further away from the altered mafic minerals, the channels are filled with amorphous silica, with limonite concentrated only on the channel walls. These channels coalesce to produce wider channels (about 0.1 mm in width), along which spalling occurs. The channels connect centers of maximum chemical alteration (mafic minerals) and they are not effective in attacking the perthite matrix. Thus, alteration occurring in this sample is restricted to mafic minerals. Plagioclase and microcline, housed within the enveloping perthitic matrix, are as fresh as that in the fresh rock.

The end-product in weathering rind sequences for the East Farrington system is a clay-rich layer developed within the rind system. The syenite possesses no clay-rich rindlet in its weathering rind system. In contrast, the most altered material in weathered syenite is not a chemically altered rindlet, but rather talus resulting from physical disintegration of adjacent in-place boulders. Talus at the foot of rind-laden boulders consists of pebble-size rock fragments embedded in a non-indurated matrix of silty sand. Although the talus is not a part of the weathering rind sequence, it represents a stage in the physical and chemical breakdown of Concord syenite. A chemical analysis of a talus sample from profile A shows concentrations similar to that in the fresh rock (Table 2). A thin section of the impregnated talus shows the sub-angular rock fragments to be composed almost entirely of the perthitic intergrowths (Plate 5 of Fritz and Ragland, 1980). The exsolved plagioclase and microcline contained within the pebble are as fresh as that in the parent rock. Hornblende and biotite retain their identity because they too are enclosed by the perthitic intergrowths comprising the rock fragments. These observations suggest the perthitic intergrowths constitute a very impregnable structure capable of preventing pore water from attacking unstable minerals like hornblende housed within the matrix. All perthite rock fragments possess iron-stained rims of varying thickness (0.05 to 0.35 mm thick). This strongly suggests that the limonite-manifested channelization within an individual rindlet becomes so extensive that it creates islands of stable mineralogy (perthites) which later, when the rindlet disagregates, form the rock fragments in the talus.

Elemental Distributions

In the East Farrington adamellite, Ca and Na behave similarly, reflecting the breakdown of plagioclase. In the Concord syenite, Ca is concentrated in hornblendes as well as plagioclase. As thin sections show progressive breakdown of hornblende and marked stability of the plagioclase with increased weathering, the small Ca loss is due to alteration of the hornblende (Figure 3).

Strontium's lack of depletion in Figure 7 is explained by the fact that this element is mostly concentrated in plagioclases rather than in the less stable hornblende. This is borne out by strontium's partition in these two minerals. Mason (1966) reported that the partition coefficient of Sr between plagioclase and hornblende in granites is about 7.5.

Most of the Na is concentrated in plagioclase, but the pyroxene identified as aegirine-augite is also a Na-bearing mineral. The behavior of Na in the syenite profile reflects the heterogeneous distribution of stable ubiquitous plagioclase. The loss of Na due to the breakdown of the minor amount of aegirine is not detectable.

The small decrease of K in inner to mid rindlets is probably due to leaching of K from biotites which thin sections of an inner rind sample reveal as being altered. The relative constancy of K concentration in the entire syenite profile is thus due to stability of the main K-bearing mineral, K-feldspar. The behavior of Ba as usual, closely follows that of K (Figures 3 and 7). Rubidium, an element whose chemical properties are similar to K, does not behave like its diadochic counterpart in this weathering rind system. An explanation is that the bulk of the Rb resides in the more unstable biotite rather than in the stable K-feldspar. Rubidium has a larger ionic radius than K and thus is more easily accomodated in high coordinated sites of minerals like biotite. Ragland and others (1968) found Rb (biotite)/Rb-(K-feldspar) in a Texas granite to be about 3. Mason (1966) reported a similar ratio for these two minerals in a California granite.

The most mobile elements of the adamellite profiles were Na and Ca. These reflected instability of plagioclase, the most unstable mineral in these profiles. In Concord syenite weathering rind profiles, Mg, not Na or Ca, is the most depleted element. It follows that Mg-bearing pyroxenes and amphiboles, not plagioclase, are the most unstable minerals in the syenite weathering system.

The erratic changes in total Fe concentration in Figure 4 reflect the heterogeneity of Fe-bearing minerals in the sampled rinds. Ferrous iron, a component of biotite, aegirine-augite and hornblende, is progressively lost from these minerals during weathering (Figure 5). The Fe^{+2} liberated from these minerals is oxidized and precipitated as limonite stain in channels.

The distribution of Ti in the profiles is erratic. Titanium can be present in significant concentrations in biotites (Deer and others, 1966). If altered biotites of the syenite also retain their Ti, then the erratic distribution of this element in the syenite profile must reflect the heterogeneous distribution of biotite and ilmenite. The same argument is also made for the Zr distribution since that element is concentrated in zircons.

The small variations of SiO_2, Al_2O_3 and H_2O indicate very little clay formation in the rinds. Weight percent of H_2O in all rindlet samples is less than 0.50 percent.

All samples plot as a tight group on the SiO_2-Al_2O_3-H_2O diagram, indicating no trend toward kaolinization in this weathering rind profile (Figure 6).

The progressive loss of Zn toward outer rindlets is due to instability of Zn-bearing amphiboles and biotites. Biotites, and especially hornblendes, are highly altered in the middle rind samples.

DISCUSSION AND CONCLUSIONS

The development of solution channels plays a major role in rindlet development because the channels are planes of weakness along which parting (rindlet development) occurs. In weathering rinds of the two described lithologies, channelization precedes the physical breakdown of the rock. This is evidenced by Plate 5 of Fritz and Ragland (1980) which shows the borders of a perthitic pebble rimmed with limonite stain. If parting primarily occurs along channel boundaries, then it is reasonable to expect that rocks having many weathering rindlets (for example, syenites) should have a higher density of channels than rocks possesing fewer weathering rindlets. Table 3 shows the channel density and mean channel width of solution channels in the two studied lithologies. The studies were performed on thin sections of the innermost weathering rind samples of these rocks in order to minimize bias caused by differing rindlet maturity. Table 3 shows that channel density varies inversely with mean channel width. Thus, granitic rocks have fewer channels per unit area but their channels are wider than those in the syenite.

Table 3. Thin sections observations showing differences of channel density and mean width of channels between the East Farrington adamellite (EFa) and the Concord Syenite (Cs).

Lithology	Number of channels per square millimeter	Mean channel width
Efa	2.5	0.08 mm
Cs	25.6	0.03 mm

This dissimilarity is explained by differences in rock texture. The syenite has a high degree of mineral intergrowths that present a relatively impermeable matrix to percolating pore water solutions. Channel development in this lithology is affected by texture in that a large number of narrow channels result. That is, the interlocking nature of the minerals effectively prevents large, through-going channels from forming. Instead, numerous, small channels develop when pore water meets the textural impasse of the perthite matrix. In contrast, large channels result in granitic rocks because the texture of these rocks is more "open". That is, few mineral intergrowths are present to bar the development of large channels. Granites are some of the most permeable of igneous rocks, having permeabilities as high as 4600 nano-Darcies (Ohle, 1951).

Clay mineral synthesis plays a major role in rindlet development in the adamellite granitic rocks but only a minor role in syenite rindlets. Fritz and Ragland (1980) discussed the role of rock texture in the development of weathering rind morphologies and state that plagioclase plays a key role in determining the mode of weathering on rind systems. This mineral is very susceptible to hydrolysis-induced kaolinization reactions which results in a creation of void space within the rock. The creation of this void space does not permit the continual propagation of the solution channel within the rock's interior because the stress at the crack's tip is dissipatated at the void (Neuber, 1958). Since rindlet boundaries are manifested on a micro-scale by coalescence of solution channels, the blunting of solution crack propogation interferes with the production of the geometric onion-skin morphology so typical of classical spheroidal weathering. The result is a few, thick rindlets that are clay rich as seen in the adamellite profile.

In contrast, the Concord syenite is a rock whose perthite texture is relatively impregnable to the invasion of solution channels. Crack development is not hindered and rindlet production is prodigious. In the absence of water-bearing solution channels, the latently unstable feldspars (especially plagioclase) in the perthite retain their identify--even in the talus pile. For this reason, the traditionally mobile elements like

Na, Ca, and Sr are not depleted. Moreover, the texturally protected feldspars produce little clay such that alumina, silica and water concentrations vary little within the weathering profile. Thus, parent rock texture can control not only the weathering rind morphology but also the elemental distribution within a weathering profile.

REFERENCES

Baird, A., 1961, A pressed-specimen die for Norelco Vacuum-path X-ray spectrograph: Norelco Reptr., v. 8, p. 108.

Bell, H., 1960, A synthesis of geologic work in the Concord area, North Carolina: U.S. Geol. Survey Prof. Paper 400-B, p. B189-B192.

Bernas, B., 1968, A new method for decomposition and comprehensive analysis of silicate rocks by atomic absorption spectrometry; Analytical Chem., v. 40, p. 1682-1686.

Butler, J. R., 1953, The geochemistry and mineralogy of rock weathering. (I) The Lizard area, Cornwall: Geochim. et Cosmochim. Acta, v. 4, p. 157-178.

Butler, J. R., and Ragland, P. C., 1969, A petrochemical survey of plutonic intrusions in the piedmont, Southeastern Appalachians: Contr. Mineralogy and Petrology, v. 24, p. 164-190.

Cabaup, J., 1969, Origin and differentiation of the gabbro in the Concord Ring Dike, North Carolina Piedmont (M.Sc. thesis): Chapel Hill, University of North Carolina, 42 p.

Deer, W. A., Howie, R. A. and Zussman, J., 1966, An Introduction to the Rock Forming Minerals. John Wiley & Sons.

Dennen, W., and Anderson, P., 1962, Chemical changes in incipient rock weathering: Geol. Soc. America Bull., v. 73, p. 375-384.

Folk, R., 1968, Petrology of Sedimentary Rock: Austin, Texas, Hemplhill's, 197 p.

Fritz, Steven J., 1976, Physical and chemical characteristics of weathering rinds from several plutons in the North Carolina Piedmont, Ph.D. dissert., University of North Carolina, 223 p.

Fritz, Steven J., and Ragland, Paul C., 1980, Weathering rinds developed on plutonic igneous rocks in the North Carolina Piedmont, Am. Jour. Sci., v. 280: p. 546-559.

Fullagar, P., 1971, Age and origin of plutonic intrusions in the piedmont of the Southeastern Appalachians: Geol. Soc. America Bull., v. 82, p. 2845-2862.

Goldich, S., 1938, A study in rock weathering: Jour. Geology, v. 46, p. 17-58.

Grant, Willard H., 1975, Chemical weathering of Panola adamellite with special reference to apatite: Southeastern Geology, v. 17, pp. 15-25.

Grim, R., 1968, Clay Mineralogy: New York, McGraw-Hill, 596 p.

Harriss, R., and Adams, J., 1966, Geochemical and mineralogical studies on the weathering of granitic rocks: Am. Jour. Sci., v. 264, p. 146-173.

Johnson, N., Likens, G., Bormann, F., and Pierce, R., 1968, Rate of chemical weathering of silicate minerals in New Hampshire: Geochim. et Cosmochim. Acta, v. 32, p. 531-545.

Krauskopf, K., 1957, Separation of manganese from iron in sedimentary processes: Geochim. et Cosmochim. Acta, v. 12, p. 61-84.

Krauskopf, K., 1967, Introduction of geochemistry: New York, McGraw-Hill, p. 721.

Krumbein, W. C., and Pettijohn, F. J., 1938, Manual of Sedimentary Petrography, D. Appleton-Century Co: New York, p. 549.

Mason, B., 1966, Principles of geochemistry: New York, John Wiley and Sons, 329 p.

Morgan, B., 1963, A gravity study of a ring dike near Concord, North Carolina (M.Sc. thesis): Chapel Hill, University of North Carolina, 78 p.

Neuber, H., 1958, Theory of notch stresses: principles for exact calculation of strength with reference to structural form and material: Berlin, Springer Publishers, 293 p.

Ohle, E., 1951, The influence of permeability on ore distribution in limestone and dolomite: Econ. Geology, v. 46, p. 667-706.

Ragland, P., Billings, G., and Adams, J., 1968, Magmatic differentiation and autometasomatism in a zoned granitic batholith from central Texas, J.S.A.: *in* Ahrens, L., ed., Origin and distribution of the elements: Oxford, Pergamon Press, p. 795-825.

Schafer, H., 1966, The determination of iron (II) oxide in silicate and refractory minerals: Analyst, v. 91, p. 763-790.

Shapiro, L., 1967, Rapid analysis of rocks and minerals by a single-solution method: U.S. Geol. Survey Prof. Paper 575-B, p. B187-B191.

Short, N., 1958, Behavior of trace elements in rock weathering and soil formation (Ph. D. dissertation): Cambridge, Massachusetts Institute of Technology, 218 p.

Stokes, W. L., and Varnes, D. J., Glossary of Selected Geologic Terms, Peerless Printing Co: Denver, 165 p.

Wagener, H., 1964, Areal modal variation in the Farrington Igneous Complex, Chatham and Orange Counties, North Carolina (M.Sc. thesis): Chapel Hill, University of North Carolina, 51 p.

Wedepohl, K., 1972, Handbook of geochemistry: v. 3, Berlin, Springer-Verlag.

THE ABUNDANT OCCURRENCE OF THE MIDDLE MIOCENE SAND DOLLAR *ABERTELLA ABERTI* IN THE HAWTHORNE FORMATION OF FLORIDA

MICHAEL L. MCKINNEY Department of Geology and Geophysics, Yale University
New Haven, Connecticut 06511

ABSTRACT

The presence of numerous fossils of *A. aberti* in the Hawthorne Formation of central and south Florida are reported for the first time. This represents a significant geographic range extension for this middle Miocene clypeasteroid which seems to have had an unusually wide range of environmental tolerances.

INTRODUCTION

The irregular echinoid *Abertella aberti* (Conrad) was first reported in the U.S. in 1842 though it was assigned to the genus Scutella (Conrad, 1842). It was assigned its current genus and family name by Durham (1953). In his major work on Cenozoic echinoids, Cooke (1959) reported its presence in the Choptank Formation (middle Miocene) of Maryland, some undesignated Miocene strata in North Carolina, and the Chipola Formation (middle Miocene) of north Florida. Kier (1983) has recently noted its occurrence in the Pungo River Formation (middle Miocene) of North Carolina.

I report here the presence of numerous fragments and whole specimens of *Abertella aberti* throughout the Hawthorne Formation of Florida, a middle Miocene unit which interfingers with the Chipola Formation in northern Florida and extends into southern Florida. Fragments of this species were noted in an exposure of the Hawthorne Formation in northern Florida by Wiliams, et al. (1977). I supplement that

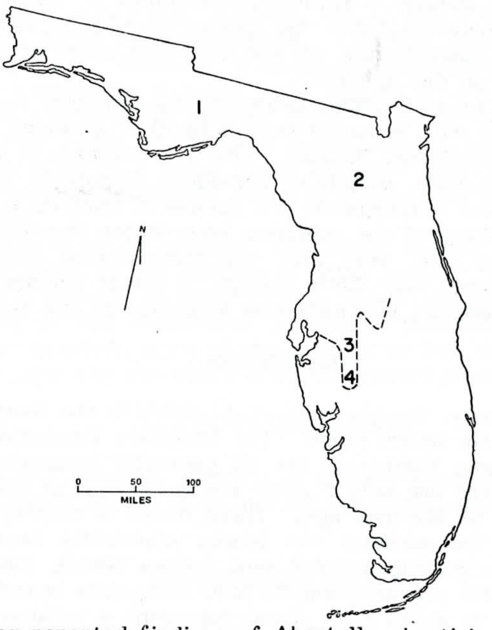

Figure 1. Map showing reported findings of Abertella aberti *in Florida: 1 = Chipola Formation in the Sopchoppy River area (Cooke, 1959), 2 = Hawthorne Formation in the western part of Alachua County (Williams, et al., 1977), 3 = Hawthorne Formation in the Polk County area in phosphate quarries around the city of Bartow, 4 = Hawthorne Formation in the Hardee County area exposed by erosion by the Peace River near the town of Zolfo Springs. Dashed line approximates the lowermost boundary of the exposed Hawthorne Formation.*

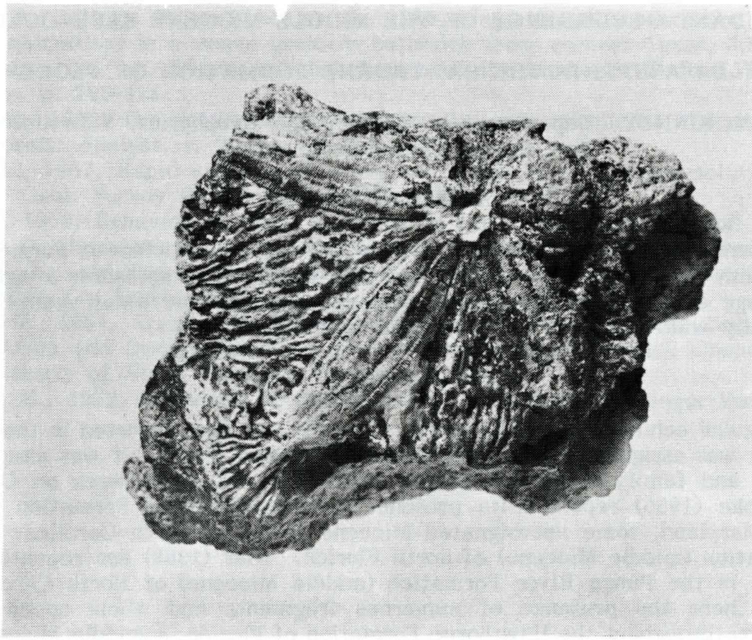

Figure 2. A typical ambulacral cast of A. aberti *common in the Hawthorne Formation of the Polk County area.*

notation by reporting the finding of numerous specimens at other places, far to the south, in the Formation indicating that the species may be found throughout the unit and is abundant in parts. I also discuss, for the first time, some general paleoecological and stratigraphic aspects of the species.

Figure 1 shows a map of Florida, indicating the previous findings of this fossil (sites 1 & 2) and the new ones reported here (sites 3 & 4) which were made by Mr. Charles E. Howlett of Casselberry, Florida. Site 3 is the area of Polk County where fragments of recognizable casts, usually of ambulacra (Figure 2), are abundant in the Hawthorne Formation where it is exposed in a number of quarries (e.g., IMC Phosphoria Mine) during phosphate mining of the overlying Bone Valley Formation. Site 4 is some 30 miles to the south of this, very near the southernmost extent of the exposed Hawthorne (Figure 1). Here, near Zolfo Springs, 3 intact specimens (e.g., Figure 3) were found, exposed by erosion of Hawthorne sediment by the Peace River.

DISCUSSION

Chronostratigraphically, the presence of *A. aberti* in the Hawthorne Formation is quite in agreement with its known range. The Choptank Formation, the Pungo River Formation, and the Chipola Formation are all generally acknowledged to also be of middle Miocene age. There are only 2 other known species of this genus and family (Abertellidae), both also of Miocene age. These occur in central America (Kier and Lawson, 1978). After the Miocene the family apparently became extinct, being displaced by northward migrating mellitid sand dollars (Smith, 1984).

Paleoecologically, this species seems to have been quite broadly adapted. For one thing, the 4 formations in which it is found represent a relatively wide variety of depositional environments. The Chipola Formation is a highly fossiliferous, argillaceous limestone in the area where Cooke (1959) reports the finding of *A. aberti*. Puri (1954) believes this formation was deposited in inner neritic conditions at a depth of about 110 m. Likewise, the upper limey beds of the Pungo River Formation, where this species is found (Kier, 1983), also seems to represent moderately deep water, from 70-150 m (Gibson and Buzas, 1973). In contrast, the Choptank Formation in Maryland which contains the species, has little calcareous content, being composed largely of silts and

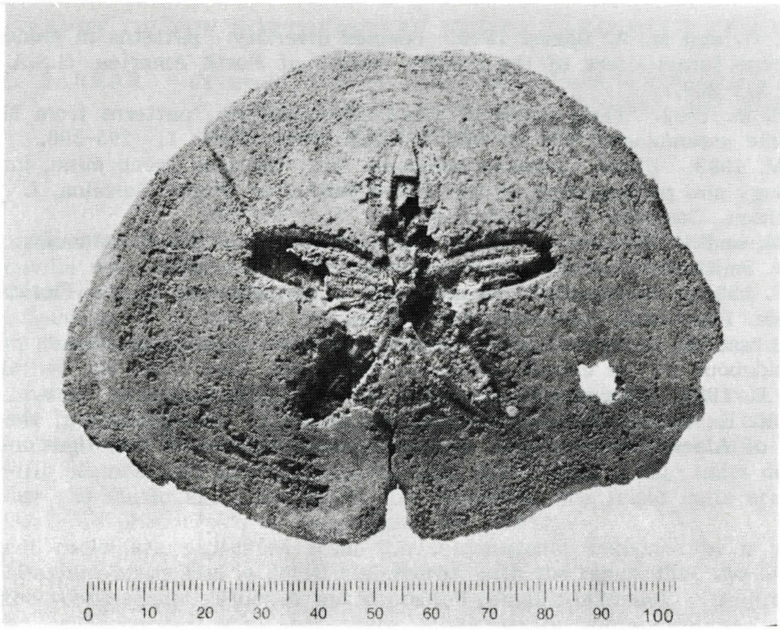

Figure 3. One of 3 intact specimens of A. aberti *found in Hawtnorne sediments near Zolfo Springs, Florida. Scale in millimeters.*

sands, representing not only more clastic terrigenous influx but shallower conditions as well, including intertidal zones (e.g., Kidwell, 1982). The Hawthorne Formation itself is so variable that it defies characterization. Puri and Vernon (1964) described it as lithologic "dumping ground". However, it certainly represents some sort of terrigenous-marine facies, where nearshore habitats were subject to significant inputs of coarse clastic material from a prograding Miocene delta. Thus, *A. aberti* seems to have been able to tolerate a wide range of sediment compositions (calcareous to siliceous) and sizes (clay to coarse sand) at a broad range of water depths. This is significant for organisms such as irregular echinoids which are often limited by substrate characteristics (Smith, 1984).

Another indication of its unusual tolerances is the fact that, unlike many echinoids, it is often found in the absence of other echinoid species: these strata do not contain significant remains of other groups. Also, the presence of abundant casts in the southern part of the Hawthorne Formation indicates that dissolution from percolating fluids has dissolved many of the remains so that the species may have been even more common here and elsewhere than the record shows.

ACKNOWLEDGEMENTS

I am indebted to Charles E. Howlett, a tireless fossil collector, for keeping me abreast of the finds which he, his wife, and his associates make during their trips into the field.

REFERENCES CITED

Conrad, T. A. 1842. Observations on a portion of Atlantic Tertiary region, with a description of new species of organic remains. Bull. Proc. Natl. Inst. for Promotion of Science, 2: 171-194.

Cooke, C. W. 1959. Cenozoic Echinoids of the Eastern U. S. U.S.G.S. Prof. Pap. 321: 126 p.

Durham, J. W. 1953. Type species of *Scutella*. J. Paleont. 27: 347-352.

Gibson, T. G. and M. A. Buzas. 1973. Species diversity: patterns in modern and Miocene foraminifera of the eastern margin of North America. G.S.A. Bull. 84: 217-238.

Kidwell, S. M. 1982. Time scales of fossil accumulation: patterns from Miocene benthic assemblages. 3rd N. Am. Paleont. Conv. Proc. 1: 295-300.

Kier, P. M. 1983. Upper Cenozoic echinoids from the Lee Creek mine, in: Geology and paleontology of the Lee Creek mine, North Carolina, I. Smithson. Contribs. to Paleobiology, No. 53: 499-507

Kier, P. M. and M. H. Lawson. 1978. Index of fossil and living echinoids, 1924-1970. Smithson. Contribs. to Paleobiology, No. 34: 182 p.

Puri, H. S. 1954. Contributions to the study of the Miocene of the Florida panhandle. Fla. Geol. Surv. Bull. 36: 345 p.

Puri, H. S. and R. O. Vernon. 1964. Summary of the geology of Florida and a guidebook to the classic exposures. Fla. Geol. Spec. Pub. No. 5: 312 p.

Smith, A. B. 1984. Echinoid Paleobiology. Allen & Unwin, Boston, Mass.: 190 p.

Williams, K. E., D. Nichol, and A. F. Randazzo. 1977. The geology of the western part of Alachua County. Fla. Bureau of Geol. Report of Investigations No. 85: 54 p.

STRATIGRAPHY OF THE NORTHEASTERN NORTH CAROLINA PIEDMONT

STEWART S. FARRAR   Orogenic Studies Laboratory, Department of Geological Sciences, Virginia Polytechnic Institute and State University, Blacksburg, Virginia 24061

ABSTRACT

The northeastern North Carolina Piedmont comprises a basement sequence of probable Grenville age, structurally overlain by a volcanogenic sequence of probable late Precambrian to early Paleozoic age. The volcanogenic sequence appears to be an eastward continuation of lithologies occurring in the Carolina slate belt. Both the basement and volcanogenic sequences have been intruded by late Paleozoic (Alleghanian) granites.

The basement sequence of gneiss and schist is characterized by relict upper amphibolite- or granulite-facies assemblages. The volcanogenic sequence consists of mafic flows, felsic and minor intermediate crystal and crystal-lithic tuffs, shallow felsic and mafic plutons, and sediments of volcanic derivation. Felsic units dominate in volume over the mafic units throughout the sequence; the felsic units are rather sodic with preserved phenocrysts of plagioclase and quartz.

Basement rocks are separated from the volcanogenic sequence by a probable regional decollement (described in detail elsewhere), with the result that the basement upon which the volcanogenic sequence was deposited remains unknown. The juxtaposed basement and volcanogenic sequences were subsequently metamorphosed, folded, intruded by numerous granitic plutons, and cut by major mylonite zones in an Alleghanian tectonic event. The Alleghanian mylonite zones cut this region into tectonic blocks, within each of which stratigraphic sequences are described. Within the central (Raleigh) block, individual formations can be traced from the greenschist-grade Eastern slate belt across the Alleghanian metamorphic gradient into the amphibolite-grade Raleigh belt. However, no formation crosses the proposed decollement separating the basement terrane from the structurally overlying volcanogenic terrane.

INTRODUCTION

Syntheses of southern Appalachian tectonics have tended to ignore the easternmost Piedmont because, although there are areas which have been studied in some detail, such as the Kiokee belt area of South Carolina (Secor and Snoke, 1978; Snoke and others, 1980) and the James River area of Virginia (Bobyarchick and Glover, 1979; Glover and others, 1982; Farrar, 1982; Farrar, 1984), there are extensive gaps between these areas.

This study describes lithostratigraphic units of the northeastern North Carolina Piedmont east of the Durham Triassic-Jurassic basin (Fig. 1). The lithologic sequences are described for three tectonic blocks which are bounded by major mylonite zones. Across the mylonite zones there are discontinuities of lithology, structure, and metamorphic grade. Detailed descriptions of the structure and metamorphism of this area appear in Farrar (in press).

The eastern North Carolina Piedmont is divided into the Carolina slate belt block, Raleigh block, and Roanoke Rapids block by the Nutbush Creek and Hollister mylonite zones (Fig. 2). A regional decollement within the Raleigh and Roanoke Rapids blocks is interpreted to separate a basement sequence of gneisses and schists from a structurally overlying metamorphosed sequence of volcanogenic sediments, mafic and felsic volcanic rocks, and cogenetic shallow intrusive rocks. The Carolina slate belt block exposes only the volcanogenic sequence.

The only radiometric age controls on rock units in the field area are the Rb/Sr ages of syn- to post-tectonic granitoid plutons which intrude both the basement and volcanogenic sequences. These ages range from 315 to 285 Ma (Kish and Fullagar, 1978; Fullagar and Butler, 1979; Farrar and others, 1981; Russell and others, in press). Rb/Sr biotite-whole rock ages indicate that regional cooling of the high-grade rocks of the Raleigh block occurred in the late Alleghanian at about 250-240 Ma (Farrar and others, 1981; Russell and others, in press).

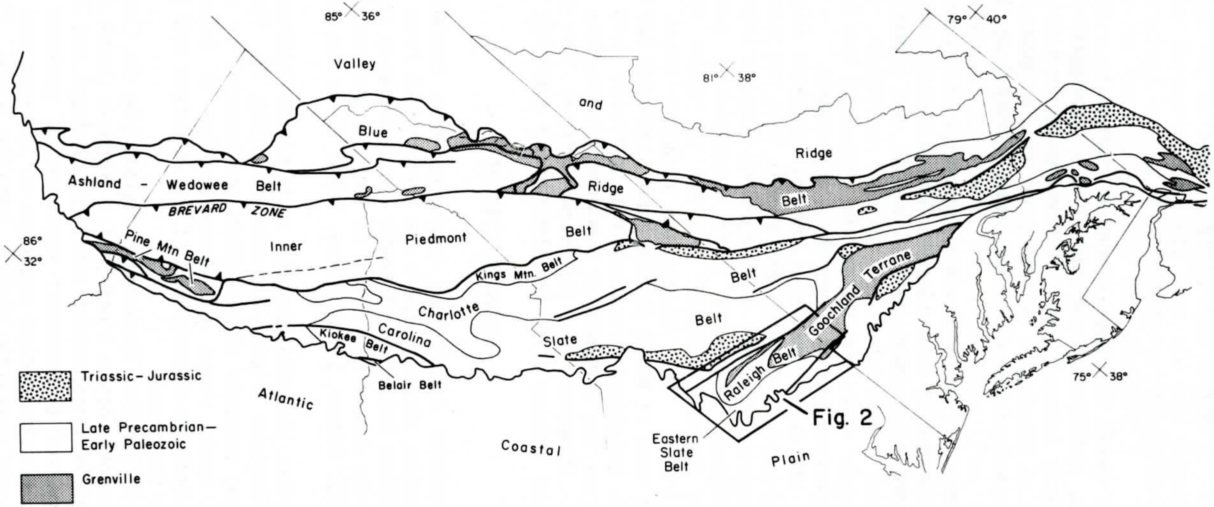

Figure 1. Geologic map of the southern Appalachians. The area shown in Figure 2 is outlined. Modified from Glover and others (1983). Paleozoic plutons are not shown.

The basement and volcanogenic sequences have not been dated in the area of this study. The basement sequence is interpreted to be Grenville in age; it may be an extension of the Goochland terrane in Virginia (Farrar and Glover, 1983; Farrar, 1984). The volcanogenic sequence is interpreted to be Late Precambrian to Early Paleozoic by extension from the main Carolina slate belt where similar sequences have been dated by Glover and Sinha (1973), St. Jean (1973), Black (1978), and Wright and Seiders (1980).

Previous published studies of the northeastern North Carolina Piedmont include: structural reconnaisance of the entire area (Parker, 1968); geology of Wake County (the southwestern part of this area) (Parker, 1979); the northwest (Parker, 1963); the northeast (Mundorff, 1946); and the south and west (Wilson and Carpenter, 1975).

STRATIGRAPHY

Lithostratigraphic units have been previously described in the western part of this area (Parker, 1963, 1979; Carpenter, 1970) and in a part of the east by Stanley (1978) and Stanley and Cavaroc (1980). An attempt is made here to develop broad lithostratigraphic units for the entire study area. These formations (Fig. 2) have been defined with the assistance of aeromagnetic, gravity, and LANDSAT data in addition to lithologic mapping and structural interpretation. Outcrop control is sparse particularly in the south and east. Locations of representative outcrops of each unit are given in Appendix 1. The author has supplied a geologic map (1:250,000) of this area to the North Carolina Division of Mineral Resources, Raleigh. This map has lithologic contacts and structural data, and shows where aeromagnetic maps were used in defining unexposed contacts.

The stratigraphy is described separately for each tectonic block (Figs. 2 and 3). Correlation between blocks is difficult, but the Smithfield formation (described below) possibly crosses from the Raleigh block into the Carolina slate belt block.

Carolina Slate Belt Block

Only that part of the Carolina slate belt block east of the Durham basin is described in this study. This block lies to the west of the Nutbush Creek mylonite zone; it consists entirely of the volcanogenic sequence. The Nutbush Creek mylonite zone forms a sharp, steeply dipping boundary at the northern and southern boundaries of this area, but in the Raleigh area it is a diffuse zone which dips moderately westward. The stratigraphic order given here is subject to modification because without top-bottom criteria pre-tectonic relations between formations are not known. In present attitude the Cary formation underlies the Fuquay-Varina complex. The Beaverdam complex intrudes the Cary formation, and the Vance County meta-trondhjemite intrudes rocks exposed to the west of the study area. The Smithfield formation, which appears to underlie the Cary formation, and the ultramafic bodies which occur within the Smithfield, are described from the Raleigh block where they are best exposed.

Cary formation: The Cary formation comprises three members. Quartz-chlorite-epidote greenstone (Cmv) at the base is overlain by felsic metatuff and quartz-albite crystal metatuff (Cfv) with the assemblage opaque + epidote + chlorite + K mica + quartz + albite. This, in turn, is overlain by opaque-epidote-chlorite-quartz-K mica phyllite (Cph). Most of these rocks are below or at biotite grade, greenschist facies metamorphism (Parker, 1979). Parker (1979) included these rocks and the western part of the Fuquay-Varina complex in his Cary sequence. Rocks of the Fuquay-Varina area are described separately as the Fuquay-Varina complex because of the spatial relation of hypabyssal quartz keratophyre intrusions occuring in the center of a large mass of felsic volcanic rocks in this area. Fortson (1958) also described some of the lithologic units which are included here in the Cary formation.

Fuquay-Varina complex: The greenschist-grade Fuquay-Varina complex comprises the Buckhorn Creek hypabyssal trondhjemite-quartz keratophyre pluton (FBk, Fig. 2), the

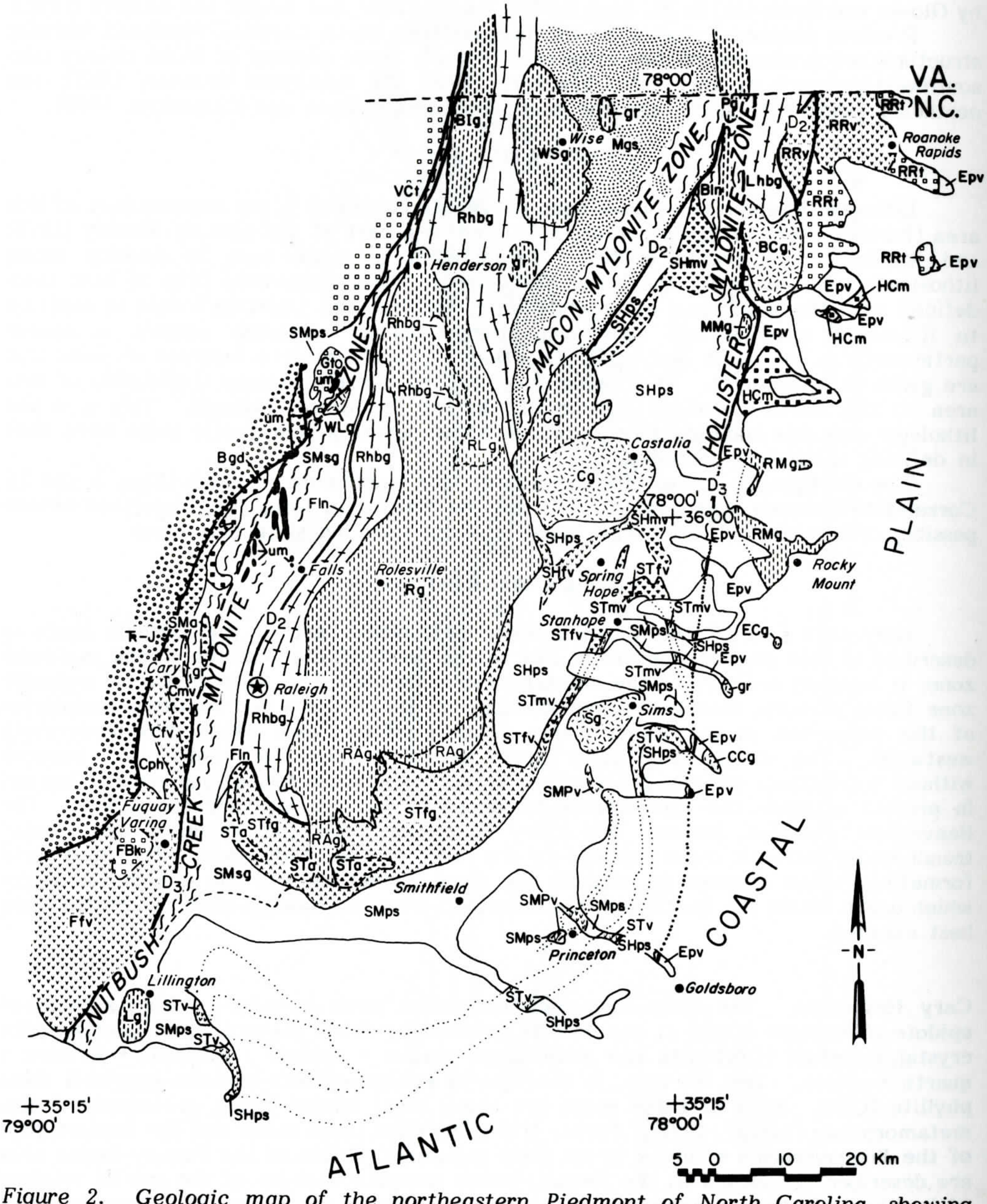

Figure 2. Geologic map of the northeastern Piedmont of North Carolina, showing formations as defined herein; modified in part from Parker (1979) and Carpenter (1970).

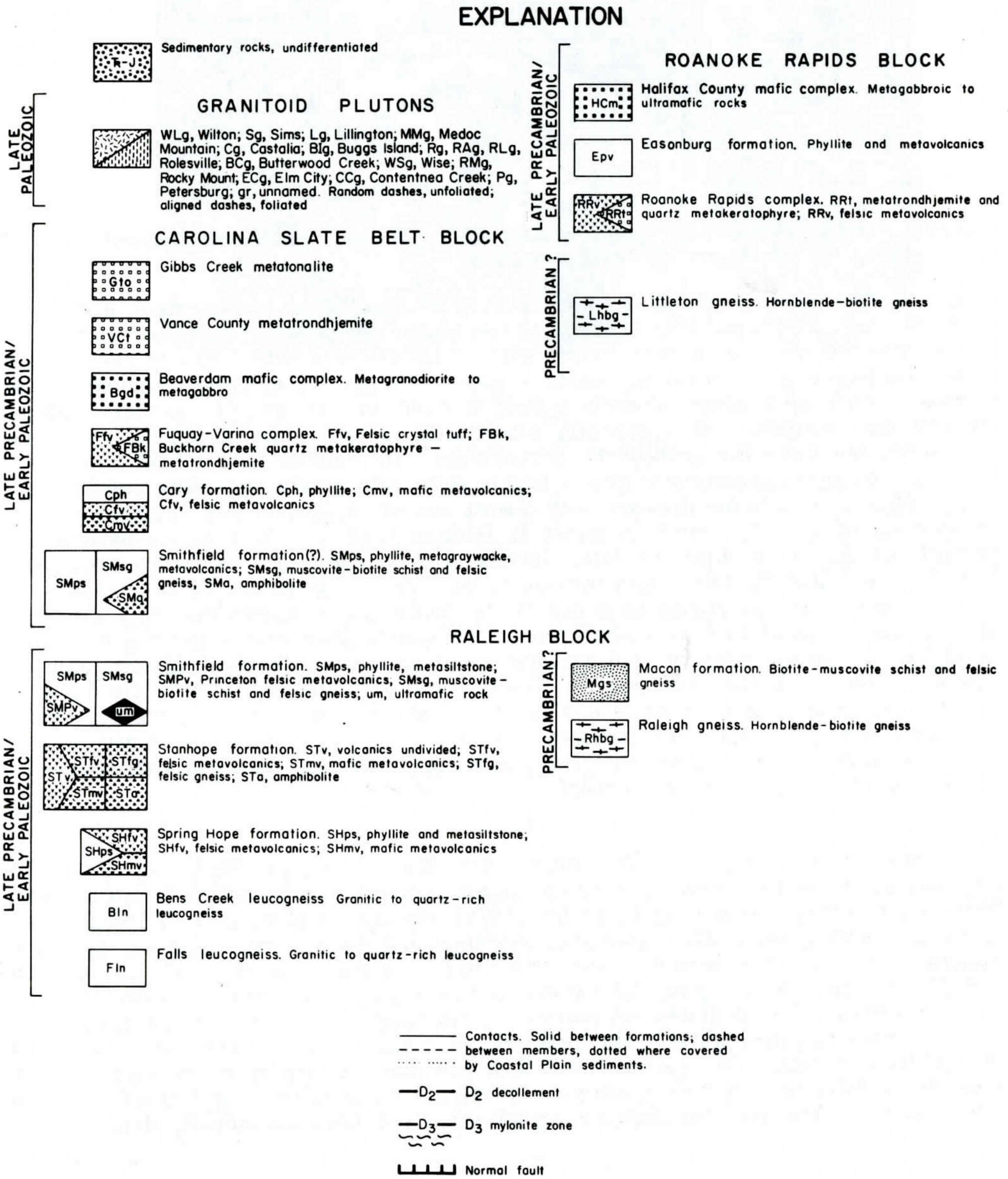

Figure 2 continued.

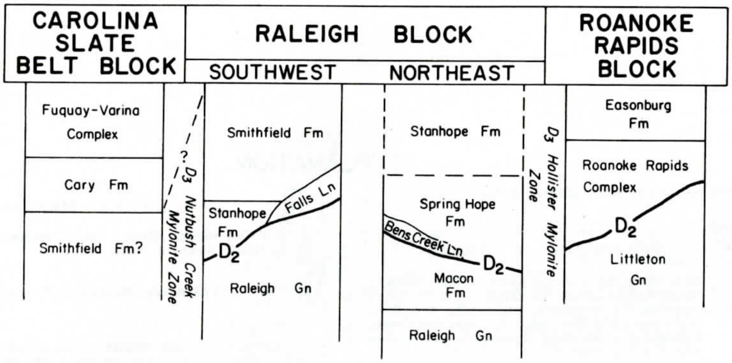

Figure 3. Schematic stratigraphic sections of the Raleigh block and adjacent areas of the northeastern Piedmont of North Carolina.

smaller Sunset Lake quartz keratophyre pluton or dike (not shown on map), and felsic albite-crystal tuff (Ffv). The Buckhorn Creek pluton comprises fine-grained, light-gray to tan trondhjemite-quartz keratophyre with albite and subordinate quartz phenocrysts in a granophyric groundmass of quartz + albite + minor to moderate amounts of K feldspar. Additional minor minerals include K mica, biotite, titanite, garnet, epidote, allanite, and opaques. An apparently subordinate facies of the pluton has the same mineralogy but has a non-granophyric groundmass. The smaller Sunset Lake hypabyssal intrusion comprises granophyric quartz keratophyre with quartz and albite phenocrysts, and porphyritic quartz keratophyre with quartz and albite phenocrysts in a fine-grained groundmass of quartz + albite + minor K feldspar (Fig. 4). Both facies have minor amounts of biotite, K mica, epidote, titanite, and opaques. The Buckhorn Creek and Sunset Lake intrusions have been previously described as granites (Parker, 1979).

These hypabyssal intrusions occur in the center of an approximately 7 km-thick pile of felsic crystal tuff with albite and some quartz phenocrysts and a groundmass of albite + quartz + minor K feldspar, and small amounts of K mica, biotite, calcite, epidote, garnet, titanite, and opaques. Interlayered with the crystal tuff are 0.5 to 2 m thick layers of muscovite schist and biotite schist. The occurrence of the hypabyssal intrusions, with porphyritic and granophyric textures, cutting a thick pile of crystal tuff of similar composition suggests that the plutons may have cut their own extrusive piles in forming the Fuquay-Varina complex.

Beaverdam mafic complex: The Beaverdam Mafic complex (Bgd, Fig. 2) is an intermediate to mafic intrusive complex metamorphosed to greenschist facies (Parker, 1979; Moye, 1981). According to Parker (1979), the northeastern part of the complex is mostly gabbro, originally comprising pyroxene and calcic plagioclase as its major minerals. The rock has been metamorphosed to hornblende (some actinolite), oligoclase and clinozoisite. The complex also includes zones of pyroxenite which has been altered to hornblendite. The southwestern portion of the complex is more felsic, ranging from quartz diorite to granodiorite. Enclaves are plentiful, including probable autoliths of the gabbroic facies. The quartz diorite and granodiorite now have the metamorphic assemblage chlorite + epidote + opaque + K mica + minor microcline + quartz + albite ± hornblende. This pre-metamorphic complex has not been isotopically dated.

Gibbs Creek metatonalite: The Gibbs Creek metatonalite pluton (Gto, Fig. 2) (quartz diorite of Carpenter, 1970), as named herein, is medium grained and light to medium gray. The rock fabric ranges from unfoliated to magmatically foliated to tectonically foliated. Numerous xenoliths of the surrounding rocks occur within the pluton. Carpenter (1970) describes the body in some detail, giving an average of five modes as 44 percent quartz, 30 percent plagioclase (An_{38}), 5 percent biotite, 6 percent epidote, 4 percent chlorite, and minor muscovite, opaques, titanite, and zircon. The pluton has apparently been metamorphosed at greenschist grade.

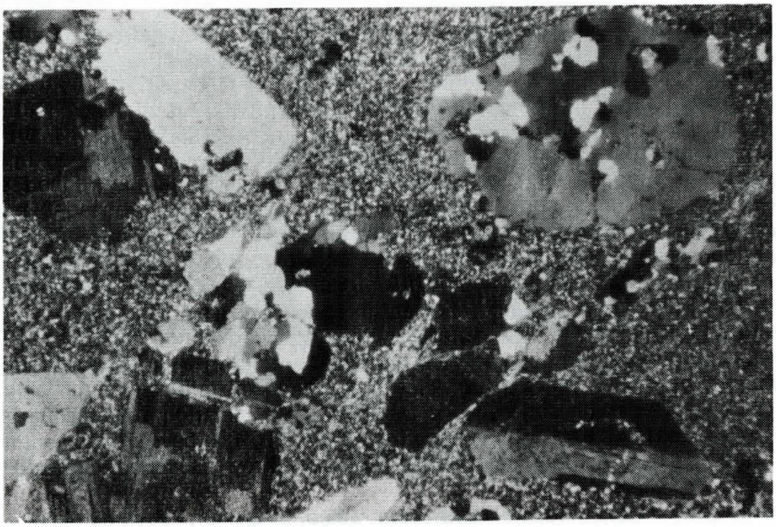

Figure 4. Photomicrograph of porphyritic quartz keratophyre with quartz and plagioclase phenocrysts in a fine-grained quartz + feldspar groundmass; from a small, hypabyssal intrusion exposed at the Sunset Lake spillway, 7 km north of Fuquay-Varina.

Vance County metatrondhjemite: The Vance County metatrondhjemitic pluton (VCt, Fig. 2) (Vance County granitic pluton of Foose and others, 1980 and of Casadevall and Rye, 1980; albite granodiorite of Parker, 1963) is a greenschist to lowermost amphibolite-grade, sodic plagioclase-rich intrusion. Seriate plagioclase is generally albite, but includes oligoclase along the eastern border. This eastern border of the pluton may be at lower amphibolite grade adjacent to the Nutbush Creek mylonite zone. The remainder of the assemblage is chlorite + biotite + minor K feldspar + quartz. The easternmost border of the pluton is mylonitized in the Nutbush Creek zone.

Smithfield formation and ultramafic bodies: Described below under Raleigh Block.

Raleigh Block

The Raleigh block forms the central, major portion of the mapped area (Fig. 2). It consists of a lower, basement sequence comprising the Raleigh gneiss and Macon formation and an upper, volcanogenic sequence comprising the Spring Hope formation, Stanhope formation, Smithfield formation, and ultramafic bodies, most of which occur within the Smithfield formation. The Falls and Bens Creek leucogneisses, which lie along the decollement between the two sequences, may have been derived by mylonitization of adjacent units or they may be deformed granitic plutons which intruded along the decollement. The basement units have been subjected to a sillimanite-grade metamorphic event which did not affect the volcanogenic sequence. A Late Paleozoic metamorphic event affecting both sequences ranged from middle greenschist grade to middle amphibolite grade. Different map units have been defined within formations for the higher-grade rocks, even where units can be traced with some confidence from low-grade areas. This distinction is made in order to emphasize the interpretative step in correlating texturally distinct metasedimentary and metavolcanic rocks of the Eastern slate belt with higher-grade rocks which lack protolith textures.

Raleigh gneiss: This formation was described by Parker (1979) as Injected Gneisses and Schists. The Raleigh gneiss (Rhbg, Fig. 2), as defined here, comprises biotite gneiss, biotite-hornblende gneiss, amphibolite, and minor muscovite-biotite schist and muscovite-quartz-feldspar pegmatite. The major portion of the formation consists of interlayered leucocratic biotite gneiss (C.I. = 2-5) and more mafic biotite-hornblende-bearing gneiss (C.I. = 10-15). The mineral assemblage is quartz + plagioclase ($An_{23}Ab_{76}Or_1$) + perthitic microcline + biotite (Fe/(Fe+Mg) = 0.57), hornblende (Fe/(Fe+Mg) = 0.64), and minor opaques, zircon, titanite, apatite, allanite, and garnet. Retrograde minerals include chlorite, muscovite, epidote, and hematite.

Numerous thin amphibolite layers in the Raleigh gneiss have the assemblage plagioclase + hornblende + biotite, minor quartz, titanite, opaques, and retrograde epidote and hematite. Small pegmatite bodies comprising quartz + K feldspar + plagioclase + muscovite are concentrated in the eastern half of the Raleigh gneiss, near the Rolesville granite. In the northern Raleigh gneiss there are thin biotite-muscovite schist layers; some contain garnet and staurolite. These schists commonly retain some relict sillimanite, most of which has been replaced by muscovite.

Although large parts of the Raleigh gneiss may be intrusive in origin, the gneiss is now strongly layered and complexly deformed, and its original contact relations with other units are obscured. The contact of the Raleigh gneiss with the younger Rolesville granite is irregular and diffuse, probably as a result of some assimilation of the gneiss by the granite.

Macon formation: The Macon formation (Mgs, Fig. 2), defined here, comprises muscovite-biotite-quartz-plagioclase gneiss, quartz-muscovite schist, chloritoid-quartz-muscovite schist with relict sillimanite, chlorite-quartz-muscovite phyllonite, and biotite-quartz-K feldspar-albite leucogneiss. The Macon formation is characterized by textures ranging from gneissic and schistose to protomylonitic and mylonitic. Various metamorphic grades are indicated by relict sillimanite + garnet-bearing assemblages in the less deformed rocks and muscovite + chlorite + quartz ± chloritoid in phyllonite. The dominant rock type of the Macon formation is muscovite-quartz-biotite-K feldspar-plagioclase gneiss with minor epidote, chlorite, opaques, apatite, and titanite. This gneiss has abundant plagioclase augen (An_{21} to An_{28}) and scattered microcline augen. Textures range from strongly foliated to protomylonitic; assemblages are of lower amphibolite grade and biotite and oligoclase were stable in the protomylonite. In the central and eastern part of the Macon formation, mylonitization in the Macon zone (Fig. 2) has reduced assemblages to greenschist facies. Textures in this area vary from protomylonite to mylonite and phyllonite. The mylonite has fluxion structures around plagioclase porphyroclasts. Biotite is replaced by chlorite, and the K feldspar and plagioclase porphyroclasts are progressively replaced by muscovite, albite, epidote and quartz in the mylonite. The final result of this process is phyllonite with the assemblage muscovite + quartz + chlorite + opaques + hematite ± epidote ± tourmaline.

Muscovite schist dominates the northern part of the Macon formation. In several outcrops the schist has the greenschist-grade assemblage chloritoid + muscovite + quartz + hematite + chlorite, with relict sillimanite surrounded by chloritoid and muscovite. Some of these outcrops also have relict garnet with chlorite and hematite rims. The chloritoid and some muscovite have grown across the pre-existing foliation in which the sillimanite lies (Fig. 5).

The Geologic Map of North Carolina (N.C. Dept. of Conservation and Development, 1958) shows part of this area as felsic metavolcanic rocks. This study indicates that these rocks are mylonites and ultramylonites of plagioclase-rich gneiss, which lack of the protolith textures necessary to determine whether or not they are volcanic in origin.

Falls leucogneiss: Parker (1979) includes this gneiss as the easternmost rock type in his "Felsic Gneisses and Schists." The Falls granitic leucogneiss (Fln, Fig. 2), as defined here, is a fine-grained, light-tan to white, magnetite-plagioclase-quartz-microcline gneiss (C.I. = 1-3) with minor garnet, biotite, titanite, allanite, apatite, chlorite, muscovite, epidote, and zircon. The Falls leucogneiss is 1.0-1.5 km thick, and it is continuous along strike for at least 40 km. Very weak layering consisting of slight concentrations of mafic minerals shows tight to isoclinal minor folds. The axes of these folds and the parallel concentration of the mafic minerals form a very strong lineation which characterises this unit; in some areas it is a pencil gneiss. Plagioclase

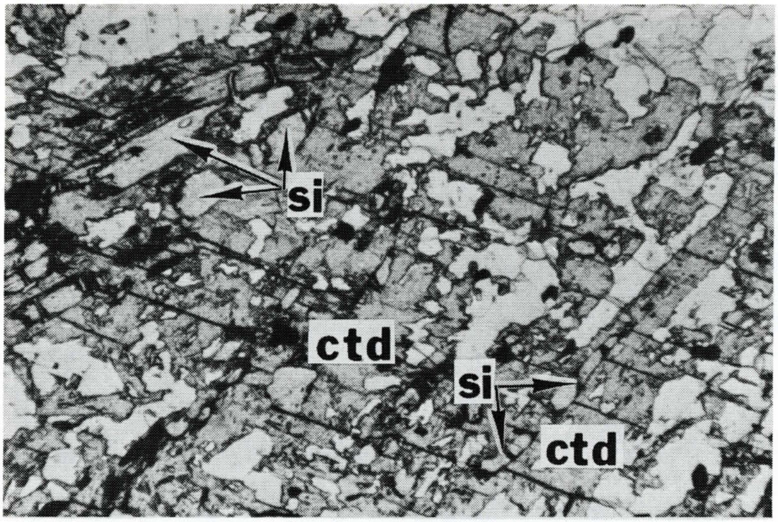

Figure 5. Photomicrograph showing chloritoid (ctd) which in part is pseudomorphic after sillimanite (si); from the Macon formation east of Warrenton, Warrenton quadrangle.

in the leucogneiss is albite ($An_6Ab_{93}Or_1$) and the microcline is microperthitic with a bulk composition of about $An_0Ab_8Or_{92}$. Biotite is of an intermediate composition with Fe/(Fe+Mg) = 0.56. Several saprolite exposures of hornblende-plagioclase amphibolite within the leucogneiss suggest that the formation may be as much as 10 to 15 percent amphibolite.

The pencil gneiss texture, fine grain size, and isoclinal folding suggest that this unit may, possibly be a recrystallized mylonite.

Bens Creek leucogneiss: The Bens Creek leucogneiss (Bln, Fig. 2), as defined here, is a fine-grained, light-tan to white, albite-quartz-microcline gneiss (C.I. = 1-3). Biotite, magnetite, garnet, titanite, apatite, chlorite, epidote, calcite and zircon are minor phases. The fine grain size and the isoclinal folds with near horizontal axes parallel to a strong mineral lineation suggest the possibility that this unit is a recrystallized mylonite adjacent to the Macon formation, in a position equivalent to that of the Falls leucogneiss which is adjacent to the Raleigh gneiss. This possible mylonite is interpreted below to be the locus of the D_2 decollement separating the basement and volcanogenic sequences. Mineral assemblages occurring in the adjacent Macon and Littleton formations suggest that the Bens Creek leucogneiss has been subjected to amphibolite-grade metamorphism.

Spring Hope formation: The Spring Hope formation, defined here, comprises interlayered phyllite, metamudstone-metasiltstone, and felsic and mafic metavolcanic rocks. Phyllite (SHps) is the most plentiful component, comprising about 60 percent of the formation. The mineral assemblage is quartz + K mica $\pm$ chlorite $\pm$ albite $\pm$ opaques. Compositional layering shows as banding on the strong foliation defined by parallel K mica flakes. This foliation is commonly crenulated by at least two later foliations. In some areas of lesser developed foliation, graded bedding is preserved in tightly folded metasiltstone-metamudstone layers.

Metavolcanic rocks comprise the remaining 40 percent of the formation. Felsic metavolcanic rocks (SHfv), including albite crystal metatuff, quartz-albite crystal-lithic metatuff, and quartz keratophyre metaporphyry, comprise about 25 to 30 percent. Greenstone-metabasalt (SHmv), some with quartz amygdules, comprises 10 to 15 percent of the Spring Hope formation. One distinctive layer of metabasalt was scoriaceous (Fig. 6), and has a fine-grained groundmass of albite + epidote + quartz +

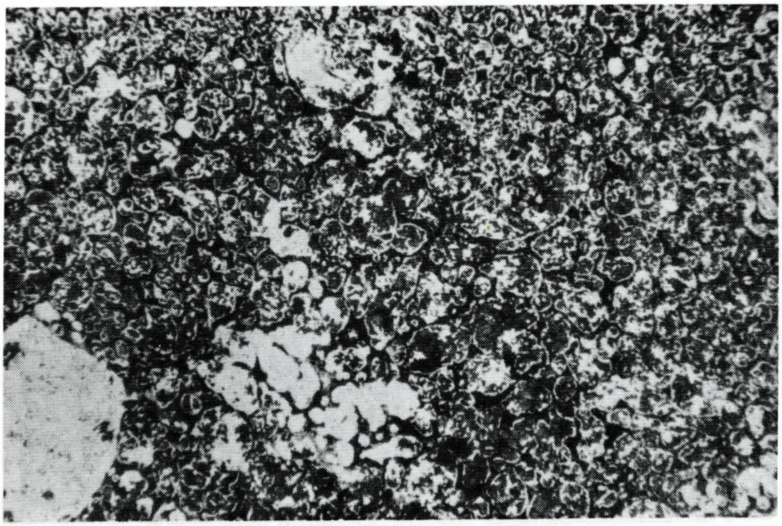

Figure 6. Photomicrograph of scoriaceous metabasalt in the Spring Hope formation. Groundmass of albite + epidote + quartz + opaque, with quartz + epidote-filled amygdules. From gravel pit adjacent to I-95, 4 km east of Spring Hope.

opaque, and numerous amygdules of quartz and epidote. Only major units of felsic and mafic metavolcanic rocks are mapped separately; other outcrops of metavolcanic rocks occur within areas mapped as dominantly phyllite.

Along the northwestern border of the formation, metamorphic grade increases. Muscovite schist has the assemblage muscovite + quartz + chlorite + staurolite + garnet + opaque. Kyanite has also been reported in this area (Stoddard and McDaniel, 1979).

Stanhope formation: The Stanhope formation is best defined in the greenschist-grade Eastern slate belt. Here it consists of massive greenstone-metabasalt (STmv, Fig. 2) overlain by felsic crystal and lapilli tuff (STfv), with thin interbedded phyllitic layers in the felsic tuff. As metamorphic grade increases into the Raleigh belt, the greenstone is recrystallized to amphibolite (STa) and the felsic metavolcanic rocks to quartz-plagioclase gneiss (STfg). The Stanhope formation is generally 1.5-2.0 km thick, and the unit is continuous along strike for more than 200 km around the Smithfield synform (Fig. 2). The ratio of felsic to mafic metavolcanic rocks is variable, but the formation appears to average about 40 percent mafic, 40 percent felsic, with 20 percent phyllite-metamudstone interlayered with the felsic rocks.

The best-exposed section is along the Tar River, near Stanhope, N.C. Massive greenstone-metabasalt at the base of the formation comprises epidote + quartz $\pm$ chlorite $\pm$ actinolite $\pm$ albite $\pm$ calcite $\pm$ opaques. Most igneous textures and minerals have been lost to recrystallization, but quartz amygdules are preserved in some outcrops. Felsic metavolcanic rock overlying the greenstone comprises albite crystal and crystal-lithic metatuff with at least one volcanic conglomerate layer 2-3 m thick. These felsic tuffs have 1-2 m thick interlayers of chlorite-K mica phyllite.

Under upper greenschist and lower amphibolite grade conditions, the rocks lose most of their distinctive volcanic textures. The felsic tuff and plagioclase-quartz crystal tuff are recrystallized to a fine-grained, plagioclase-rich gneiss (STfg). In some lesser-deformed areas, the relict plagioclase phenocrysts are plentiful. The mineral assemblage comprises plagioclase (albite or oligoclase) + quartz + minor K feldspar + muscovite + epidote + opaque $\pm$ garnet $\pm$ calcite $\pm$ titanite $\pm$ biotite. Muscovite schist layers within the felsic gneiss are the recrystallized equivalents of phyllite layers occurring in the lower-grade felsic metavolcanic rocks. The mafic volcanic rocks, which occur as greenstones at lower grade, have been recrystallized to plagioclase-hornblende amphibolite (STa) with minor quartz and opaque. Intermediate-grade samples of quartz-chlorite-albite-epidote-amphibole amphibolite occur in the south-eastern part of the amphibolite member.

Smithfield formation: Metasiltstone-metamudstone and phyllite (SMps), and subordinate felsic metavolcanic rocks (SMPv) comprise the Smithfield formation, as defined here, which is exposed in the Smithfield synform (see Fig. 2, and STRUCTURE). This is interpreted to be the uppermost stratigraphic unit of the Eastern slate belt. Outcrop width of the formation is as much as 25 km and thickness is estimated at 8 to 10 km. As the Raleigh belt is approached, recrystallization increases, resulting in an interlayered sequence of schist and gneiss (SMsg) of amphibolite grade. On the west side of the Raleigh block, north of the Wilton granite (Fig. 2), metamorphic grade drops again, and rocks which may comprise part of the Smithfield formation extend into the Carolina slate belt block where they comprise interlayered phyllite, metagraywacke, felsic metavolcanic rocks, and minor mafic metavolcanic rocks (SMps) (Carpenter, 1970).

Metasiltstone, metamudstone, and phyllite comprise the metasedimentary portion of this formation in the Eastern slate belt. The metamudstone-metasiltstone is generally green gray, with the assemblage quartz + K mica + chlorite + albite + epidote + opaques $\pm$ titanite. Graded beds a few mm thick are common with quartz + albite-rich layers grading into K mica + chlorite-rich layers. Rare quartz-rich layers have magnetite + zircon heavy mineral concentrations. Bedding is cut by two or three foliations. S_1 is a strong planar orientation of K mica and chlorite. S_2 and S_3 are crenulation foliations.

The phyllite is very rich in K mica, with the assemblage K mica + quartz + chlorite $\pm$ albite $\pm$ tourmaline $\pm$ hematite $\pm$ opaques. S_1 and S_2 foliations are particularly strong. Bedding is commonly isoclinally folded. It is visible as color or mineralogical banding on foliation surfaces, producing a strong lineation.

Felsic metavolcanic rocks occur in the Princeton member (SMPv), which is dominated by albite and albite-quartz crystal metatuffs. Several felsic flows in the unit have flow layering defined by alternating albite-, K mica-, and epidote-rich layers. These flows are amygdaloidal with quartz-filled vesicles from 2 to 3 cm in diameter in some layers (Fig. 7). The amygdules are flattened in the plane of combined S_1 + S_2. The felsic metavolcanic rocks are minor in volume, but they crop out quite well because of their resistance to erosion. Near Princeton these rocks form a ridge which protrudes through Coastal Plain cover. This ridge is visible on LANDSAT images.

The Smithfield formation has a characteristic aeromagnetic anomaly pattern (U.S. Geological Survey, 1974). The metasediments cause a flat, low anomaly which is interrupted by a high-amplitude, short-wavelength high intensity pattern, corresponding to the Princeton felsic metavolcanic member along the southeastern limb of the synform. A mirror image of this short-wavelength aeromagnetic high occurs along the northwestern limb of the synform. Although outcrops have not been found, it is assumed that the felsic metavolcanic member also produces this anomaly.

Gneisses and schists of the high-grade portion of the Smithfield formation (SMsg) comprise the following: (1) muscovite-biotite-quartz-albite gneiss (felsic metavolcanic rock); (2) quartz-muscovite schist and muscovite quartzite; (3) muscovite-biotite schist; (4) muscovite graphite schist; and (5) amphibolite. This map unit comprises parts of two units of Parker (1979), his Mica Gneisses and Schists with Interlayered Hornblende Gneiss, and Felsic Gneisses and Schists.

Muscovite-biotite-quartz-albite gneiss and mylonitic gneiss with minor tourmaline, microcline, opaques, apatite, chlorite, titanite, and calcite comprise most of the western third of the map unit in the Nutbush Creek mylonite zone. The gneiss is very fine grained, and has a strong foliation of the micas axial planar to dismembered isoclinal folds of the compositional layering. The unit appears to be a recrystallized mylonite with the intensity of recrystallization increasing to the east. Some relict plagioclase phenocrysts remain as evidence of the volcanic origin of this rock.

An amphibolite body (SMa) lies within the quartz-albite-muscovite-biotite gneiss. The least deformed portions of this amphibolite consist of hornblende with fine-grained opaque inclusions and plagioclase. The opaque inclusions are interpreted to have exsolved from igneous clinopyroxene which has completely reacted to hornblende. The distribution of the inclusions preserves a relict ophitic texture (Fig. 8), indicating that this was a gabbroic intrusion or thick flow in contrast to the fine-grained metabasalt of flows in the Stanhope formation to the southeast.

East of the felsic gneiss (metavolcanic) unit is a zone of interlayered and

Figure 7. Quartz-filled amygdules in felsic metavolcanic flow rock in the Princeton member of the Smithfield formation. Inactive Nello Teer quarry at Princeton.

complexly folded felsic gneiss, muscovite quartzite, muscovite-biotite schist, and muscovite-graphite schist. The graphite layers are shown by Parker (1979). Some felsic layers in this unit have relict plagioclase phenocrysts; these layers appear to be felsic crystal metatuffs. The muscovite quartzite and schists are amphibolite-grade equivalents of the metamudstone and metasiltstone of the Smithfield formation. Variable metamorphic grade in this area results in a great variety of mineral assemblages, ranging from retrograde greenschist assemblages in some of the Nutbush Creek mylonite rocks to kyanite-staurolite-grade assemblages adjacent to the Falls leucogneiss on the east. Excluding zones of retrogression in the Nutbush Creek mylonite zone, the metamorphic grade increases from west to east.

Ultramafic bodies: Numerous ultramafic bodies (um) occur within the Smithfield formation north of Raleigh. These bodies, some with cores of pyroxenite, have been metamorphosed with the surrounding rocks. Rock types include serpentinite, soapstone, talc-chlorite schist, and actinolite-chlorite rocks according to Parker (1979), Carpenter (1970), and Moye (1981). Primary mineralogy cannot be determined in most of the bodies. Observed contacts are tectonic. It is postulated here, and by Moye (1981) and Stoddard and others (1982a, 1982b) that these lens-shaped bodies were emplaced as tectonic slices, probably during the D_2 event; they were not intruded as magmas as postulated by Dickey (1963) and Carpenter (1970).

Roanoke Rapids Block

The Roanoke Rapids block, comprising the eastern edge of the Piedmont, ranges in metamorphic grade from middle greenschist facies to middle amphibolite facies. Because of the lack of outcrop due to Coastal Plain overlap, the stratigraphic sequence

Figure 8. Photomicrograph of amphibolite derived from gabbro or thick basalt flow. Igneous clinopyroxene and much of the igneous plagioclase have reacted to form hornblende. Finely dispersed opaque inclusions in the hornblende are interpreted to have exsolved from the igneous clinopyroxene. Although the pyroxene is gone, the inclusions preserve the relict ophitic texture of the pyroxene with respect to plagioclase. Some relict cores of igneous plagioclase are preserved with hornblende overgrowths. Outcrop is at intersection of Ebenezer Church Road, CR 1649, and Crabtree Creek, 4 km northwest of Raleigh.

cannot be defined with much confidence. The Littleton gneiss and the Roanoke Rapids complex are the best exposed; descriptions of the other formations are based on very sparse outcrops.

The Littleton gneiss is interpreted to be part of the Grenville-age Goochland basement terrane. It is separated by the D_2 decollement (Fig. 2) from the structurally overlying volcanogenic sequence comprising the Roanoke Rapids complex, Easonburg formation, and Halifax County mafic complex.

Littleton gneiss: The amphibolite-grade Littleton gneiss (Lhbg), as defined here, is essentially identical to the Raleigh gneiss. It comprises biotite gneiss, hornblende-biotite gneiss, and minor amphibolite and muscovite-biotite schist. As in the Raleigh gneiss, the more leucocratic (C.I. = 3-5) biotite gneiss predominates over the more mafic hornblende-biotite gneiss (C.I. = 10-15). The typical mineral assemblage of the hornblende-biotite gneiss is hornblende + biotite + oligoclase + quartz + microcline, with minor opaques, zircon, titanite, allanite, and apatite; secondary minerals include epidote, muscovite, and chlorite.

Roanoke Rapids complex: The Roanoke Rapids complex, as defined here, comprises greenschist-grade, hypabyssal, intrusive (RRt) and extrusive (RRv) felsic, to intermediate rocks. The hypabyssal intrusion may have been the center of volcanism. It is irregular in shape and approximately 20 km in diameter. It is surrounded by felsic metavolcanic rocks with interlayered metasediments of probable volcanogenic origin. The intrusion ranges from trondhjemitic to quartz dioritic in composition. The mineral assemblage comprises albite + amphibole + biotite + quartz + K feldspar + epidote + chlorite + K mica + titanite + opaque. The intrusion is cut by quartz keratophyre dikes which have quartz and albite phenocrysts in a granophyric quartz-K feldspar-albite groundmass (Fig. 9). These intrusive rocks are characterized by a high content of sodic feldspar and a relative lack of K feldspar. They exhibit greenschist-facies mineral assemblages.

Figure 9. Photomicrograph of quartz and plagioclase phenocrysts set in the quartz-feldspar granophyric groundmass of a quartz keratophyre dike in the Roanoke Rapids complex. Outcrop is in the Roanoke River at Weldon, Weldon quadrangle.

Extrusive rocks of the Roanoke Rapids complex comprise plagioclase crystal and crystal-lithic metatuff, and relatively rare felsic flows. One probable flow consists of albite phenocrysts connected by thin films of quartz-albite-K feldspar granophyre to form layers (Fig. 10). The layers are separated by lenticles of quartz. This rock is interpreted to have been a flow or lava dome which crystallized rapidly, producing the granophyric texture and trapping vapor. Quartz fills the large flattened vesicles.

Metamorphosed pyroclastic and volcaniclastic rocks are common in the area surrounding the Roanoke Rapids intrusion. Crystal and crystal-lithic metatuff interlayered with phyllite and metagraywacke occur along the tailrace below the Roanoke Rapids dam and along both shores of Roanoke Rapids Lake. The crystal metatuff has albite and quartz phenocrysts in a groundmass of albite + quartz + microcline + K mica + calcite $\pm$ epidote $\pm$ biotite $\pm$ chlorite $\pm$ titanite $\pm$ garnet $\pm$ opaques. The crystal-lithic metatuff and crystal-lithic lapilli metatuff have albite and quartz phenocrysts and lapilli as large as 10 cm in diameter in a groundmass of albite + quartz + epidote + chlorite $\pm$ calcite $\pm$ opaques. The lapilli have sharp contacts with the groundmass and are commonly rounded; smaller fragments are commonly angular. Flattening in the plane of S_1 or S_2 foliation is common. Lapilli include the following varieties: very fine-grained, felty, albite-quartz groundmass with albite phenocrysts; fine-grained, equigranular quartz-albite groundmass with quartz and albite phenocrysts; and fragments of intrusive rocks from the complex. No nonvolcanic lithic fragments have been found.

Metasedimentary rocks of the complex include K mica-quartz-chlorite phyllite and a volcaniclastic metagraywacke with the assemblage quartz + albite + calcite + epidote + chlorite + opaques.

The complex has also been intruded by dikes which vary from quartz keratophyre to basalt in composition. Mafic dikes, metamorphosed to greenstone, are exposed in the tailrace of the Roanoke Rapids dam.

Easonburg formation: The Easonburg formation (Epv), as defined here, includes interlayered felsic volcanic and phyllitic rocks exposed south of the Roanoke Rapids complex and to the east of the Hollister mylonite zone. These rocks are exposed sporadically in the deeper stream valleys which cut the overlying Coastal Plain sediments. This formation may be equivalent to the Spring Hope formation, but it cannot be correlated with confidence across the Hollister mylonite zone.

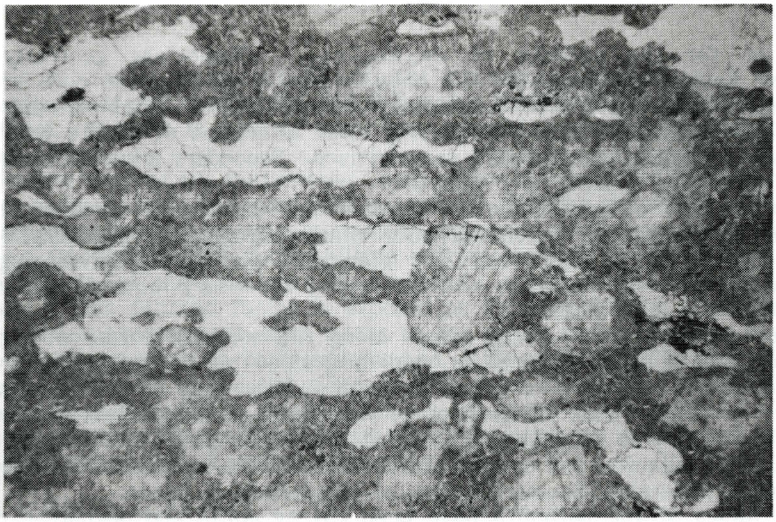

Figure 10. Photomicrograph of quartz keratophyre flow of the Roanoke Rapids complex. Ribbons of plagioclase phenocrysts, surrounded by films of granophyric quartz-feldspar, are separated by lenticles of quartz. Sample is from 2 km northwest of Thelma, Thelma quadrangle.

Halifax County mafic complex: The Halifax County mafic and ultramafic rocks (HCm) have been described by Stoddard and Teseneer (1978) and Kite and Stoddard (1984). They comprise metaperidotite, metagabbro, and metabasalt. Metaperidotite consists of serpentine + magnetite ± chlorite ± talc and relict clinopyroxene ± olivine ± Cr-spinel. Metagabbro comprises actinolite + epidote ± chlorite and relict plagioclase ± clinopyroxene. The metabasalt comprises blue-green amphibole + albite + epidote ± chlorite and relict plagioclase ± oxides.

Granitoids

The northeastern Piedmont of North Carolina has been intruded by numerous syn- and post-tectonic granitoid plutons. Granitoids occurring in amphibolite-grade country rock are generally syn-tectonic, with a moderate to weak biotite foliation (S_3) parallel to country rock foliation. Feldspars and quartz in these granitoids show minor to moderate recrystallization. Granitoids occurring in greenschist-grade country rock are essentially undeformed or are cut by discrete mylonite zones. Foliation is weak to absent. The foliation which does occur is an igneous flow foliation, and is generally parallel to the contacts of the pluton. Because both the deformed and undeformed granites fall in the age range 313-285 Ma (see below), it is concluded that granites in the high-grade belt were subjected to a ductile deformational event which did not affect the granites of the low-grade belts. Rock classification is that of the IUGS (Streckeisen, 1976).

Rolesville granite batholith: The Rolesville granite was named by Stuckey (1965) for the community of Rolesville near a large quarry in the granite. The body was descibed as a batholith by Parker (1968). The Rolesville batholith comprises three texturally-defined granite facies, and a border facies which contains a large component of country rock gneiss occurs along the western edge of the batholith. The modal average for 19 samples of Rolesville granite point-counted on slabs and thin sections is: plagioclase 37%, K feldspar 33%, and quartz 25%. The C.I. is 5% (Becker and Farrar, 1977).

The Rolesville main facies (Rg) consists of medium- to coarse-grained biotite granite, with weak compositional layering cut by a later weak to moderate biotite foliation. Alkali feldspar is microperthitic microcline + albite with an average composition for the perthite of $An_0Ab_8Or_{92}$. Plagioclase generally has weak oscillatory zoning ($An_{18}Ab_{81}Or_1$ to $An_{24}Ab_{75}Or_1$). Thin albite rims are common. Biotite has Fe/(Fe+Mg) = 0.58. Accessory minerals include allanite, opaques, zircon, apatite, and titanite. There is commonly some alteration of biotite to chlorite, and plagioclase is slightly to moderately saussuritized. Secondary minerals include chlorite, epidote, muscovite, calcite, and hematite.

The Archers Lodge porphyritic facies (RAg) constitutes much of the southern margin of the batholith. It contains microcline macroperthite phenocrysts 1-4 cm in length. Quartz, biotite, plagioclase, and microcline microperthite averaging 4-5 mm in length comprise the groundmass. Accessory and secondary minerals are the same as in the Rolesville main phase.

The Louisburg facies (RLg) occurs along the northern border of the Rolesville batholith. It is a foliated, fine- to medium-grained biotite granite with quartz and feldspar grains averaging 1 to 2 mm in length. Microcline in the Louisburg facies is microperthitic with a bulk composition of $An_0Ab_6Or_{94}$. Plagioclase is normally zoned from $An_{22}Ab_{77}Or_1$ to $An_{19}Ab_{80}Or_1$, and it has albite rims. Accessories present are zircon, apatite, allanite, and opaques; hematite, chlorite, epidote, and muscovite occur as secondary minerals. Saussuritization of plagioclase is minor.

All facies of the batholith have been cut by aplite and pegmatite dikes a few centimeters to tens of centimeters thick. The main facies of Rolesville is cut by large dikes of biotite leucogranite which apparently were late stage granitic melts. The leucogranite has microcline microperthite ($An_0Ab_7Or_{93}$) and plagioclase ($An_{14}Ab_{85}Or_1$). The minor biotite is almost completely altered to chlorite. Saussuritization of the plagioclase is relatively strong.

Castalia granite: The Castalia pluton (Cg), mapped by Julian (1972), is a medium- to coarse-grained biotite granite. The Rb/Sr isochron age of the Castalia is 313 $\pm$ 13 Ma (Fullagar and Butler, 1979). The eastern part of the pluton is essentially unfoliated. The northwestern part has a weak foliation parallel to regional country rock foliation, and the rock closely resembles the Rolesville main facies. The average grain size is approximately 5 mm. The K feldspar is microcline microperthite. Plagioclase is weakly to moderately zoned ($An_{29}Ab_{70}Or_1$ to $An_{18}Ab_{81}Or_1$) and moderately saussuritized. Other minerals are chlorite, epidote, calcite, muscovite, garnet, titanite, zircon, allanite, apatite, and opaques. The unfoliated portion of the pluton is notable for its uniformity of texture and composition.

Butterwood Creek granite: This granite (BCg) is named herein for Butterwood Creek which flows across the granite south of Littleton, North Carolina (Fig. 2). This area is designated granite, metavolcanic rocks and mica gneisses on the Geologic Map of North Carolina (N.C. Dept. of Conservation and Development, 1958). Most of the Butterwood Creek consists of coarse-grained, amphibole-biotite granite with K feldspar megacrysts. An earlier, more mafic facies occurs as autoliths and as a border facies; a third facies is a foliated fine- to medium-grained muscovite-biotite leucogranite.

The eastern two-thirds of the Butterwood Creek is undeformed and unfoliated coarse-grained amphibole-biotite granite. The granite (C.I. = 5-8) has microcline perthite megacrysts (up to 2-3 cm, some with wiborgitic texture), quartz, plagioclase (0.5-1.5 cm in diameter) with weak to moderate oscillatory zoning ($An_{23}Ab_{76}Or_1$ to $An_{19}Ab_{79}Or_2$). Biotite is of intermediate composition (Fe/(Fe+Mg) = 0.46), and the amphibole has Fe/(Fe+Mg) = 0.48. Quartz has undulose extinction, and there has been minor recrystallization of the borders of plagioclase. Accessory euhedral titanite is distinctive. Other accessory minerals include opaques, zircon, apatite, and allanite. Secondary minerals include chlorite, muscovite, and epidote. Minor quartz veins cutting the granite contain trace amounts of molybdenite.

The earlier mafic facies is a biotite-amphibole granodiorite with C.I. = 15 to 20. Mineral compositions are similar to those of the coarse-grained facies. Some antiwiborgite texture is present. This is believed to be an early facies of the pluton.

A fine- to medium-grained, muscovite-biotite leucogranite facies (C.I. = 1-2) occurs on the southwestern margin of the Butterwood Creek pluton. K feldspar is microperthitic microcline with plentiful adjacent myrmekite. Plagioclase is oligoclase. Biotite is partially altered to chlorite, and muscovite occurs as an interstitial, possibly primary mineral. Epidote is a minor secondary mineral. Accessories include garnet, opaques, and zircon.

The western third of the Butterwood Creek pluton is cut by the Hollister mylonite zone. As the mylonite zone is approached, a tectonic foliation develops in the granite. In the coarse-grained facies, quartz is strongly deformed, with subgrain development; feldspars are fractured, with recrystallized edges; biotites are bent and kinked; titanites are fractured and rounded. No amphibole occurs in the deformed coarse-grained facies. This foliated facies is exposed at Panacea Springs in the Littleton quadrangle. Similar textural changes occur in the other facies, but the muscovite-biotite leucogranite appears to be less deformed, although it is foliated. Within the mylonite zone, grain size is greatly reduced, with some zones of ultramylonite. The textural gradation suggests that these facies are all parts of one pluton.

The whole-rock Rb/Sr age of the Butterwood Creek pluton is 292 ± 31 Ma (Farrar and others, 1981; Russell and others, in press).

Medoc Mountain granite: A small pluton of medium- to coarse-grained biotite granite (MMg) occurs about 2 km south of the southern edge of the Butterwood Creek pluton. This pluton has been described from surface exposures and drill core by Robertson and others (1947) and Harvey (1974). The Boy Scout-Jones and Moss-Richardson molybdenite prospects are associated with this pluton. The pluton has been dated as 301 ± 6 Ma (Fullagar and Butler, 1979). The granite is unfoliated, but faulted and fractured in some areas (Harvey, 1974). Cu-Mo mineralization is associated with quartz veins cutting the granite and surrounding phyllite. There is minor to moderate alteration of the granite with secondary minerals including chlorite, muscovite, epidote, and carbonate.

Sims granite: The Sims granite (Sg), also known as the Conner Stock, is a coarse-grained, unfoliated biotite granite dated by Wedemeyer and Spruill (1980) at 287 ± 9 Ma. The pluton is approximately elliptical with a long axis of about 10 km, and it has a thin layer of Coastal Plain sediments over most of its eastern half. Mineralogically, the Sims comprises perthitic microcline, quartz, zoned plagioclase (from about An_{20} to An_{16}) which is moderately to strongly saussuritized, and biotite ($Fe/(Fe+Mg) = 0.56$). Relatively high fluid content has resulted in plentiful subsolidus alteration which produced muscovite, epidote, chlorite and minor fluorite. A pelitic xenolith has the assemblage biotite + andalusite + fibrolite + quartz + muscovite. At the contact of the granite, the quartz-K mica phyllite country rock has been recrystallized to a coarse-grained quartz-muscovite hornfels.

Rocky Mount granitoid: The Rocky Mount pluton (RMg) lies along the Piedmont-Coastal Plain boundary (Fig. 2). It has been briefly described by Watson and Laney (1906), Mundorff (1946), Councill (1954), and Parker (1968). The pluton is mostly covered by Coastal Plain sediments, but as outlined from water well and aeromagnetic data, its boundaries correspond to a -30 milligal gravity anomaly (Dept. of Defense Gravity Data, 1976). The Rocky Mount pluton comprises three major facies (Farrar, 1980): biotite monzogranite which crops out along the Tar River; hornblende-biotite granodiorite which is exposed only in the RM1 drillcore in the center of the pluton, which is also the center of the gravity anomaly (Farrar, 1980); and biotite-hornblende tonalite which forms the northwestern boundary of the pluton.

The biotite monzogranite is light gray, equigranular, medium- to fine-grained, weakly to moderately foliated, and has a C.I. of 2-3. Biotite (up to 1.5 mm in diameter) is the only ferromagnesian silicate. Perthitic microcline, plagioclase, and quartz grains range up to 4 mm in diameter. The feldspars are sub- to anhedral; quartz has subgrain development, and is flattened slightly parallel to the foliation defined by biotite. The plagioclase (An_{15}) has weak normal zoning and weakly to moderately saussuritized cores. Accessory minerals include apatite, zircon, allanite, magnetite, and small euhedral titanites; secondary minerals include epidote and chlorite after biotite, and minor epidote, calcite, and muscovite from saussuritization of plagioclase. Enclaves of fine-grained biotite-hornblende tonalite are common in some outcrops, and these may be related to the coarser-grained tonalite which occurs to the north.

The RM1 drillcore comprises medium- to coarse-grained hornblende-biotite granodiorite, which has not been found in the exposed portion of the pluton. Minor facies in the core include a dike of fine-grained biotite monzogranite and several 1-2 cm thick quartz-feldspar pegmatite and aplite veins. The hornblende-biotite granodiorite has euhedral to subhedral plagioclase, somewhat strained, up to 0.5-1.0 cm long, and with oscillatory zoning An_{32-23}. The plagioclase comprises up to 45 modal percent of the rock. Anhedral quartz and sub- to anhedral microcline perthite comprise 20 to 25 modal percent each. Biotite (7%) and amphibole (2%) comprise the ferromagnesian silicates. Accessory minerals include large, 2-3 mm in diameter, euhedral titanite, and smaller apatite, allanite, zircon, pyrite, and magnetite. Secondary minerals include minor chlorite and epidote after biotite, and minor epidote and calcite after plagioclase.

The hornblende-biotite tonalite is medium-gray, medium-grained, and weakly foliated. It contains 55 modal percent plagioclase (An_{40-30}, up to 8 mm in diameter), 20 percent quartz (2-4 mm), 10-15 percent each of biotite and amphibole (2-4 mm); and very minor microcline microperthite. Accessory minerals include apatite, zircon, and large (1-3 mm in diameter) euhedral titanites. Secondary minerals include traces of epidote, calcite, and muscovite from the saussuritization of plagioclase.

Other granites: The *Elm City granite* (ECg) lies to the southwest of the aeromagnetic anomaly caused by the Rocky Mount pluton. Outcrops of the two plutons are separated by Coastal Plain cover. The Elm City pluton, a medium- to coarse-grained biotite granite, is exposed in an abandoned quarry alongside the Atlantic Coast Line railroad about 3.5 km north of Elm City. Water well cuttings (Mundorff, 1946) suggest that the pluton is small. The mineralogy is microcline perthite, quartz, plagioclase (approximately An_{20}, with slight zoning and minor saussuritization), biotite (commonly altered to chlorite), with accessory allanite, zircon, and opaques, and secondary epidote, muscovite, and chlorite. This pluton is also described by Councill (1954).

The *Contentnea Creek granite* (CCg) (Councill, 1954 and Watson and Laney, 1906) is a coarse-grained biotite granite exposed in fractured condition along Contentnea Creek south of Wilson. It was not examined in this study.

The *Wilton granite* (WLg) (Carpenter, 1970), is a small pluton about 3 km east of Wilton in Granville County, within the Nutbush Creek mylonite zone. It is a pink, medium-grained, foliated biotite granite with a Rb/Sr age of 285 ± 10 Ma (Fullagar and Butler, 1979). Its mineral assemblage is microcline perthite, plagioclase, quartz, biotite, with accessory opaques, allanite, titanite, zircon, and secondary chlorite, muscovite, and calcite. There is some saussuritization of plagioclase, and biotite is commonly altered to chlorite. C.I. is 2 to 5. The granite has been weakly deformed, having moderately to strongly strained quartz. Fractures have quartz-molybdenite-sulfide mineralization.

The *Buggs Island granite* (BIg) is a medium-grained, foliated, biotite granite similar to the Rolesville. The Buggs Island, most of which lies in Virginia, has been dated by Rb/Sr at 313 ± 8 Ma (Kish and Fullagar, 1978). It lies in the northwestern Raleigh belt and is bounded on the west by the Nutbush Creek mylonite zone.

The *Wise granite* (WSg) lies within the northern Raleigh belt, and has not been dated. It is a complex pluton comprising medium-grained, muscovite-biotite granite and garnet-biotite-muscovite leucogranite. Both facies are foliated; they are well exposed in abandoned quarries within 0.5 km northwest and southeast of Wise in the Warrenton quadrangle.

The *Lillington granite* (Lg) is a medium-grained, foliated, biotite granite cropping out south of Lillington in the southwesternmost part of the Raleigh block. This granite has been dated at 290 Ma by Rb/Sr (Kish and Fullagar, 1978).

METAMORPHISM AND DEFORMATION

Three regional metamorphic events have been distinguished in this area (Fig. 11) (Farrar, in press). The basement sequence was metamorphosed to sillimanite (or possibly granulite) grade in a Grenville(?) event (M_g) which did not affect the cover sequence. The volcanogenic cover sequence was metamorphosed to greenschist grade (M_1), probably in the Taconic, as was the Carolina slate belt to the west (Kish and others, 1979; Glover and others, 1983). This M_1 greenschist-grade event may or may not have affected the basement sequence. A third metamorphic event (M_2) overprinted the sillimanite-grade basement rocks and the greenschist-grade volcanogenic rocks. M_2 assemblages reached amphibolite-grade in the Raleigh belt. These grade outward with decreasing temperature into the pre-existing M_1 greenschist-grade assemblages. M_2 was accompanied by the intrusion of numerous granitic plutons. Plutons which intrude the amphibolite-grade Raleigh belt have no definable contact aureoles (e.g., Rolesville); those which intrude greenschist-grade Eastern slate belt have distinct aureoles (e.g., Sims).

Four regional deformational events have been defined in this area (Farrar, in press). The first, a composite of possibly several early events (D_g), isoclinally folded compositional layering during the sillimanite-grade metamorphism of the basement sequence. The second (D_1) produced a penetrative S_1 foliation and minor folds in the volcanogenic sequence coincident with M_1 P,T conditions. Possible D_1 effects in the basement sequence have not been distinguished. D_2 (Taconic?) thrusting of the volcanogenic sequence over the basement resulted in the juxtaposition of the terranes along a decollement (D_2; Fig. 11). Regional scale F_2 folds, overturned to the northwest, formed in the volcanogenic sequence during this event. D_2 occurred during late M_1 or early M_2 under greenschist-grade conditions. During an Alleghanian D_3 event, regional-scale F_3 folds (Fig. 11) folded the pre-existing D_2 decollement and F_2 folds into their present geometry. D_3 mylonite zones (Nutbush Creek, Hollister, and Macon, Fig. 11) developed along the limbs of these F_3 folds. S_3 foliation developed axial planar to the F_3 folds.

DISCUSSION

The Raleigh gneiss, Macon formation and Littleton gneiss are interpreted to be a Grenville basement terrane by correlation with the Grenville-age Goochland terrane granulite-facies rocks along strike to the north (Farrar and Glover, 1983) (Fig. 1). Pelitic rocks of the Goochland terrane have relict Grenville-age assemblages of coarse-grained sillimanite (Fig. 5) and/or sillimanite + K feldspar assemblages. These are partially replaced by probable Alleghanian assemblages which contain kyanite and/or staurolite at amphibolite grade and muscovite $\pm$ chloritoid $\pm$ chlorite at upper greenschist grade. Within the Raleigh block basement terrane, the pelitic rocks consistently have relict coarse-grained sillimanite; the coarse-grained sillimanite does not occur in the structurally overlying volcanogenic sequence. The highest-grade assemblages of the volcanogenic rocks contain kyanite $\pm$ staurolite which are prograde from greenschist facies.

The boundary between the basement and overlying units could be either an unconformity or a fault. Other Grenville basement terranes of the southern Appalachians, including the Blue Ridge, Sauratown Mountains, and Pine Mountain belt, are overlain by terrestrial and/or shallow marine deposits derived from a continental source. The basement terrane of this area appears to lack such a cover. In the area where the contact is best exposed between the Castalia and Butterwood Creek plutons (Fig. 2), basement is directly overlain by the Spring Hope formation. The contact zone appears to be a recrystallized mylonite. This contact needs to be examined more thoroughly, but from existing evidence it is interpreted to be a regional decollement, separating the Grenville(?) basement from the structurally overlying volcanogenic sequence (Farrar, in press).

The volcanogenic sequences of the Carolina slate belt block, Raleigh block, and Roanoke Rapids block are assumed to be approximately the same age and to be equivalent in age to part of the Carolina slate belt. The volcanic rocks are probably bimodal, like those of the Carolina slate belt. The volcanics appear to represent

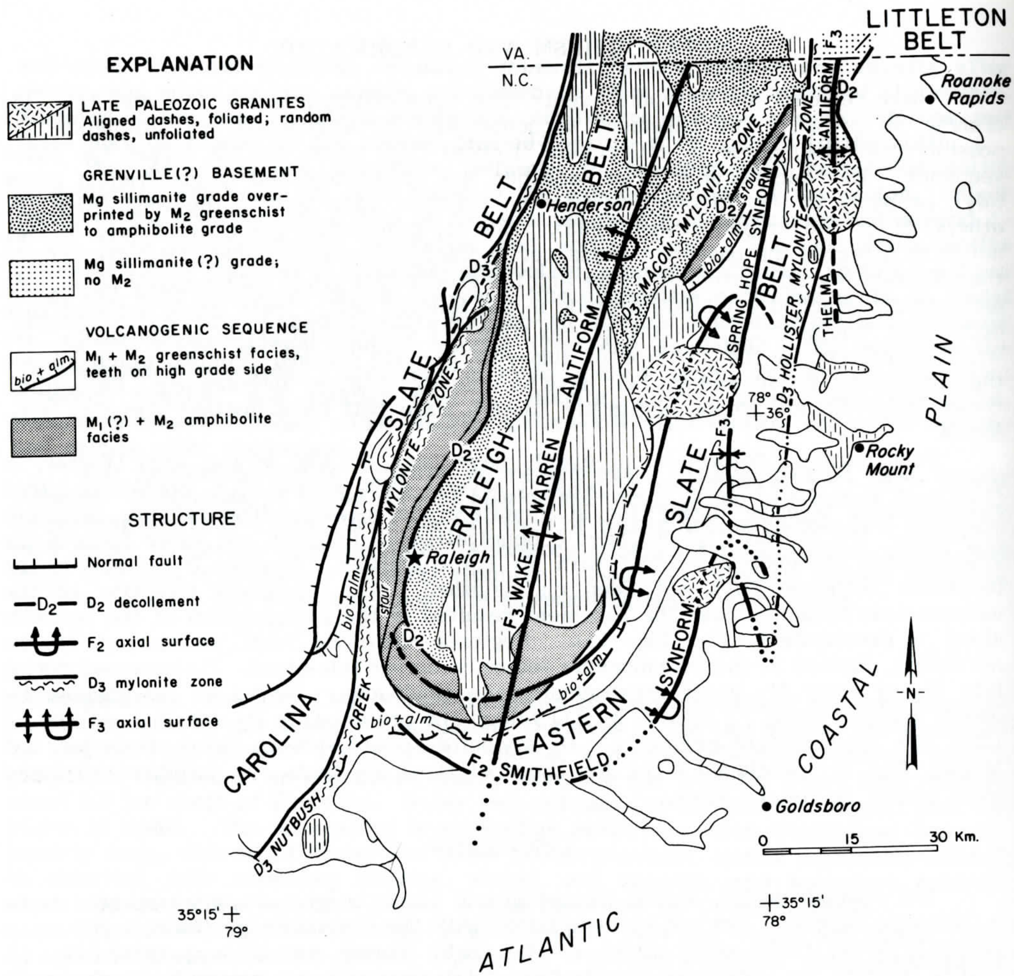

Figure 11. Metamorphic and structural map of the northeastern North Carolina Piedmont.

several local accumulations, including the Fuquay-Varina complex and the Roanoke Rapids complex. With such local volcanic centers and no radiometric ages, it would be premature to attempt correlation of units between this area and the main Carolina slate belt west of the Durham-Wadesboro Triassic-Jurassic basin.

CONCLUSIONS

The easternmost North Carolina Piedmont comprises a Grenville(?) basement sequence interpreted to be the southern continuation of the Goochland terrane of the eastern Virginia Piedmont (Farrar and Glover, 1983). These rocks are structurally overlain by a volcanogenic sequence of probable Late Precambrian-Early Paleozoic age which is an eastward continuation of the Carolina slate belt. The basement sequence of gneiss and schist is characterized by relict upper amphibolite- or granulite-facies assemblages. The volcanogenic sequence is characterized by relatively sodic bimodal volcanic rocks, associated shallow intrusions, and volcanogenic sediments. The basement and cover sequences were metamorphosed, folded, intruded by numerous granites, and cut by major mylonite zones in an Alleghanian tectonic event. The Alleghanian mylonite zones cut the area into separate tectonic blocks. Within the Raleigh block, individual formations have been traced from the greenschist-grade Eastern slate belt into the amphibolite-grade Raleigh belt.

This study illustrates the importance of defining stratigraphic units which are independent of metamorphic grade, yet recognizing that metamorphic discontinuities may also indicate stratigraphic discontinuities. The metamorphic transition from greenschist-grade Eastern slate belt to amphibolite-grade Raleigh belt, described by Parker (1979) in the southwest and Boltin and Stoddard (1983) in the northeast, occurs within the volcanogenic sequence and is an Alleghanian feature (Farrar and others, 1981; Russell and others, in press), whereas the relict high-grade assemblages in the basement can be used to define the important stratigraphic discontinuity between the basement and the volcanogenic cover.

ACKNOWLEDGEMENTS

This research began as part of an investigation of low-temperature, geothermal resources supported by the U.S. Department of Energy (Contracts Nos. EV-76-S-05-5103 and ET-78-C-05-5648 to J. K. Costain, L. Glover, III, and A. K. Sinha, and Contract No. DE-AC05-78ET27001 to J. K. Costain and L. Glover, III) with supplemental support from the Los Alamos Scientific Laboratory (Contract N28-77506-1 to A. K. Sinha, J. K. Costain, and L. Glover, III) and the U. S. Geological Survey (Contract 14-08-0001-G-685 to L. Glover, III and J. K. Costain). Assistance in this research by J. A. Speer and S. W. Becker is greatly appreciated. This work has benefited from reviews by J. A. Speer, S. W. Becker, G. S. Russell, L. Glover, III, D. T. Secor, E. F. Stoddard, R. L. Mauger and an anonymous reviewer.

Appendix 1: Locations of Representative Outcrops

CAROLINA SLATE BELT BLOCK

Cary Formation
- Greenstone. CR 1652, 1.2 km north of Cary in the Cary quadrangle.
- Felsic metatuff. Unnumbered road, 1 km west of CR 1300 at the southern edge of the Cary quadrangle.
- Phyllite. 2 km north of Holly Springs on N.C. 55, Apex quadrangle.

Fuquay-Varina Complex
- Buckhorn Creek pluton. Buckhorn Creek, 6 km west of Fuquay-Varina.
- Sunset Lake pluton. Spillway of Sunset Lake, 7 km north of Fuquay-Varina.
- Crystal tuff. CR 1427, 3.5 km west of Chalybeate Springs in the Fuquay-Varina quadrangle.

Beaverdam Mafic Complex
- Along Upper Barton Creek at CR 1841, Bayleaf quadrangle. See Parker (1979) for additional outcrops.

Gibbs Creek Metatonalite
- Along the Tar River as described by Carpenter (1970).

Vance County Metatrondhjemite
- CR 1308 at Nutbush Creek, Townsville quadrangle.

RALEIGH BLOCK

Raleigh Gneiss
- Streambed north of Enloe High School in Raleigh, Raleigh East quadrangle.

Macon Formation
- Gneiss. 2 km east of Warrenton along N.C. 58, Warrenton quadrangle.
- Phyllonite. CR 1057 at Little Fishing Creek, Macon quadrangle.
- Sillimanite + chloritoid schist. 2 km east of Warrenton along U.S. 158, Warrenton quadrangle.

Falls Leucogneiss
- At Falls on the Neuse River.

Bens Creek Leucogneiss
- 1 km northwest of Littleton, along the east side of Little Stone House Creek, Littleton quadrangle.

Spring Hope Formation

Quartz keratophyre metaporphyry. Roadcut at intersection of unnumbered road and Seaboard Coast Railroad 2.5 km west of Spring Hope, Bunn East quadrangle.

Felsic metatuff. Southern contact of Castalia pluton.

Greenstone with quartz amygdules. Spillway of Bodies Mill Pond, 2 km southeast of the Castalia pluton.

Scoriaceous metabasalt. Temporary gravel pit for I-95 construction, 4 km east of Spring Hope.

Stanhope Formation

Greenstone and felsic metavolcanics. Minor streams, both sides of N.C. 581, 2 km north of Stanhope, Spring Hope quadrangle.

Felsic gneiss. Along Swift Creek 10-15 km northwest of Smithfield, Powhatan quadrangle.

Amphibolite. Along Middle Creek, 6-8 km east of Willow Springs, Angier quadrangle.

Smithfield Formation

Metasediments. Several stream valleys northwest of Smithfield, and spillway of Holts Pond, 3 km southwest of Smithfield.

Princeton volcanic member. Spillway of Holts Pond, 2 km west of Princeton, and at two Nello Teer quarries northeast of Princeton.

Felsic gneiss. Crabtree quarry, west of Raleigh in Raleigh West quadrangle.

Amphibolite. CR 1649, south of Crabtree Creek, Raleigh West quadrangle.

Muscovite quartzite and schists. Crabtree Creek behind Crabtree Valley Mall on U.S. 70, Raleigh West quadrangle.

Ultramafic Bodies

See Carpenter (1970), Parker (1979), Moye (1981).

ROANOKE RAPIDS BLOCK

Littleton Gneiss

Along Deep Creek, 2.5 km southwest of Summit, Thelma quadrangle.

Roanoke Rapids Complex

Metatrondhjemite. Roanoke River at Weldon, and CR 1665, 1 km south of N.C. 48 in the Roanoke Rapids quadrangle.

Quartz keratophyre flow. 2 km northwest of Thelma, Thelma quadrangle.

Pyroclastic rocks and metasediments. Raceway below Roanoke Rapids dam.

Metagraywacke. South side of Roanoke River on N.C. 48 at Roanoke Rapids.

Phyllite. Along Deep Creek, 1 km south of Roanoke Rapids Lake.

Easonburg Formation

Crystal tuff. Along Tar River, 2 km south of Easonburg.

Phyllite. Along Swift Creek, 2 km south of Hilliardston, Red Oak quadrangle.

Halifax County Mafic Complex

Along Fishing Creek, 4 km north of Salem, Ringwood quadrangle.

GRANITOIDS

Locations are given only for those defined, or redefined here.

Rolesville Granite

Main facies. Quarries at Lassiter, Knightdale, Wendell, and Garner.

Archers Lodge facies. Middle Creek, north of Coats Crossroads, Edmonston quadrangle.

Louisburg facies. Roadcut on N.C. 39 at northern edge of Louisburg.

Butterwood Creek Granite

Coarse-grained, undeformed facies. CR 1001, 1.8 km west of Aurelian Springs, Aurelian Springs quadrangle.

Fine-grained, muscovite-biotite facies. Abandoned quarry, north of CR 1315, 1.2 km southwest of N.C. 4, Hollister quadrangle.

Deformed coarse-grained facies. Drillcore LIT-1, next to Butterwood Creek, 1.1 km south of Littleton, Littleton quadrangle.

Rocky Mount Granite

Biotite monzogranite. Along Tar River and tributaries in and west of Rocky Mount.

Hornblende-biotite granodiorite. RM 1 drillcore, 1 km south of Battleboro on Beech Brook, Drake quadrangle.

Biotite-hornblende tonalite. Along Swift Creek and Flat Rock Branch, northwest of Drake, Drake quadrangle.

REFERENCES

Becker, S. W. and Farrar, S. S., 1977, The Rolesville batholith: *in* Costain and others, Evaluation and Targeting of Geothermal Resources in the Southeastern United States, Progress Report, November 1, 1976-March 31, 1977.

Black, W. W., 1978, Chemical characteristics and Rb/Sr ages of metavolcanics from the Carolina slate belt of North Carolina: Geological Society of America Abstracts with Programs, v. 10, p. 162-163.

Bobyarchick, A. R. and Glover, L., III, 1979, Deformation and metamorphism in the Hylas zone and adjacent parts of the eastern Piedmont in Virginia: Geological Society of America Bulletin, v. 90, p. 739-752.

Boltin, W. R., and Stoddard, E. F., 1983, Transition from Raleigh belt to Eastern slate belt near Hollister, North Carolina: Geological Society of America Abstracts with Programs, v. 15, p. 111.

Carpenter, P. A., III, 1970, Geology of the Wilton area, Granville County, North Carolina (M.S. Thesis): Raleigh, North Carolina State University, 106 p.

Casadevall, T., and Rye, R. O., 1980, The Tungsten Queen deposit, Hamme district, Vance County, North Carolina: A stable isotope study of a metamorphosed quartz-huebnerite vein: Economic Geology, v. 75, p. 523-537.

Councill, R. J., 1954, Commercial granites of North Carolina: North Carolina Division of Mineral Resources Bulletin 67, 59 p.

Department of Defense, 1976, Department of Defense gravity library, North Carolina and South Carolina USGS Project, scale 1:250,000.

Dickey, J. B., 1963, The geology of Barton Creek area, northern Wake County, North Carolina (M.S. Thesis): Raleigh, North Carolina State University, 55 p.

Farrar, S. S., 1980, Petrology of the Rocky Mount granitoid pluton, North Carolina, and comparison to other granitoid plutons of the southern Piedmont: *in* Sinha, A. K., Costain, J. K., and Glover, L. III, eds., Distribution and Analysis of 300 m.y. old Granites as a Potential Geothermal Resource, Petrology Section, Report VPI&SU-LASL2, Virginia Polytechnic Institute and State University Contract N27-77506-1, p. 1-24.

Farrar, S. S., 1982, The Goochland granulite terrane, eastern Piedmont, Virginia: Petrographic evidence of Grenville granulite facies and Alleghanian amphibolite facies metamorphism: Geological Society of America Abstracts with Programs, v. 14, p. 17.

Farrar, S. S., 1984, The Goochland granulite terrane: Remobilized Grenville basement in the eastern Virginia Piedmont: *in* Bartholomew, M. J. (ed.), The Grenville Event in the Appalachians and Related Topics, Geological Society of America Special Paper 194, p. 215-227.

Farrar, S. S., in press, Tectonic evolution of the easternmost Piedmont, North Carolina: Geological Society of America Bulletin.

Farrar, S. S. and Glover, L. III, 1983, Grenville basement in the Piedmont east of the pre-Appalachian (Pre-Caledonian) edge(?) of the North American craton: Geological Society of America Abstracts with Programs, v. 15, p. 123.

Farrar, S. S., Russell, G. S., Russell, C. W., and Glover, L., III, 1981, Alleghanian deformation and metamorphism in the eastern Piedmont of North Carolina: New evidence from Rb-Sr whole-rock and biotite ages: Geological Society of America Abstracts with Programs, v. 13, p. 449-450.

Foose, M. P., Slack, J. F., and Casadevall, T., 1980, Textural and structural evidence for a predeformation hydrothermal origin of the Tungsten Queen deposit, Hamme district, North Carolina: Economic Geology, v. 75, p. 515-522.

Fortson, C. W., 1958, Geology of the Crabtree Creek area, northwest of Raleigh, North Carolina (M.S. thesis): Raleigh, North Carolina State College, 101 p.
Fullagar, P. D. and Butler, J. R., 1979, 325 to 265 m.y.-old post-metamorphic granitic plutons in the Piedmont of the southeastern Appalachians: American Journal of Science, v. 279, p. 161-185.
Glover, L., III, Mose, D. G., Costain, J. K., Poland, F. B., and Reilly, J. M., 1982, Grenville basement in the eastern Piedmont of Virginia: a progress report: Geological Society of America Abstracts with Programs, v. 14, p. 20.
Glover, L., III and Sinha, A. K., 1973, The Virgilina deformation, a late Precambrian(?) orogenic event in the central Piedmont of Virginia and North Carolina: American Journal of Science, v. 273-A, p. 234-251.
Glover, L., III, Speer, J. A., Russell, G. S., and Farrar, S. S., 1983, Ages of regional metamorphism and ductile deformation in the central and southern Appalachians: Lithos, v. 162, p. 223-245.
Harvey, B. W., 1974, The microscopic petrography and ore microscopy of the Boy Scout-Jones molybdenum prospect, Halifax County, North Carolina (M.S. thesis): Raleigh, North Carolina State University, 85 p.
Julian, E. L., 1972, The Castalia adamellite in Franklin and Nash Counties, North Carolina, and the petrogenesis of some associated aplites and pegmatites (M.S. thesis): Raleigh, North Carolina State University, 61 p.
Kish, S. A. and Fullagar, P. D., 1978, Summary of geochronological data for Late Paleozoic plutons from high grade metamorphic belts of the eastern Piedmont of North Carolina, South Carolina, and Virginia: in, Snoke, A. W., ed., Geological investigations of the eastern Piedmont, southern Appalachians: Carolina Geological Society, 1978 Guidebook, South Carolina Geological Survey, Columbia, S. C., p. 61-64.
Kish, S. A., Butler, J. R., and Fullagar, P. D., 1979, The timing of metamorphism and deformation in the central and eastern Piedmont of North Carolina: Geologigical Society of America Abstracts with Programs, v. 11, p. 184-185.
Kite, L. E. and Stoddard, E. F., 1984, The Halifax County complex: Oceanic lithosphere in the eastern North Carolina Piedmont: Geological Society of America Bulletin, v. 95, p. 422-432.
Mundorff, M. J., 1946, Ground water in the Halifax area, North Carolina: North Carolina Division of Mineral Resources Bulletin 51, 76 p.
North Carolina Department of Conservation and Development, Division of Mineral Resources, 1958, Geologic Map of North Carolina, scale 1:500,000.
Parker, J. M., III, 1963, Geologic setting of the Hamme tungsten district North Carolina and Virginia: U.S. Geological Survey Bulletin 1122-G, p. G1-G69.
Parker, J. M., III, 1968, Structure of easternmost North Carolina Piedmont: Southeastern Geology, v. 9, p. 117-131.
Parker, J. M., III, 1979, Geology and mineral resources of Wake County: North Carolina Division of Mineral Resources Bulletin 86, 122 p.
Robertson, A. F., McIntosh, F. K., and Ballard, T. J., 1947, Boy Scout-Jones and Moss-Richardson molybdenum deposits, Halifax County, N.C.: U.S. Bureau of Mines Report of Investigations 4156.
Russell, G. S., Russell, C. W. and Farrar, S. S., in press, Alleghanian deformation and metamorphism in the eastern North Carolina Piedmont: Geological Society of America Bulletin.
St. Jean, J., Jr., 1973, A new Cambrian trilobite from the Piedmont of North Carolina: American Journal of Science, v. 273-A, p. 196-216.
Secor, D. T., Jr. and Snoke, A. W., 1978, Stratigraphy, structure, and plutonism in the central South Carolina Piedmont: *in* Snoke, A. W., ed., Geological investigations of the eastern Piedmont, southern Appalachians: Carolina Geological Society 1978 Guidebook, South Carolina Geological Survey, South Carolina State Development Board, p. 65-123.
Snoke, A. W., Kish, S. A., and Secor, D. T., Jr., 1980, Deformed Hercynian granitic rocks from the Piedmont of South Carolina: American Journal of Science, v. 280, p. 1018-1034.

Stanley, L. G., 1978, A eugeosynclinal orthoquartzite facies in the Eastern slate belt rocks of Nash County, North Carolina (M.S.thesis): Raleigh, North Carolina State University, 81 p.

Stanley, L. G. and Cavaroc, V. V., 1980, Orthoquartzite sandstone in a eugeosynclinal facies of the Eastern slate belt of North Carolina: The Journal of the Elisha Mitchell Scientific Society, v. 96, p. 12-19.

Stoddard, E. F. and McDaniel, R. D., 1979, Geology of the Raleigh belt in eastern Franklin and Warren Counties, North Carolina: A preliminary report: Geological Society of America Abstracts with Programs, v. 11, p. 214.

Stoddard, E. F., Kite, L. E., and Moye, R. J., 1982, Ophiolitic terranes of the eastern Piedmont of North Carolina and their tectonic implications: Geological Society of America Abstracts with Programs, v. 14, p. 86.

Stoddard, E. F., Moye, R. J., Kite, L. E., and Won, I. J., 1982, Eastern North Carolina ophiolite terranes: setting, petrology, and implications: Geological Society of America Abstracts with Programs, v. 14, p. 626.

Stoddard, E. F. and Teseneer, R. L., 1978, Associated mafic and ultramafic igneous rocks, southwestern Halifax County, North Carolina: Geological Society of America Abstracts with Programs, v. 10, p. 199.

Streckeisen, A., 1976, To each plutonic rock its proper name: Earth Science Reviews, v. 12, p. 1-33.

Stuckey, J. L., 1965, North Carolina: Its geology and mineral resources: Raleigh, North Carolina Department of Conservation and Development, 550 p.

United States Geological Survey, 1974, Aeromagnetic map of parts of the Greensboro and Raleigh 1^{o} by 2^{o} quadrangles, North Carolina: U.S. Geological Survey Open-file Map 74-29.

Watson, T. L. and Laney, F. B., 1906, The building and ornamental stones of North Carolina: North Carolina Geological Survey Bulletin 2, 283 p.

Wedemeyer, R. G. and Spruill, R. K., 1980, Geochemistry and geochronology of the Sims granite, eastern Carolina slate belt, North Carolina: Geological Society of America Abstracts with Programs, v. 12, p. 211.

Wilson, W. F. and Carpenter, P. A., 1975, Region J geology: A guide for North Carolina mineral resource development and land use planning: North Carolina Mineral Resources Section, Regional Geology Series 1, 76 p.

Wright, J. E. and Seiders, V. M., 1980, Age of zircon from volcanic rocks of the central North Carolina Piedmont and tectonic implications for the Carolina volcanic slate belt: Geological Society of America Bulletin, v. 91, p. 287-294.